

HIGH PRESSURE SOLUBILITIES OF CARBON DIOXIDE IN  
THE AROMATIC SOLVENTS BENZENE, NAPHTHALENE,  
PHENANTHRENE, AND PYRENE

By

MARK W. BARRICK

Bachelor of Science

Oklahoma State University

Stillwater, Oklahoma

1985

Submitted to the Faculty of the Graduate College  
of the Oklahoma State University  
in partial fulfillment of the requirements  
for the Degree of  
MASTER OF SCIENCE  
May, 1985

Thesis  
1985  
B275h  
cop. 2



HIGH PRESSURE SOLUBILITIES OF CARBON DIOXIDE IN  
THE AROMATIC SOLVENTS BENZENE, NAPHTHALENE,  
PHENANTHRENE, AND PYRENE

Thesis Approved:

*Robert L. Robinson Jr.*  
\_\_\_\_\_  
Thesis Adviser

*Tom Wagoner*  
\_\_\_\_\_

*Walter L. Foutel*  
\_\_\_\_\_

*Norman N. Durham*  
\_\_\_\_\_  
Dean of the Graduate College

## PREFACE

An isothermal bubble-point apparatus was designed, tested, and operated in this work to measure the high pressure solubilities of carbon dioxide in the aromatic solvents benzene, naphthalene, phenanthrene, and pyrene. Measurements were made over a temperature range of 40 to 160°C and a pressure range of 100 to approximately 1550 psia.

Empirical binary interaction parameters for both the Soave-Redlich-Kwong and Peng-Robinson equations as well as Henry's constants and partial molar volumes of carbon dioxide in the aromatic solvents have been evaluated from resulting experimental data.

I wish to express my sincere appreciation to my adviser, Dr. R. L. Robinson, Jr., for his guidance, support, and patience throughout the course of this study.

I must thank Mr. J. McRay Anderson for his contributions to the design, testing, and operation of the apparatus used in this study. Mr. Anderson and I worked jointly on this project although studying different systems. The procedure chapter contained in this text was written by Mr. Anderson while his text contains an experimental apparatus section written by myself. I would also like to thank Mr. Heinz Hall for his help in constructing the apparatus and Mr. Khaled Gasem for his help in regressing the experimental data. Thanks must also go to Mrs. Kenda Morris for her valuable assistance and patience during preparation of this text.

Financial support was gratefully received from the United States Department of Energy (DE-FG22-83PC60039).

## TABLE OF CONTENTS

| Chapter   | Page |
|---|------|
| I. INTRODUCTION . . . . .   | 1    |
| II. LITERATURE REVIEW. . . . .                                      | 2    |
| Experimental Data . . . . .   | 2    |
| Thermodynamic Prediction Methods. . . . .                           | 3    |
| III. REVIEW OF PHASE EQUILIBRIUM THERMODYNAMICS . . . . .           | 9    |
| IV. EXPERIMENTAL APPARATUS . . . . .                                | 19   |
| General Description . . . . .                                       | 20   |
| Equilibrium Cell. . . . .   | 22   |
| Rotating Magnet Assembly. . . . .                                   | 27   |
| Storage Vessels . . . . .   | 27   |
| Pressure Measurements . . . . .                                     | 29   |
| Volumetric Injection Pumps. . . . .                                 | 30   |
| Constant Temperature Baths. . . . .                                 | 30   |
| Degassing Trap. . . . .   | 31   |
| Fittings, Tubing, and Valves . . . . .                              | 33   |
| Chemicals . . . . .   | 33   |
| V. EXPERIMENTAL PROCEDURE . . . . .                                 | 35   |
| Cleaning the Storage Cell . . . . .                                 | 36   |
| Cleaning the Equilibrium Cell . . . . .                             | 40   |
| Charging and Degassing the Solvent. . . . .                         | 42   |
| Injecting the Solvent . . . . .                                     | 44   |
| Injecting the Solute Gas. . . . .                                   | 47   |
| Measuring the Bubble Point. . . . .                                 | 49   |
| Proper Determination of the Isothermal Solubility<br>Curve. . . . . | 54   |
| Calibration of Pressure Transducers . . . . .                       | 56   |
| VI. ERROR ANALYSIS AND DATA REDUCTION. . . . .                      | 59   |
| Error Analysis. . . . .   | 59   |
| Data Reduction. . . . .   | 62   |
| VII. EXPERIMENTAL RESULTS AND DISCUSSION. . . . .                   | 64   |

| Chapter   | Page |
|---|------|
| VIII. CONCLUSIONS AND RECOMMENDATIONS. . . . .  | 100  |
| Conclusions . . . . .   | 100  |
| Recommendations . . . . .   | 101  |
| SELECTED BIBLIOGRAPHY. . . . .  | 103  |
| APPENDIXES . . . . .  | 107  |
| APPENDIX A - EXPLANATION OF THE PROGRAM USED TO CALCULATE<br>PERCENTAGE UNCERTAINTY IN CO <sub>2</sub> DENSITY. . . . .           | 108  |
| APPENDIX B - COMPUTER PROGRAM USED TO CALCULATE CO <sub>2</sub><br>DENSITY AS A FUNCTION OF TEMPERATURE AND<br>PRESSURE . . . . . | 109  |
| APPENDIX C - COMPUTER PROGRAM USED IN CALIBRATION OF<br>PRESSURE TRANSDUCERS . . . . .  | 116  |
| APPENDIX D - ERROR PROPAGATION IN MOLE FRACTION AND<br>BUBBLE-POINT PRESSURE. . . . .   | 121  |

## LIST OF TABLES

| Table  | Page |
|--|------|
| I. Summary of CO <sub>2</sub> + Benzene Equilibrium Data. . . . .  | 3    |
| II. Chemicals and Their Purities . . . . .   | 34   |
| III. Maximum Error in Bubble-Point Pressure . . . . .  | 62   |
| IV. Vapor Pressure Test Results. . . . .   | 64   |
| V. Solubility of CO <sub>2</sub> in Benzene . . . . .  | 66   |
| VI. Soave and Peng-Robinson Equation of State<br>Representations of CO <sub>2</sub> Solubility Data. . . . . | 68   |
| VII. Solubility of CO <sub>2</sub> in Naphthalene . . . . .  | 72   |
| VIII. Solubility of CO <sub>2</sub> in Phenanthrene. . . . .   | 77   |
| IX. Solubility of CO <sub>2</sub> in Pyrene. . . . .   | 85   |
| X. Critical Properties Used in Equations of State . . . . .  | 88   |
| XI. Henry's Constants and Partial Molar Volumes for CO <sub>2</sub> . . . . .                                | 94   |
| XII. Densities and Volumes used to Calculate Solubilities . . . . .  | 95   |



## LIST OF FIGURES

| Figure  | Page |
|---|------|
| 1. Schematic Diagram of the Isothermal Bubble-Point Apparatus. . . . .                                | 21   |
| 2. Overhead View of the Bubble-Point Apparatus. . . . .   | 23   |
| 3. Stirred Equilibrium Cell . . . . .   | 24   |
| 4. Section View of Stirrer. . . . .   | 26   |
| 5. Rotating Magnet Assembly . . . . .   | 28   |
| 6. Degassing Trap . . . . .   | 32   |
| 7. Schematic Diagram of the Apparatus with Valve Identification . .                                   | 37   |
| 8. Injection Sheet. . . . .   | 45   |
| 9. Percentage Uncertainty in CO <sub>2</sub> Density Versus Pressure. . . . .                         | 48   |
| 10. P-V Data Sheet . . . . .  | 51   |
| 11. Graphical Bubble-Point Determination . . . . .  | 52   |
| 12. Typical Bubble-Point Data for CO <sub>2</sub> + Solvent. . . . .                                  | 55   |
| 13. Comparison of Bubble-Point Data for CO <sub>2</sub> + Benzene at 40°C. . . .                      | 67   |
| 14. Comparison of Solubility Data for CO <sub>2</sub> in Benzene at 40°C . . . .                      | 71   |
| 15. Bubble-Point Data for CO <sub>2</sub> + Naphthalene at 100°C . . . . .                            | 73   |
| 16. Bubble-Point Data for CO <sub>2</sub> + Naphthalene at 150°C . . . . .                            | 74   |
| 17. Soave and Peng-Robinson Representations of CO <sub>2</sub> Solubility<br>in Naphthalene . . . . . | 76   |
| 18. Bubble-Point Data for CO <sub>2</sub> + Phenanthrene at 110°C. . . . .                            | 78   |
| 19. Bubble-Point Data for CO <sub>2</sub> + Phenanthrene at 150°C. . . . .                            | 79   |
| 20. Soave and Peng-Robinson Representations of CO <sub>2</sub> Solubility<br>in Phenanthrene. . . . . | 81   |

| Figure   | Page |
|--|------|
| 21. Comparison of Binary Interaction Parameters for<br>CO <sub>2</sub> + Phenanthrene . . . . .  | 82   |
| 22. Solubility of CO <sub>2</sub> in Phenanthrene at One Atmosphere. . . . .                     | 84   |
| 23. Bubble-Point Data for CO <sub>2</sub> + Pyrene at 160°C. . . . .                             | 86   |
| 24. Soave and Peng-Robinson Representations of CO <sub>2</sub> Solubility<br>in Pyrene. . . . .  | 87   |
| 25. Binary Interaction Parameters Versus the Number of<br>Benzene Rings in the Solvent . . . . . | 90   |
| 26. Binary Interaction Parameters Versus Solvent<br>Molecular Weight . . . . .                   | 91   |
| 27. Binary Interaction Parameters Versus the Solvent<br>Liquid Density . . . . .                 | 92   |

## LIST OF SYMBOLS

### Symbol

|            |   |
|------------|---|
| a          | attraction parameter for equations of state   |
| b          | van der Waals covolume for equations of state |
| f          | fugacity                                      |
| g          | acceleration due to gravity                   |
| h          | height  |
| H          | Henry's constant                              |
| HC         | head correction                               |
| k          | binary interaction parameter                  |
| l          | binary interaction parameter                  |
| MW         | molecular weight                              |
| n          | moles   |
| N          | number of chemical species or data points     |
| P          | pressure                                      |
| Q          | quantity to be minimized                      |
| R          | universal gas constant                        |
| T          | temperature                                   |
| V          | volume  |
| x          | liquid phase mole fraction                    |
| y          | vapor phase mole fraction                     |
| z          | mixture mole fraction                         |
| Z          | compressibility factor                        |
| $\sigma^2$ | variance                                      |

### Greek symbols

|            |                         |
|------------|-------------------------|
| $\alpha$   | attraction parameter    |
| $\gamma$   | activity coefficient    |
| $\epsilon$ | error                   |
| $\kappa$   | characteristic constant |
| $\mu$      | chemical potential      |
| $\rho$     | density                 |
| $\phi$     | fugacity coefficient    |
| $\omega$   | acentric factor         |

### Subscripts

|                 |                                  |
|-----------------|----------------------------------|
| 1               | initial value or component "one" |
| 2               | final value or component "two"   |
| b               | bubble point                     |
| c               | critical property                |
| cb              | cell bath                        |
| CO <sub>2</sub> | carbon dioxide                   |
| GIP             | gas injection pump               |

## Subscripts

|        |                                  |
|--------|----------------------------------|
| HC     | hydrocarbon                      |
| Hg     | mercury                          |
| Hgcell | mercury in equilibrium cell      |
| i      | specie or data point index       |
| if     | oil-mercury interface            |
| j      | specie or data point index       |
| m      | mixture parameter                |
| o      | original value                   |
| oil    | dead weight guage oil            |
| P      | pressure                         |
| pb     | pump bath                        |
| r      | reduced property                 |
| ref    | dead weight guage reference mark |
| S      | solvent                          |
| SG     | solute gas                       |

## Superscripts

|      |                        |
|------|------------------------|
| calc | calculated             |
| exp  | experimental           |
| ~    | partial molar property |
| o    | pure liquid state      |
| +    | pure reference state   |
| ^    | real mixture           |
| -    | molar property         |

## CHAPTER I

### INTRODUCTION

To effectively design and operate processes for conversion of coal to fluid fuels, the phase behavior of the mixtures encountered in the conversion process must be known.

Equations of state are widely used in industry to model the phase behavior of mixtures present in the many stages of the conversion process. The prediction accuracy of equations of state can be enhanced while retaining their simplicity by employing empirical binary interaction parameters. The purpose of this work was to determine the solubilities of carbon dioxide in the aromatic solvents benzene, naphthalene, phenanthrene, and pyrene. Binary interaction parameters were then regressed from the resulting experimental data for each binary system.

Data on these systems is of interest to the energy industry because all of the above-named chemicals are found in coal. The data on these binary systems can also be used to test generalized correlations for predicting binary interaction parameters from the physical properties of chemical species.

## CHAPTER II

### LITERATURE REVIEW

During the course of this study, a review of literature relevant to the present work was performed. Literature concerning experimental vapor-liquid equilibrium (VLE) data and methods for predicting vapor-liquid behavior were surveyed; special attention was focused on the systems studied in the present work.

#### Experimental Data

A large amount of data exists on CO<sub>2</sub> + hydrocarbon binary mixtures for systems in which the hydrocarbon is a liquid at room temperature. However, very limited data are available on systems involving CO<sub>2</sub> and heavy aromatic solvents which are solids at room temperature. Such data are needed to predict phase behavior of mixtures encountered during conversion of coal to fluid fuels (1).

Of the systems studied in this work, the system CO<sub>2</sub> + benzene was found to have the most previous experimental data. Donohue (2), Gupta et al. (3), Nagarajan et al. (4), and Ohgaki and Katayama (5) have measured isothermal phase compositions at various pressures. In addition, Gasem (6) and Gupta et al. (3) determined bubble-point pressures of CO<sub>2</sub> + benzene binary mixtures at constant temperature. Table I presents a summary of the temperatures at which the above authors conducted their experiments.

TABLE I  
SUMMARY OF CO<sub>2</sub> + BENZENE  
EQUILIBRIUM DATA

| Temperatures (K)       | Pressures (MPa) | Reference<br>Number |
|------------------------|-----------------|---------------------|
| 313.35, 352.95, 393.15 | 2.119 - 6.270   | (2)                 |
| 313.2, 353.2, 393.2    | 0.740 - 13.395  | (3)                 |
| 344.3                  | 6.895 - 10.960  | (4)                 |
| 298.15, 313.15         | 0.894 - 7.750   | (5)                 |
| 313.2                  | 0.754 - 5.171   | (6)                 |

Two references were found for the system CO<sub>2</sub> + phenanthrene. Chen et al. (7) measured the solubilities of several solutes (including CO<sub>2</sub>) in phenanthrene at one atmosphere pressure and temperatures ranging from 378.15 to 418.15 K. Phase compositions of the binary CO<sub>2</sub> + phenanthrene were measured at pressures from 200 to 1600 psia and temperatures 220 to 800°F by DeVaney et al. (8).

A reference for the system CO<sub>2</sub> + naphthalene by Orlov and Cherkasova (9) was found but could not be obtained. No data on the system CO<sub>2</sub> + pyrene could be found.

#### Thermodynamic Prediction Methods

Several investigators have studied the use of equations of state to predict the phase behavior of mixtures. Two equations of state, the

Soave-Redlich-Kwong (SRK) and Peng-Robinson (P-R) (these equations are presented in detail in Chapter III), have been found particularly useful for this purpose due to their overall simplicity and accuracy.

The general consensus of studies performed have shown that while the SRK and P-R equations can predict the phase behavior for hydrocarbon mixtures with reasonable precision, their accuracy is reduced when non-hydrocarbon gases are present in the mixture.

Huron et al. (10) investigated the ability of the SRK equation to predict VLE and critical locus curves for binaries of paraffins (methane through n-decane) with CO<sub>2</sub> and H<sub>2</sub>S. This study concluded that on the whole, critical points and VLE are correctly represented by the SRK with the use of the binary interaction parameter,  $k_{ij}$ , for systems with non-hydrocarbon components. Also the parameter  $k_{ij}$  determined from critical points did not differ significantly from the value of  $k_{ij}$  determined from VLE data.

To determine the optimum values for  $k_{ij}$ , Huron et al. minimized the sum of the squares of errors,  $Q$ , in the calculated vapor mole fractions of the components and calculated pressures of the system (at given temperature and liquid mole fraction):

$$Q = \sum_{i=1}^N \{(y_i^{\text{Exp}} - y_i^{\text{Calc}})^2 + [(p_i^{\text{Exp}} - p_i^{\text{Calc}})/p_i^{\text{Exp}}]^2\} \quad (2.1)$$

No correlation was found between  $k_{ij}$ 's and any characteristic parameters of the hydrocarbons studied by Huron et al. However,



although no relationship was found, they stated their belief that some non-obvious relationship does exist.

The use of the SRK for VLE calculations was also studied by Graboski and Daubert (11). The systems studied involved CO<sub>2</sub>, H<sub>2</sub>S, N<sub>2</sub>, and CO in the paraffins methane through n-decane. In this work, they found that for hydrocarbon mixtures, no interaction parameters were needed. However, with non-hydrocarbon components present, the binary interaction parameter,  $k_{ij}$ , greatly improved equilibria predictions. They also concluded that  $k_{ij}$  can be related to the solubility parameter difference between the hydrocarbon and non-hydrocarbon. Thus, generalized correlations for interaction parameters for each non-hydrocarbon/hydrocarbon binary can be found.

The values of  $k_{ij}$  determined by Graboski and Daubert ranged from 0.00 to 0.25. The value increased with molecular size. Generally,  $k_{ij}$  is assumed to be a constant for a binary pair, independent of temperature and pressure. However, they found that this was not always the case.

The optimum values of  $k_{ij}$  determined by Graboski and Daubert were obtained from two search-optimization routines. One minimized the bubble-point pressure variance,  $\sigma_p^2$ ,

$$\sigma_p^2 = \sum_{i=1}^N [(P_i^{\text{Exp}} - p_i^{\text{Calc}})/P_i^{\text{Exp}}]^2 \quad (2.2)$$

and the other minimized the flash volume variance,  $\sigma_V^2$

$$\sigma_V^2 = \sum_{i=1}^N [(L_i^{\text{Exp}} - L_i^{\text{Calc}})^2 + (V_i^{\text{Exp}} - V_i^{\text{Calc}})^2]. \quad (2.3)$$

No difficulty in convergence was encountered with the bubble-point method but some problems arose with the flash procedure. In the end, the bubble-point method was deemed the better of the two methods by showing a greater sensitivity to the value of  $k_{ij}$  (this confirms the choice of the bubble-point method used in this work to determine optimum values for interaction parameters).

Mundis et al. (12) calculated equilibrium ratios (K values) for  $\text{CO}_2$  and  $\text{H}_2\text{S}$  in paraffinic, naphthenic, and aromatic solvents using the SRK equation with optimum values for  $k_{ij}$ . The purpose of their study was to gain some understanding of the influence that the chemical composition of absorber solvent oils would have on  $\text{CO}_2$  and  $\text{H}_2\text{S}$  K values. The particular systems studied included  $\text{CO}_2$  and  $\text{H}_2\text{S}$  in methane + n-heptane, methane + methylcyclohexane, and methane + toluene at 20.0, -20 and -40°F and in methane + n-octane at 0 and -20°C. Average errors in the predicted K values for these systems were approximately 5%.

The ability of the P-R equation to predict K values for  $\text{CO}_2$  plus hydrocarbon systems was examined by Lin (13). The range of hydrocarbons studied included selected paraffins from methane to n-octadecane and a few naphthenic and aromatic compounds. In this work, Lin presents optimized P-R values for  $k_{ij}$  and also discussed the state of efforts to derive a generalized correlation for estimating values of  $k_{ij}$ .

On the whole, Lin found the P-R equation able to predict the K-values  $\text{CO}_2$  + hydrocarbon mixtures with an average error of 5.4 to 8.0%. Best results were obtained by using optimum values of  $k_{ij}$  (at

each temperature), but for rough approximations, Lin found a constant value of  $k_{ij} = 0.125$  gave results consistent with experimental data in most cases. The majority of optimum  $k_{ij}$  values using the P-R equation were in the range 0.11 to 0.13. Lin believes his results demonstrated that there was no need to treat  $k_{ij}$  as temperature-dependent for  $\text{CO}_2$  + hydrocarbon mixtures.

Turek et al. (14) investigated the use of two binary interaction parameters,  $k_{ij}$  and  $l_{ij}$ , to predict phase equilibria of  $\text{CO}_2$  + multicomponent hydrocarbon systems. This was done to better predict phase behavior of  $\text{CO}_2$  + hydrocarbon mixtures over a wide range of  $\text{CO}_2$  concentrations which may be encountered in  $\text{CO}_2$  miscible reservoir processes. In this work, a modified form of the Redlich-Kwong equation (as suggested by Yarborough (15)), with mixing rules developed to predict phase behavior over a wide range of  $\text{CO}_2$  concentrations, was used for predictions.  $\text{CO}_2$ /hydrocarbon binary interaction parameters were determined simultaneously through numerical regression of binary VLE data from the literature. The regression program used to determine these parameters minimized the square of the fugacity deviation between phases for each component. The binary interaction parameters were expressed as continuous functions of hydrocarbon acentric factor and the parameters were determined through simultaneous regression on many binary systems. This approach was taken because it permits interpolation (or extrapolation) of binary interaction parameters for binaries lacking experimental data.

The work of Turek et al. included tests of their correlation on  $\text{CO}_2$  + synthetic oil (made up of selected hydrocarbons) and  $\text{CO}_2$  + a true reservoir oil. The properties of each of these systems were determined

experimentally. The modified Redlich-Kwong equation was then used (with the empirically determined values of  $k_{ij}$  and  $l_{ij}$ ) to predict the experimentally observed behavior.

Overall, the results showed much improved prediction of physical properties of the systems analyzed using two interaction parameters relative to the use of only one interaction parameter. Also concluded was that the modified Redlich-Kwong equation with appropriate parameters is capable of predicting the complex phase equilibria found in  $\text{CO}_2$  + hydrocarbon systems.

All of the authors studying the use and correlation of interaction parameters cited discrepancies in VLE data among experimenters as a problem. These discrepancies cause scatter in optimum values of  $k_{ij}$ , which hampers efforts to determine generalized correlations for interaction parameters. Further, there is insufficient VLE data available on naphthenic and aromatic compounds to begin correlation efforts specifically for these compounds or test the applicability of generalized correlations (based on other hydrocarbons) to these compounds.

## CHAPTER III

### REVIEW OF PHASE EQUILIBRIUM THERMODYNAMICS

The determination of CO<sub>2</sub> solubilities in heavy aromatic solvents in this study involved the measurement of bubble-point pressures of binary mixtures of CO<sub>2</sub> in selected aromatic compounds. The bubble-point pressure of a mixture is an equilibrium property governed by the laws of thermodynamics. Classical thermodynamics provides a general criterion for equilibrium between a fixed number of stable phases in a non-reactive system containing any number of components. By combination of the first and second laws of thermodynamics, the following conditions can be shown to hold at equilibrium in a simple system (16):

- a) the phases must be at the same temperature  $T$  and pressure  $P$
- b) the chemical potential for each specie must be identical in all phases throughout the system

For a two-phase binary mixture, these conditions can be written mathematically as

$$T' = T'' \quad (3.1)$$

$$P' = P'' \quad (3.2)$$

$$\mu_i' = \mu_i'' \quad (i = 1,2) \quad (3.3)$$

where the superscripts (') and (") indicate separate phases.

These relationships can be applied directly to calculate equilibrium properties in terms of temperature, pressure, and chemical potential. To do this, some model must be employed to represent the

chemical potential of components in terms of the measurable quantities of phase composition, temperature, and pressure. However, the chemical potential is not a "well behaved" mathematical function at limiting conditions and is normally replaced by a "better behaved" function, fugacity.

Fugacity can be related to chemical potential most easily by first considering a pure component ideal gas (16)

$$\left(\frac{\partial \mu_i}{\partial P}\right)_{T,n} = \bar{V}_i = \frac{RT}{P}. \quad (3.4)$$

Integrating this expression yields

$$\bar{\mu}_i - \mu_i^+ = RT \ln (P/P^+) \quad (3.5)$$

where  $\bar{\mu}_i$  is the chemical potential of the pure substance and  $\mu_i^+$  is the pure reference state chemical potential.

Similarly, the value of the chemical potential of a component in an ideal gas mixture relative to its value in a pure state at  $P^+$  is

$$\tilde{\mu}_i - \mu_i^+ = RT \ln (Py_i/P^+). \quad (3.6)$$

To retain the simplicity of the above equations for non-ideal gas systems, fugacity and is defined in relation to the chemical potential (by analogy to Equation (3.6)) as

$$\tilde{\mu}_i - \mu_i^+ \equiv RT \ln (\hat{f}_i/P^+) \quad (3.7)$$

and

$$\lim_{P \rightarrow 0} (\hat{f}_i / Py_i) \equiv 1.0. \quad (3.8)$$

The pressure,  $P^+$ , is the reference pressure selected for the ideal gas.

Equation (3.7) can be written for both phases of a two-phase binary mixture,

$$\tilde{\mu}_i' - \mu_i^+ = RT \ln (\hat{f}_i' / P^+) \quad (3.9)$$

$$\tilde{\mu}_i'' - \mu_i^+ = RT \ln (\hat{f}_i'' / P^+). \quad (3.10)$$

If the mixture is at equilibrium  $\tilde{\mu}_i'' = \tilde{\mu}_i'$ , and therefore  $\hat{f}_i'$  must equal  $\hat{f}_i''$ . Thus, an equilibrium condition similar to Equation (3.3) can be written as

$$\hat{f}_i' = \hat{f}_i'' \quad (i = 1, 2). \quad (3.11)$$

Fugacity, like chemical potential, is a function of phase composition, temperature, and pressure, but the fugacity is more convenient for practical applications.

Fugacities of vapor and liquid phases are normally described in terms of their deviations from some "idealized behavior" reference. One such reference is the ideal gas.

The fugacity of an ideal gas is given by

$$\hat{f}_i = Py_i \quad (3.12)$$

and fugacities can be expressed in terms of the fugacity coefficient,  $\phi$ , which is defined as (16)

$$\phi_i \equiv \frac{\text{actual fugacity of component "i" in a mixture}}{\text{fugacity of component "i" in an ideal gas mixture}}$$

from which it follows that

$$\phi = \hat{f}_i / Py_i. \quad (3.13)$$

The fugacity coefficient approach is often applied to both vapor and liquid phases.

Another possible reference is an "ideal" liquid solution. An ideal solution is defined as one which exhibits (17)

- a) no volume change on mixing
- b) no heat effect on mixing, and
- c) random distribution of molecules in the mixture

The fugacity of a component "i" in an "ideal" liquid solution is then given as



$$\hat{f}_i = x_i f_i^0 \quad (3.14)$$

where  $f_i^0$  is the fugacity of component "i" in the pure liquid state at the system temperature and pressure. Using this reference, the deviation from the "ideal" liquid solution fugacity for component "i" is defined as the activity coefficient (16),  $\gamma_i$ ,

$$\gamma_i = \frac{\text{actual fugacity of component "i" in a mixture}}{\text{fugacity of component "i" in an ideal solution}}$$

from which it follows that

$$\gamma_i = \hat{f}_i / x_i f_i^0 \quad (3.15)$$

The activity coefficient approach to determining fugacities is normally used only for the liquid phase.

The fugacity coefficient can be related to the volumetric properties of a mixture by the exact relation (16)

$$\ln \phi_i = \frac{1}{RT} \int_0^P \left[ \bar{V}_i - \frac{RT}{P} \right] dP \quad (3.16)$$

or more commonly

$$\ln \phi_i = \frac{1}{RT} \int_{\infty}^V \left[ \frac{RT}{V} - \left( \frac{\partial P}{\partial n_i} \right)_{T,V,n_j} \right] dV - \ln Z \quad (3.17)$$

Similarly, the activity coefficient is related to the volumetric properties of a mixture by the expression

$$\ln \gamma_i = \frac{1}{RT} \int_0^P (\tilde{V}_i - \bar{V}_i) dP \quad (3.18)$$

where  $\tilde{V}_i$  and  $\bar{V}_i$  represent partial molar volume and molar volume of component "i", respectively.

In this study, the fugacity coefficient approach was used to evaluate fugacities of the components in both the liquid and vapor phases. The usual approach to calculate fugacity coefficients is to employ an equation of state as the model for the mixture behavior and relate the fugacity coefficient to pressure, volume, temperature behavior by using Equation (3.17).

Two equations of state used widely in industry for this purpose are the Soave-Redlich-Kwong (SRK) and Peng-Robinson (P-R) equations. The SRK equation of state is (18)

$$p = \frac{RT}{V-b} - \frac{a(T)}{V(V+b)} \quad (3.19)$$

where

$$a(T) = a_c \alpha(T) \quad (3.20)$$

$$b = 0.0664 RT_c/P_c \quad (3.21)$$

and

$$a_c = 0.42747 R^2 T_c^2 / P_c \quad (3.22)$$

$$\alpha(T)^{0.5} = 1 + \kappa (1 + T_r^{0.5}) \quad (3.23)$$

$$\kappa = 0.480 + 1.574\omega - 0.176\omega^2. \quad (3.24)$$

The Peng-Robinson equation of state is of similar form (19)

$$p = \frac{RT}{V-b} - \frac{a(T)}{V(V+b) + b(V-b)} \quad (3.25)$$

where  $a(T)$  and  $b$  are given as

$$a(T) = a_c \alpha(T) \quad (3.26)$$

$$b = 0.07780 RT_c / P_c \quad (3.27)$$

where

$$a_c = 0.45724 R^2 T_c^2 / P_c \quad (3.28)$$

$$\alpha(T)^{0.5} = 1 + \kappa(1 - T_r^{0.5}) \quad (3.29)$$

$$\kappa = 0.37464 + 1.54226\omega - 0.26992\omega^2. \quad (3.30)$$

To apply the SRK or P-R equation of state to mixtures, the values of  $a$  and  $b$  can be determined using the mixing rules (14)

$$a_m = \sum_{i=1}^N \sum_{j=1}^N z_i z_j (1 - k_{ij})(a_i a_j)^{0.5} \quad (3.31)$$

$$b_m = 0.5 \sum_{i=1}^N \sum_{j=1}^N z_i z_j (1 + l_{ij})(b_i + b_j) \quad (3.32)$$

In Equations (3.31) and (3.32) the quantities  $k_{ij}$  and  $l_{ij}$  are empirical "binary interaction parameters" characterizing the binary interactions between components "i" and "j". Values for  $k_{ij}$  and  $l_{ij}$  must be determined from experimental data (such as the bubble-point pressures of the binary mixtures studied here). Using values for  $k_{ij}$  and  $l_{ij}$  determined by regression of experimental data generated in this study, the abilities of the SRK and P-R equations to represent the solubilities of  $\text{CO}_2$  in the aromatic solvents benzene, naphthalene, phenanthrene, and pyrene were evaluated.

In addition to the solubilities of  $\text{CO}_2$  in the above mentioned solvents, Henry's constants and partial molar volumes of  $\text{CO}_2$  were also estimated using a method of Krichevsky and Kasarnovsky (20). This method is applicable to systems where the solubility of the solute ( $\text{CO}_2$ ) in the solvent is small and the solvent has a low vapor pressure.

For binary systems, at constant temperature and pressure, Henry's law can be used to estimate the fugacity of a component

$$\hat{f}_i = H_i x_i \quad (\text{@ constant } T, P) \quad (3.33)$$

However, saturation pressure versus solubility data are not at constant pressure; the effect of pressure on the fugacity of a component (at constant temperature and pressure) is related to a change in pressure by

$$RT \ln \hat{f}_i \cong \tilde{V}_i dP \quad (3.34)$$

and by integrating this expression from  $P_1$  to  $P_2$  yields

$$RT \ln (\hat{f}_{i,P_2} / \hat{f}_{i,P_1}) = \int_{P_1}^{P_2} \tilde{V}_i dP. \quad (3.35)$$

If the partial molar volume of component "i" is taken to be constant, then

$$RT \ln (\hat{f}_{i,P_2} / \hat{f}_{i,P_1}) = \tilde{V}_i (P_2 - P_1). \quad (3.36)$$

If  $P_1$  in Equation (3.33) is taken to be the vapor pressure of the solvent,  $P_{HC}^0$ , then combining Equations (3.33) and (3.36) yields an expression which can be written for any pressure,  $P$ ,

$$\ln (\hat{f}_{i,P} / x_i) = \ln H_i + \tilde{V}_i (P - P_{HC}^0) / RT. \quad (3.37)$$

The solvents studied in this work (with the exception of benzene) are of very low volatility and the vapor phase can be assumed to be essentially pure  $\text{CO}_2$ . Thus,  $\hat{f}_{i,p}$  may be replaced by the fugacity of the pure solute,  $f^0_{\text{CO}_2}$ , at the system pressure. Rewriting Equation (3.36) in the form used in this study then results in

$$\ln (f^0_{\text{CO}_2, P_b} / x_{\text{CO}_2}) = \ln H_{\text{CO}_2, \text{HC}} + \tilde{V}_{\text{CO}_2} (P_b - P^0_{\text{HC}}) / RT. \quad (3.38)$$

Inspection of Equation 3.37 shows the K-K equation can be plotted the form of straight line. Thus, determining the y-intercept and slope of a plot of  $\ln(f^0_{\text{CO}_2} / x_{\text{CO}_2})$  versus  $P_b - P^0_{\text{HC}}$  yields the Henry's constant and partial molar volume of the solute ( $\text{CO}_2$ ), respectively.

The K-K equation yields best results when its application is limited to

- a) low solubilities of solute (values of  $x_i$ )
- b) pressures such that  $P_b - P^0_{\text{HC}}$  is not great and well away from the mixture critical pressure
- c) solvents of low volatility

## CHAPTER IV

## EXPERIMENTAL APPARATUS

Many experimental apparatus and operating procedures have been used to study vapor-liquid equilibrium. In most cases investigators use variations of one of the three following methods:

- a) phase compositions are measured as a function of pressure at a constant temperature,
- b) phase compositions are measured as a function of temperature at constant pressure, or
- c) the pressures and/or temperatures where condensation or boiling occurs are measured at constant composition.

Experimental apparatus which encompass each of the above mentioned methods are currently in use (21, 22, 23). Of special interest to this study are those investigators who developed their apparatus to incorporate the bubble-point approach (method c above) to vapor-liquid equilibrium data acquisition. Sage et al. (23) developed such an apparatus, and the method employed in this study is similar to theirs with added design details for handling solvents which are solid at room temperature and a new method of agitating the binary mixture. Tiffin et al. (24) have also developed a similar apparatus; however they use a method other than the bubble-point approach to acquire data.

The bubble-point approach to VLE data acquisition was chosen for this study for several reasons. The bubble-point method is simple and precise and does not require use of analytical instruments (such as chromatographs) for phase analysis. It is efficient and produces data which are quite adequate for present purposes and very reliable. Details of the bubble-point method and the apparatus used in this study are discussed in the following sections. Because the apparatus and procedure were the same as those used for the acquisition of Mr. J. McRay Anderson's (25) data, the following sections are identical in both theses.

#### General Description

The apparatus used in this study was designed for measurement of isothermal bubble-point pressures of liquid mixtures. Of particular interest were measurements on solute gases in solvent liquids which would solidify at room temperature. The apparatus was originally designed and operated by Gasem (6), but it was extensively redesigned and reconstructed for the present study. The modifications increased the rate of data collection and eliminated effects of room temperature fluctuations on the measured pressures. A schematic diagram of the apparatus is shown in Figure 1 and a description is given below.

The operation of the apparatus, to measure bubble-point pressures of binary mixtures, involves combining known amounts of solute gas and solvent liquid in an equilibrium cell. The mixture, maintained at constant temperature, is stirred and compressed so that the solute gas is forced into solution in the solvent. The bubble-point pressure for the given mixture is taken as the pressure at which the vapor phase



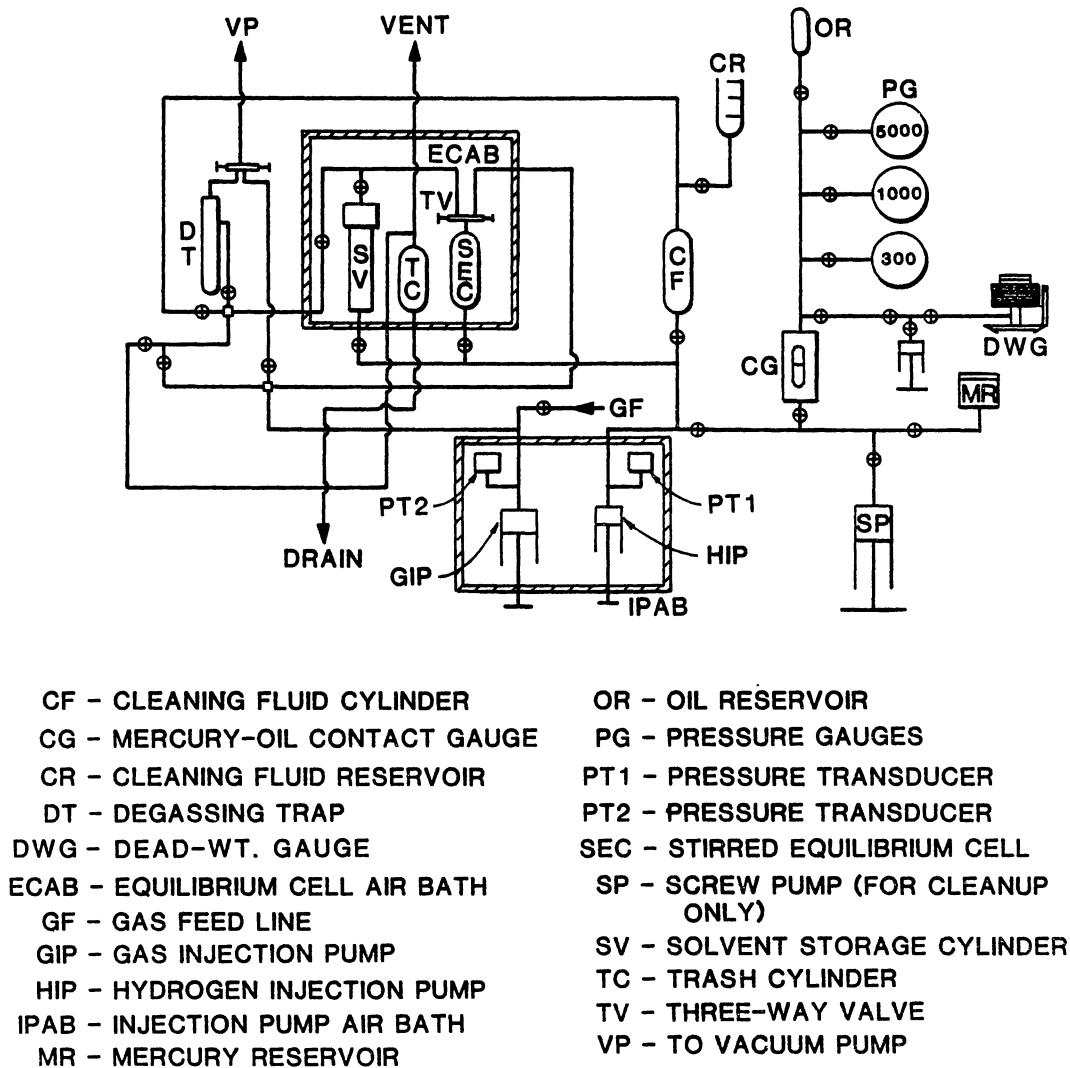


Figure 1. Schematic Diagram of the Isothermal Bubble-Point Apparatus

disappears. A general description of the arrangement of the apparatus follows.

The bubble-point apparatus is supported on two adjacent tables (see Figure 2). The larger table holds the equilibrium cell air bath (ECAB, abbreviations refer to nomenclature of Figures 1 and 3) and the control panel, with the equilibrium cell air bath temperature controller on a lower shelf. Upon the smaller table is the injection pump air bath (IPAB). A lower shelf was built into the smaller table to house the cleaning pump (CP) and the injection pump air bath temperature controller.

The control panel supports much of the apparatus, including the valves, tubing, magnet drive motor controller, pressure gauges, and digital pressure and temperature indicators. The degassing trap (DT), cleaning fluid storage cell (CF), and cleaning fluid reservoir (CFR) are also mounted on the control panel.

### Equilibrium Cell

The central component of the apparatus is a variable volume stirred equilibrium cell. This equilibrium cell is a 304 stainless steel tubular reactor (High Pressure Equipment Company Incorporated, catalog number TOC-6), modified to become the stirred equilibrium cell (SEC) shown in Figure 3.

The first modification of the reactor was to machine the top 2.25 inches of the reactor from an outside diameter of 1.50 inches to 1 inch. This was done to increase the magnetic coupling between the drive magnets (DM) and stirrer magnets (SM). Next, the bottom port of the top plug was tapped to allow attachment of a stirrer support pin (SSP).

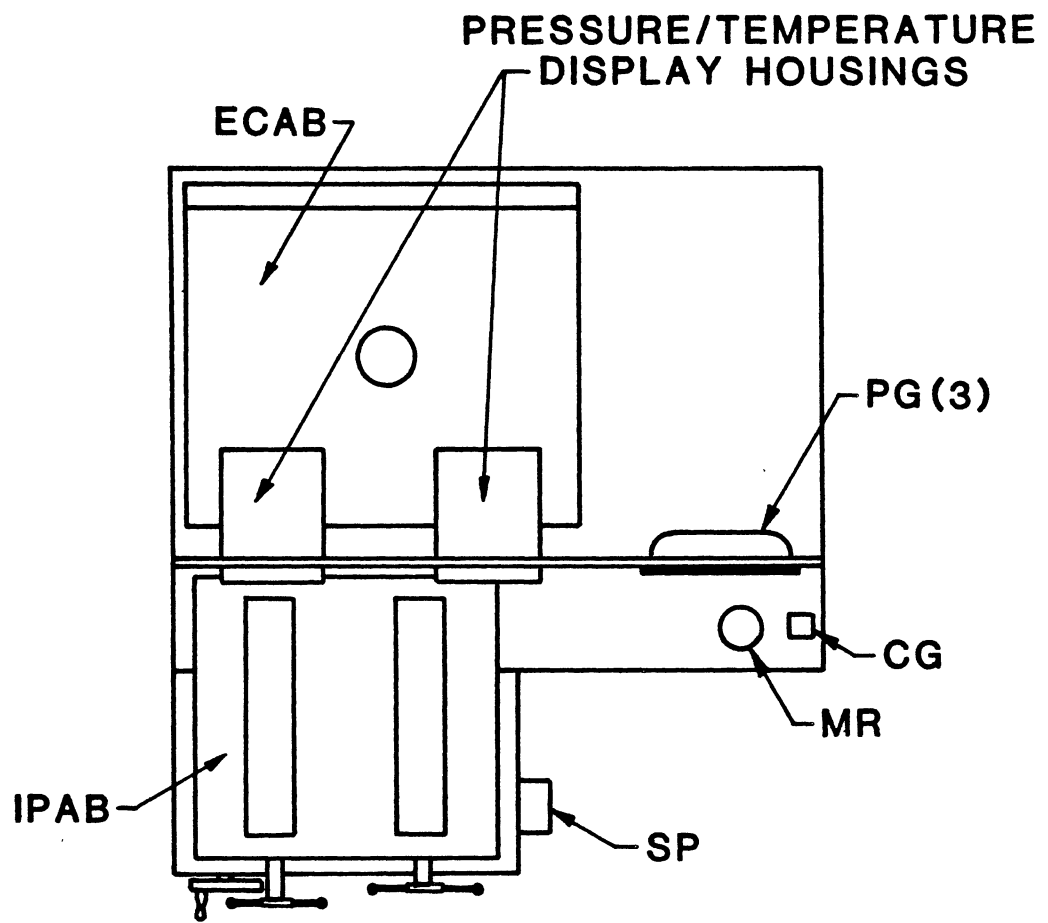
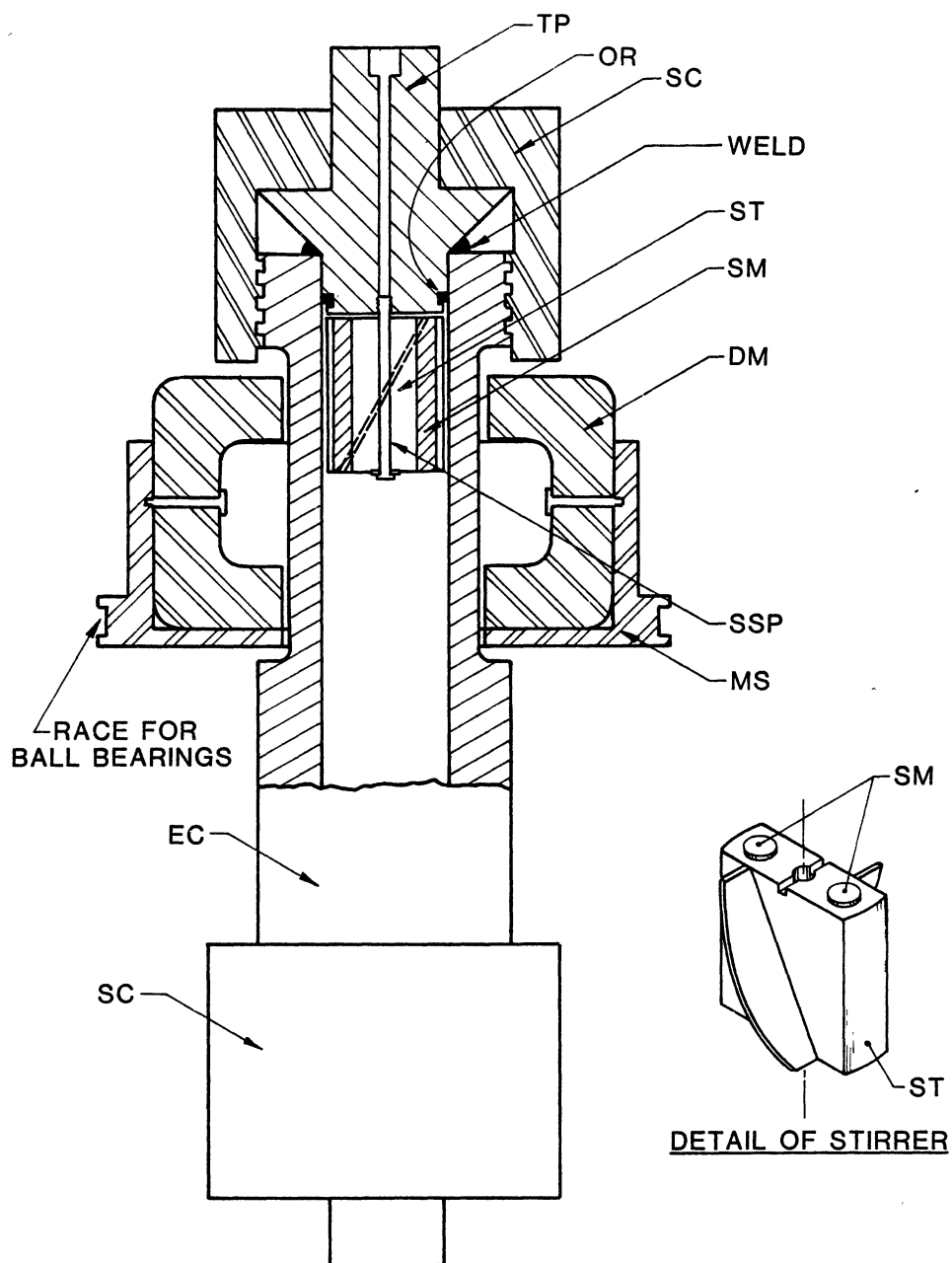


Figure 2. Overhead View of the Bubble-Point Apparatus



- DM - DRIVE MAGNETS  
 EC - EQUILIBRIUM CELL (CYLINDRICAL)  
 MS - ROTATING MAGNET SUPPORT  
 OR - O RING  
 SC - SCREW CAP  
 SM - STIRRER MAGNETS  
 SSP - STIRRER SUPPORT PIN  
 ST - STIRRER  
 TP - TOP PLUG

Figure 3. Stirred Equilibrium Cell

After modification of the cell, a persistent high pressure leak from the "O" ring seal on the top plug (TP) was discovered. To eliminate this leak, the top plug was beveled downward (to avoid trapping chemicals) and welded to the body of the equilibrium cell.

The stirrer, machined from cylindrical aluminum stock, is 1" long and has a rectangular body with an impeller blade on each side (see detail, Figure 3). Two cylindrical stirrer magnets were mounted in the stirrer symmetrically about and parallel to the stirrer vertical exit. The stirrer is attached to the base of the top plug by the stirrer support pin (SSP).

A flow channel for introduction or removal of chemicals from the top of the equilibrium cell was made by drilling a hole down the center of the stirrer support pin for the length of its threads. A second hole was then drilled horizontally across the threads, intersecting the first hole (see Figure 4). The threads were then filed flat on planes perpendicular to the horizontal hole. In addition, the stirrer was slotted across the top. Acting together, these modifications allowed easy chemical access to the inside of the equilibrium cell for injecting or cleaning purposes.

The equilibrium cell has an internal volume of approximately 37 cc. The effective volume of the cell can be varied by introduction or withdrawal of mercury (which acts as a fluid piston) through the bottom of the cell. Chemical injections to the cell were made at the top of the cell through a short section of small diameter stainless steel tubing connected to a stainless steel three way valve (High Pressure Equipment Company Incorporated, catalog number 15-15 AF1). Separate

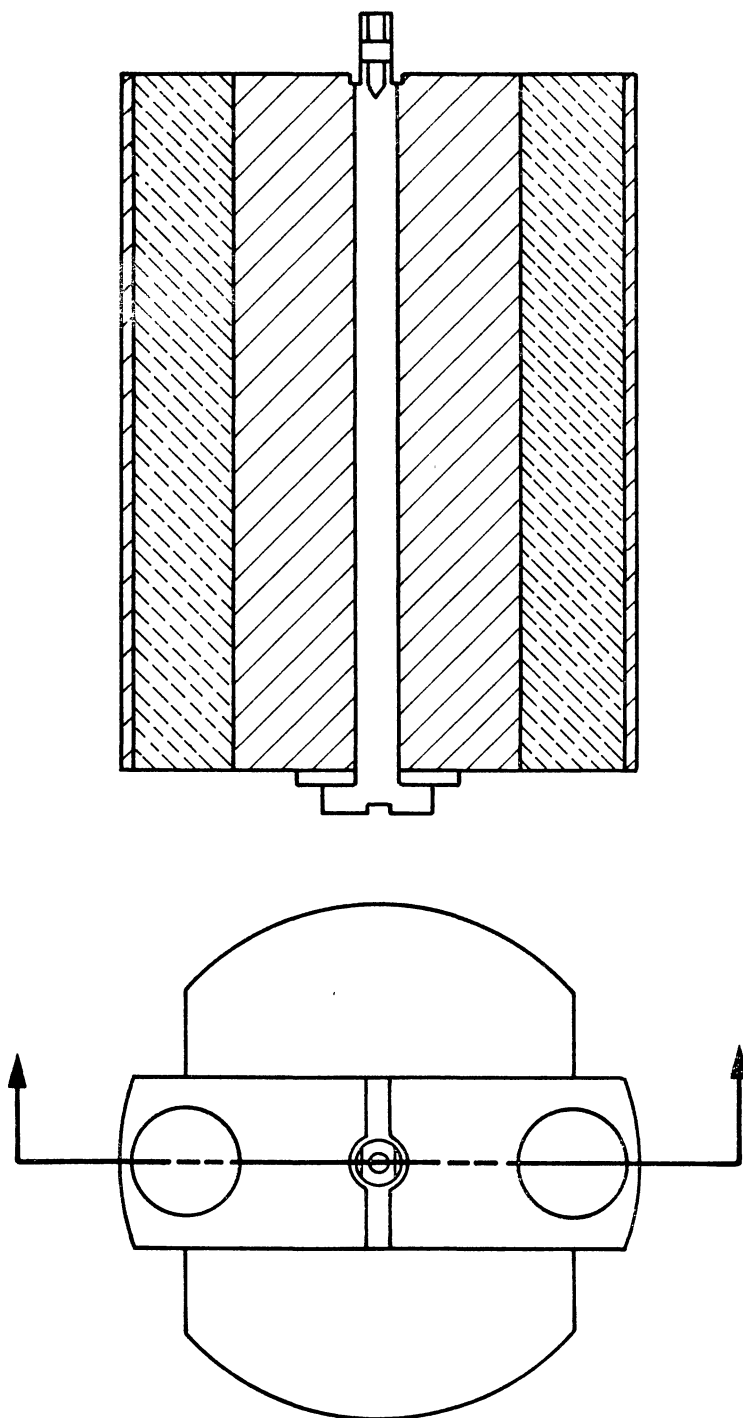


Figure 4. Section View of Stirrer

inlet lines for the solute gas and solvent liquid were connected to this valve, which controlled chemical access to the cell.

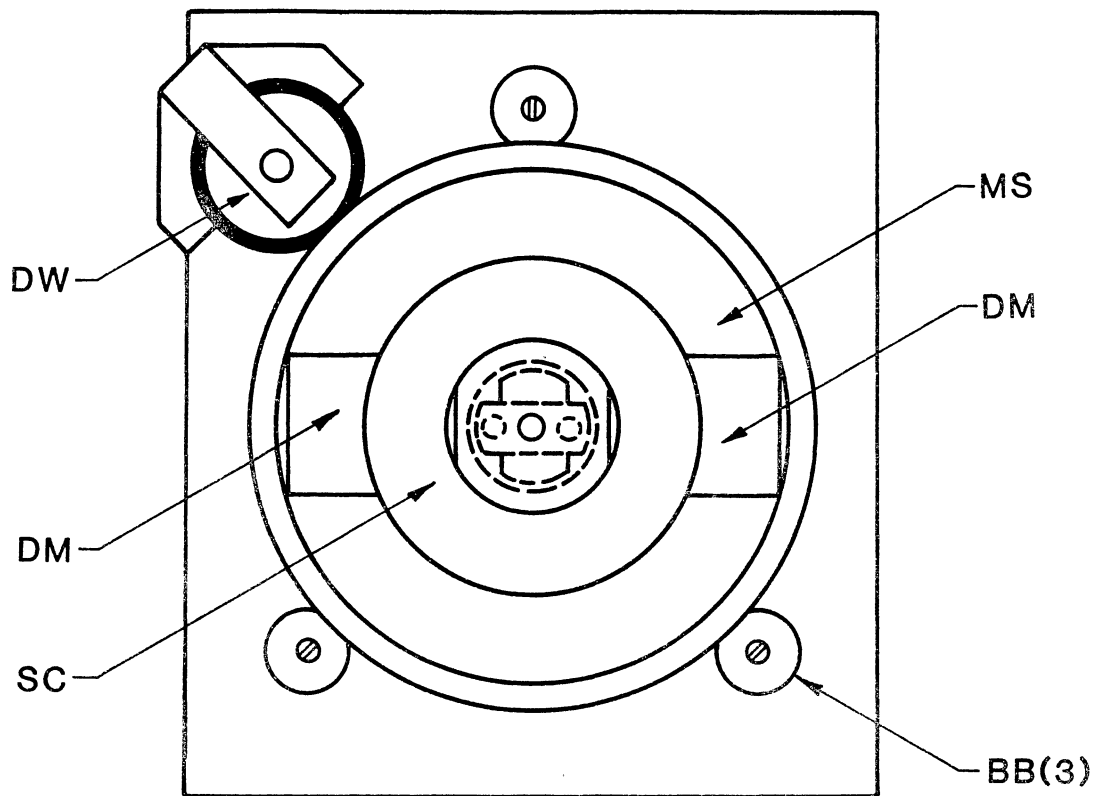
### Rotating Magnet Assembly

A rotating magnet assembly was used to drive the stirrer within the equilibrium cell. Figure 5 shows a top view of this assembly.

Three ball bearings (BB) (Fafnir, catalog number S5KDD) held the rotating magnet support (MS) in place while allowing it to spin freely. The rotating magnet support is doughnut shaped and was fabricated in two sections so it can be opened to allow removal of the equilibrium cell from the air bath. The two drive magnets (DM) are bolted, opposite each other, to the walls of the rotating magnet support. A 1/50 horsepower variable speed motor (Bodine Electric Company, model series 200, type NSH-12) is used to power the drive wheel (DW), which contacts the edge of the rotating magnet support. The motor is mounted on top of the equilibrium cell air bath and is connected to the drive wheel by a variable-length drive shaft. A motor speed controller (Bodine Electric Company, model 901, type BSH-200) was used to maintain the rotating magnet support speed of 124 revolutions per minute.

### Storage Vessels

Several cylinders were employed for either injection or storage purposes (see Figure 1). The solvent storage cylinder (SV) is a high-pressure reactor bomb with a screw type closure (High Pressure Equipment Company Incorporated, catalog number OC-3). It is housed inside the equilibrium cell air bath so that heavy solvents (solids at room



BB - BALL BEARINGS  
DM - DRIVE MAGNETS  
DW - DRIVE WHEEL  
MS - ROTATING MAGNET SUPPORT  
SC - SCREW CAP

Figure 5. Rotating Magnet Assembly



temperature but liquids at operating temperature) can be melted and degassed prior to their use. The solute gas is stored in a 25 cc gas injection pump (GIP). The injection pump (Temco Incorporated, model 25-1-10-HAT), kept at constant temperature within the injection pump air bath, facilitates direct injection of the solute gas to the equilibrium cell.

The cleaning fluid cylinder (CF), a 250 cc high pressure stainless steel cylinder, is used to store cleaning fluid for injection to the equilibrium cell or solvent storage cylinder during clean up before or after experimental runs. A 150 cc glass buret was used as a reservoir (CR) for charging cleaning fluid to the cleaning fluid storage cylinder. Solvent and cleaning fluid could be displaced from the solvent storage cylinder or cleaning fluid storage cylinder, respectively, by injecting a volume of mercury into the bottom of these cylinders, which displaces an equal volume of their contents.

The trash cylinder (TC), a 250 cc stainless steel cylinder, is housed within the equilibrium cell air bath and used to receive liquids being expelled from the apparatus during clean up.

A 250 cc mercury reservoir (MR) was used to maintain an adequate volume of mercury within the system.

#### Pressure Measurements

Equilibrium cell, solvent injection, and solute injection pressures were measured with pressure transducers (Sensotec Incorporated, model STJE 1890) with a range of 0-3000 psi. These pressure transducers were kept at constant temperature in the injection pump air bath. Pressures

are displayed on digital readouts (Sensotec Incorporated, model 450D) with a resolution of 0.1 psi.

Pressures within the equilibrium cell, solvent storage cylinder, and cleaning fluid cylinder are transmitted directly to the solvent transducer (PT1) through mercury-filled lines. The pressure of the solute gas is measured directly by the solute transducer (PT2). At the beginning of the study of each binary mixture, the hydrocarbon pressure transducer was calibrated against a dead weight tester (Ruska Instrument Corporation, model number 2400.1).

#### Volumetric Injection Pumps

Three precision positive displacement pumps were used to operate the apparatus. A 10 cc pump (Temco Incorporated, model 10-1-12 H) was used for injecting solvent and for varying the effective volume of the equilibrium cell during data collection. This pump has a pressure rating of 10,000 psi and a resolution of 0.005 cc. Solute injections were made with a 25 cc pump (Temco Incorporated, model 25-1-10-HAT) which has a pressure rating of 10,000 psi and a resolution of 0.005 cc. Both pumps were maintained at constant temperature in the injection pump air bath.

To clean the apparatus, a 500 cc pump (Ruska Instrument Corporation, model 2210-801) was used. This pump is rated at 12,000 psi and has a resolution of 0.02 cc.

#### Constant Temperature Baths

Two air baths were used to maintain constant temperatures for components of the apparatus used for injection and pressure measuring

purposes. The equilibrium cell air bath (ECAB) (Hotpack, model 200001) houses the equilibrium cell, solvent storage cylinder, and trash cylinder. Temperature of this oven is maintained within  $0.1^{\circ}\text{C}$  by a Halikainen proportional-integral controller, model 1053 A, which was used to replace the original temperature control system on the air bath.

The injection pumps and pressure transducers are housed in the injection pump air bath. This air bath was fabricated from  $1/2$ " plywood and lined with fiberglass insulation. A Halikainen proportional-integral controller, model 1053 A, is also used to maintain the temperature in this air bath within  $0.1^{\circ}\text{C}$  of the setpoint, which was  $50.0^{\circ}\text{C}$  throughout this study.

The temperatures of both air baths are measured with precisions of  $0.1^{\circ}\text{C}$  using separate platinum resistance thermometers connected to identical digital readouts (Fluke Incorporated, model 2180 A) which have a resolution of  $0.01^{\circ}\text{C}$ . Periodic ice point measurements confirmed the claimed accuracy of  $0.1^{\circ}\text{C}$ .

#### Degassing Trap

Prior to bubble-point measurements, the solvent liquid must be degassed to remove air or any volatile contaminants in the solvent storage cylinder.

The degassing trap is a 100 cc, 1" diameter glass tube with a ground glass connection and a glass top which accommodates inlet and outlet lines (see Figure 6). To degass the solvent, the solvent storage cylinder is evacuated. If any of the solvent vaporizes during degassing, it is carried along and condensed at the bottom of the

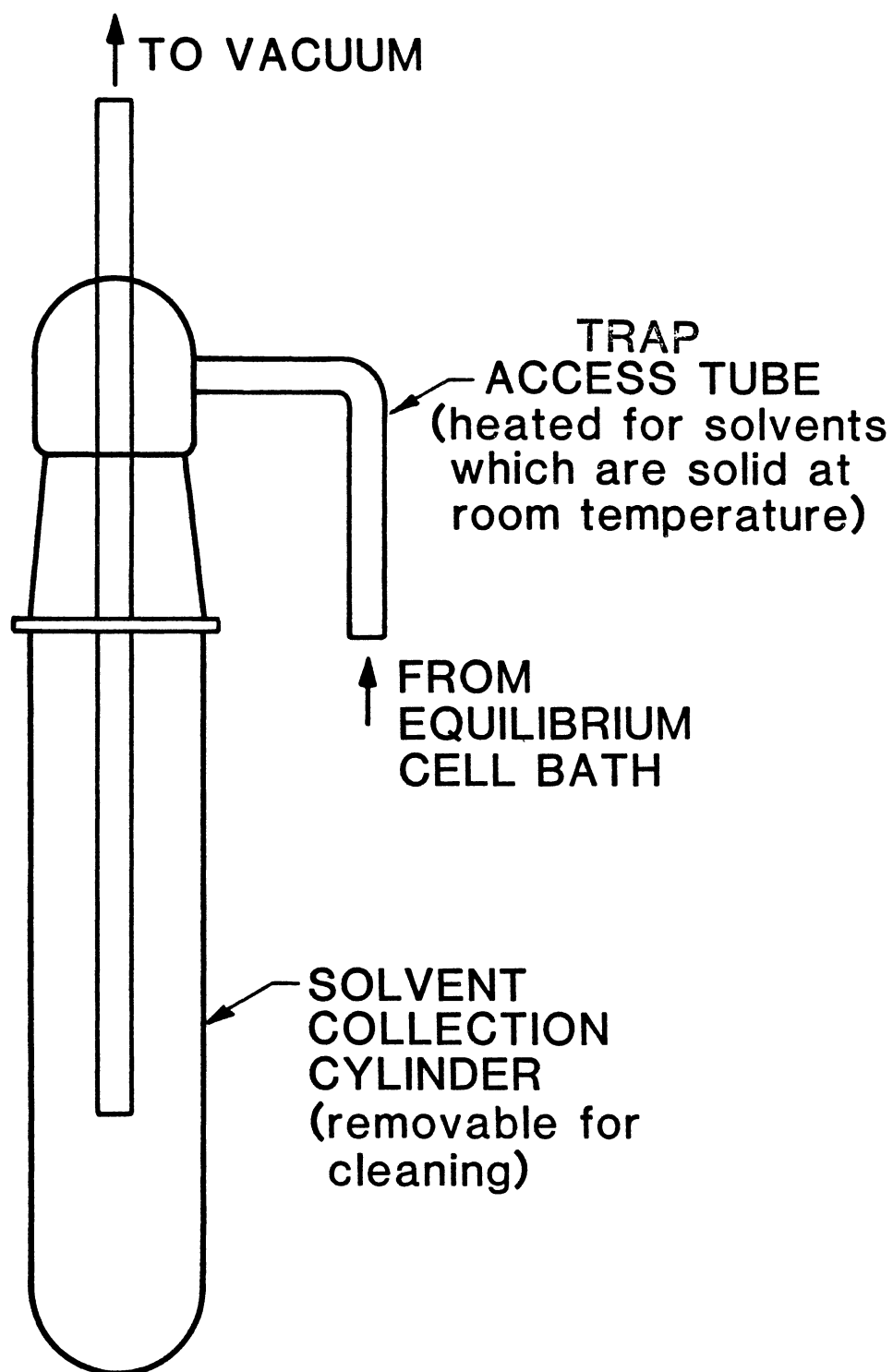


Figure 6. Degassing Trap

degassing trap, ahead of the vacuum pump. Once degassing of the solvent has been completed, the bottom tube of the trap is removed and emptied.

The lines between the solvent storage cylinder and degassing trap were wrapped with heating tape to prevent solvent solidification in the lines. A variac was used to control the temperature of the heating tapes.

#### Fittings, Tubing, and Valves

All fittings, tubing, and valves (High Pressure Equipment Company) used in construction of this apparatus were made of 316 stainless steel and rated at 15,000 psi. One-sixteenth inch tubing and valves were used for pressure measurement lines to minimize dead volumes where necessary. One-eighth inch tubing and valves were used throughout the rest of the apparatus.

#### Chemicals

All materials used in this study were obtained from commercial suppliers and no further purification was attempted. The suppliers and stated purities of the chemical are given in Table II.

TABLE II

## Chemical and Their Purities

| Chemicals      | Source                    | Stated Purity<br>(mol %) |
|----------------|---------------------------|--------------------------|
| Carbon Dioxide | Union Carbide Company     | 99.99                    |
| n-Pentane      | Fisher Scientific Company | Spectro Grade            |
| Benzene        | Aldrich Chemical Company  | Reagent Grade            |
| Naphthalene    | Aldrich Chemical Company  | 99+                      |
| Phenanthrene   | Aldrich Chemical Company  | 99+                      |
| Pyrene         | Aldrich Chemical Company  | 99+                      |

## CHAPTER V

### EXPERIMENTAL PROCEDURE

This chapter contains a step-by-step procedure for properly measuring solubilities using the apparatus described in the previous section. Two steps in the operation of the apparatus are extremely critical in obtaining accurate data: injection of the solvent/solute and measurement of the pressure which determines the solubility (bubble-point pressure). Special care must be taken during the injections to assure accurate measurement of the amount of each component injected into the equilibrium cell so that the composition of the mixture in the cell will be evaluated correctly. Caution and patience must also be exercised when measuring the bubble-point pressure; some mixtures require up to two hours to reach a stable pressure after they have been disturbed. Methods are suggested herein for detecting if an isotherm of data is possibly in error. These simple yet reliable methods are included as a check against errors made in either of the two critical steps mentioned above.

Throughout this chapter, the terms solubility and bubble-point pressure are used interchangeably. Because different terminologies exist in thermodynamic literature, the terms solubility and bubble point are both used to describe a single phase binary mixture at the point where the gas phase has just dissolved totally into the liquid phase. Thus, the data taken in this work may be viewed as the solubility of the

gas (mole fraction) in the liquid at given temperature and pressure or as the bubble-point pressure of the mixture at given temperature and composition.

### Cleaning The Storage Cell

Before the solvent storage vessel (SV, Figure 1) can be used to store a hydrocarbon solvent, it must be properly cleaned of the previous contents so that the new solvent is not contaminated. The cleaning procedure is as follows:

1. If the storage vessel contains solvents which are solid at room temperature, turn on the heating tape and allow the disposal lines outside the equilibrium cell air bath (ECAB) to come to a temperature above the melting point of the solvent. Open valves V1, V6, V10, and OV1 (for location of all valve abbreviations, refer to Figure 7). Using the cleaning pump (CP), purge any solvent from the solvent storage vessel by pumping mercury into the bottom of the storage vessel until mercury can be seen in the sight tube (ST) located just down-line from the trash cylinder (TC). The sight tube is viewed through a window in the equilibrium cell air bath so that the bath can remain closed and at constant temperature during cleanup.

2. Open V2 and purge the sight tube with solute gas (typically the solute gas is kept at approximately 200 psia for purge purposes). Close V1 and V2 once the mercury and solvent in the sight tube have been blown into the trash cylinder. If the solute gas does not displace the mercury and solvent from the sight tube, a plug may have formed somewhere in the trash lines. Heat any exposed trash lines directly with a heat gun until the solute gas has cleared the plug from the lines



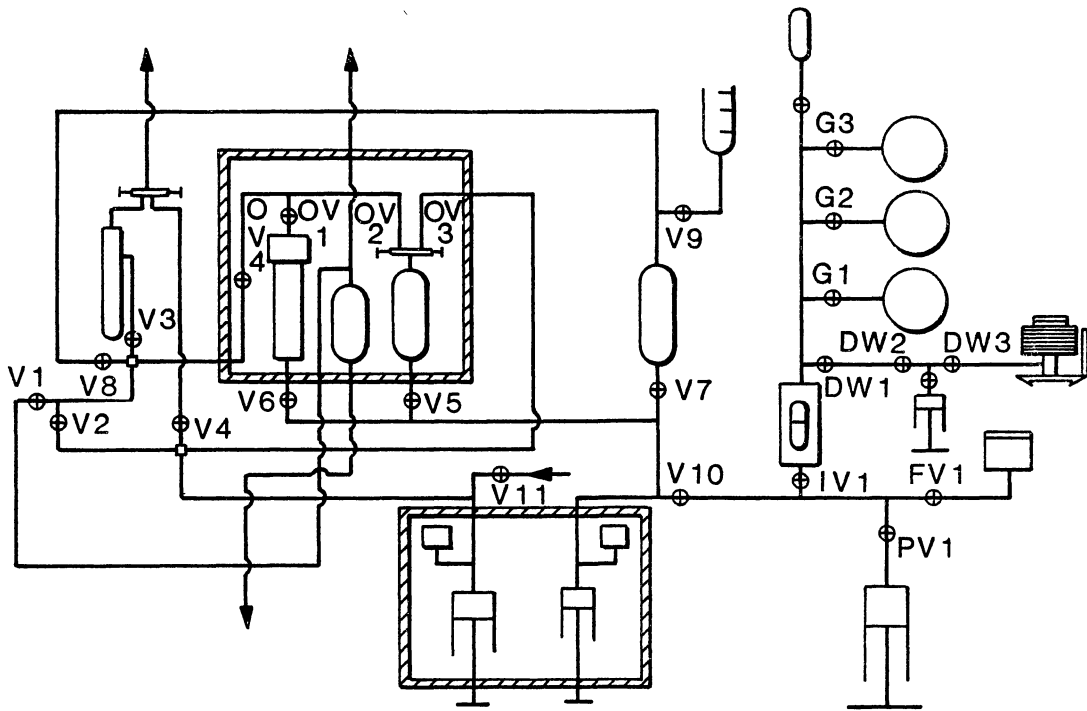


Figure 7. Schematic Diagram of the Apparatus with Valve Identification

and purged the sight tube of any mercury or solvent left from the storage vessel.

3. Withdraw mercury from the bottom of the solvent storage vessel to create a 70 to 80 cc space in the storage vessel. By opening V2, a pressure head may be established above the mercury in the storage vessel to aid in the removal of mercury from the cell. Solute gas used for a pressure head must be vented through V1 after the mercury has been removed from the vessel.

4. Close V1 and V6, open V7 and V9, and inject mercury into the cleaning fluid storage cylinder (CF) using the cleaning pump until mercury can be seen in the bottom of the cleaning fluid reservoir (CR). Fill the reservoir with approximately 100 cc of cleaning fluid (normally n-pentane or benzene) by pouring the fluid into the opening at the top of the reservoir. Draw the cleaning fluid into the cleaning fluid storage cylinder by withdrawing 80 to 90 cc of mercury back into the cleaning pump, then close V9.

5. Pressurize the cleaning fluid to assure it is totally liquid by pumping mercury from the cleaning pump into the cleaning fluid storage cylinder until a pressure reading higher than the vapor pressure of the cleaning fluid is indicated on the hydrocarbon transducer readout. Open V8 and inject cleaning fluid into the storage vessel by use of the cleaning pump. Continue until the storage cell is full of cleaning fluid. Close V7 and V8, open V6 and increase the pressure in the storage vessel to a level which assures that the cleaning fluid in the vessel is all liquid. Allow the cleaning fluid to remain in the solvent storage vessel for a period of time (15 to 20 minutes) so that any

remaining solvent in the storage vessel will dissolve in the cleaning fluid.

6. Repeat steps 1 through 5 twice to clean the cell a total of three times. After the charge of cleaning fluid has been removed following steps 1 and 2 and 80 to 90 cc of space have been left in the storage vessel as explained in step 3, remove any residual cleaning fluid vapors from the vessel by turning on the vacuum pump, allowing it to create a sufficient vacuum, and then opening valves VV1, V3, and OV1.

A sufficient vacuum is indicated when the vacuum gauge reads 500 millitorr or less. A "perfect" vacuum would register zero millitorr on the vacuum gauge; however, the current vacuum system is capable of producing a vacuum of only 200 millitorr under the best possible circumstances (ie. clean trash trap, tight seals on all connections, clean oil in vacuum pump, vacuum pump working properly). During most evacuations of the storage vessel the vacuum gauge registers 500 millitorr. This measure of vacuum has proved sufficient in all cleanings of the storage vessel; however, allowing the vacuum to register above 500 millitorr should be avoided because this will not assure proper evacuation of the storage vessel.

Because the hydrocarbon transducer was set at 0.0 psia under vacuum conditions, the pressure reading from the hydrocarbon transducer should fall immediately and approach 0.0 psia after OV1 has been opened. The transducer will indicate a small pressure reading (2.0 to 3.0 psia) as long as vapors from the cleaning fluid remain in the storage vessel; however, the pressure reading should fall slowly to 0.0 psia as the cleaning fluid vapors are evacuated from the storage cell. If the pressure in the storage vessel does not fall immediately after OV1 has

been opened, a plug has formed somewhere in the vacuum lines. To remedy this problem apply direct heat with the heat gun to any exposed areas of the lines until the pressure falls as expected.

### Cleaning the Equilibrium Cell

To measure correct solubilities, the equilibrium cell must be properly cleansed of any foreign material prior to beginning a run. The following procedure will create a clean cell ready for injection of solute and solvent.

1. If the solvent being removed from the equilibrium cell is solid at room temperature, turn on the heating tape and allow it to come to temperature above the melting point of the solvent. Close valve OV1, V3, VV1, and V6 and open valves V1, V5, and OV2. Using the cleaning pump, displace any mixture from a previous experiment out of the equilibrium cell (SEC) by injecting mercury into the bottom of the equilibrium cell until mercury can be seen in the sight tube.

2. Open V2 and purge the sight tube with solute gas (watch for plugs and remove as described earlier). Close V1 and V2 after the sight tube is clear.

3. Remove mercury from the cell to create a 20 cc space in the equilibrium cell. By opening V2, solute gas pressure may be established above the mercury in the equilibrium cell to aid in removal of mercury from the cell. This solute gas must be vented through V1 after the mercury has been removed from the cell.

4. Close V1 and V5, open V7 and V9, and inject mercury into the cleaning fluid storage cylinder (using the cleaning pump) until mercury can be seen in the bottom of the cleaning fluid reservoir. Fill the

cleaning fluid reservoir with 70 to 80 cc of cleaning fluid. Draw cleaning fluid into the storage cylinder by withdrawing 70 to 80 cc of mercury back into the cleaning pump then close V9 and V7.

5. Open V7 and pressurize the cleaning fluid to assure it is completely liquid. Open V8 and inject cleaning fluid into the equilibrium cell by use of the cleaning pump. Continue until the equilibrium cell is full of cleaning fluid. Close V7, V8, and OV2, open V5 and pressurize the equilibrium cell to a level which assures that the cleaning fluid remains liquid in the cell. Turn on the stirrer to assist the cleaning fluid in dissolving any remaining solvent. Allow the cleaning fluid to remain in the equilibrium cell for 10 to 15 minutes before removing it.

6. Repeat steps one through five twice omitting step four each time. Step four is omitted the second and third time because enough cleaning fluid has been placed in the cleaning fluid storage cylinder initially to complete all three subsequent cleaning fluid injections. After the third charge of cleaning fluid has been removed and a 20 cc space created in the equilibrium cell, switch on the vacuum pump. Open VV1 and V3 after the vacuum gauge indicates the vacuum pump is creating a sufficient vacuum (as explained in step six of solvent storage vessel cleaning procedure). Open OV2 and allow the equilibrium cell to be evacuated for six to seven hours to assure all cleaning fluid vapors and foreign matter are evacuated from the cell. The hydrocarbon pressure transducer reading should fall immediately after OV2 is opened; approaching zero as the cleaning fluid vapors are removed from the equilibrium cell.

### Charging and Degassing the Solvent

1. After being properly cleaned and evacuated, the solvent storage vessel is ready to be charged with solvent. To charge the storage vessel, unscrew the cap from the top of the vessel and carefully remove the plug by pulling straight up (to avoid scratching the sealing surface of the storage vessel). Examine the empty storage vessel by holding a mirror over the top opening of the vessel and adjusting the mirror so that the inside of the vessel can be viewed. If the vessel walls and mercury in the vessel both appear clean, fill the vessel with hydrocarbon solvent. Should residue be observed on the vessel walls or on the mercury at the bottom of the vessel, then the vessel should be swabbed with a soft cloth or rag dipped in cleaning fluid, always being careful not to scratch the sealing surface of the storage vessel. Solid hydrocarbons should be tightly packed into the solvent storage vessel so that a maximum amount of hydrocarbon can be placed in the cell (a space of 20 to 30 cc must be left above the hydrocarbon solvent in the storage vessel to allow room for replacement of the plug). To complete the charging procedure carefully replace the plug and screw down the cap of the storage vessel.

2. After properly charging the storage vessel, turn on the vacuum pump and allow it to create a sufficient vacuum. If a solid hydrocarbon has been placed in the storage vessel, the heating tape must be turned on to supply heat to all of the exposed lines used in degassing, thus preventing a solid plug of solvent from forming in these lines. Before proceeding, the heating system should run for fifteen minutes to allow the lines to reach a temperature above the melting point of the solvent.

3. Open VV1, V3, and OV1 to allow any dissolved air to be removed from the solvent in the storage vessel. The transducer reading should fall immediately after OV1 has been opened, approaching zero as air is removed from the storage vessel. If the pressure in the vessel does not drop, a plug has probably formed in the degassing lines and must be removed by direct heating from the heat gun.

4. Allow the hydrocarbon solvent to degas for approximately four hours while checking periodically for traces of solvent in the degassing trap (DT). Any solvent collected in the degassing trap can not be used for injection, so it is important to keep the amount of solvent lost to the degassing trap to a minimum. Volatile hydrocarbon solvents must be watched closely because they evaporate readily under vacuum and much of the solvent can be lost to the degassing trap. When valve OV1 is opened, air is pulled into the degassing trap, normally carrying traces of solvent with it as it bubbles up the trap access tube (Figure 6) into the trap. As more air is evacuated from the storage vessel, the bubbling is reduced and eventually subsides (normally after approximately four hours; less time for volatile solvents). When the solvent can not be seen bubbling up the trap access tube, the degassing is complete. Close OV1, V3, and VV1 to isolate the solvent from the vacuum lines and turn off the vacuum pump. Pump mercury from the cleaning pump into the storage vessel to move solvent into the evacuated space left in the storage vessel and injection lines after degassing. Vent the pump by breaking the connections from the pump to the light condensable trap located in the hood.

## Injecting the Solvent

So that a complete record of the injection can be kept for future reference, an injection sheet (Figure 8) is used to record all necessary information. The sheet is prepared by recording the date and the name, density, and molecular weight of the solvent in their designated places. Once the sheet is prepared, the solvent is injected as described below.

1. When the desired temperatures have been set and both air baths allowed to come to temperature (normally requiring four to five hours for all metal parts in the ovens to reach thermal equilibrium), record the temperatures on the injection sheet, then open V5 and OV1. After the evacuated lines leading to the equilibrium cell from the storage vessel have been completely filled with solvent, compress the solvent to a level above the solvent vapor pressure. Once the solvent has been compressed, close V10 and monitor the pressure in the storage vessel until it becomes constant. In practice, approximately one hour is required to reach a constant pressure in the storage vessel.

2. When the storage vessel pressure becomes constant, record the pressure reading on the injection sheet. Note the initial volume reading on the hydrocarbon injection pump (HIP) and record this value on the sheet also. After recording the volume, open OV2 and advance the injection pump until approximately 7cc (for CO<sub>2</sub> solubility studies) of solvent have been injected into the equilibrium cell. To finish the injection, close OV2 and adjust the hydrocarbon injection pump until the pressure in the storage vessel returns to the original value recorded before OV2 was opened. After reestablishing the original pressure reading, record the final volume reading from the injection pump.



## INJECTION SHEET

Date: \_\_\_\_\_

SOLVENT INJECTION

Solvent Name: \_\_\_\_\_

Time<sub>i</sub>: \_\_\_\_\_P<sub>i</sub>: \_\_\_\_\_Temp Pump  
Bath : \_\_\_\_\_x<sub>i</sub>: \_\_\_\_\_Temp Cell  
Bath : \_\_\_\_\_x<sub>f</sub>: \_\_\_\_\_Time<sub>f</sub>: \_\_\_\_\_P<sub>f</sub>: \_\_\_\_\_ $\Delta V = ( \text{_____} ) ( \text{_____} ) = \text{_____}$ Solvent  $\rho = \text{_____}$  M. Wt. = \_\_\_\_\_  
( ) $\Delta n$  solvent = \_\_\_\_\_

n solvent = \_\_\_\_\_

SOLUTE INJECTION

Solute Name: \_\_\_\_\_

Time<sub>i</sub>: \_\_\_\_\_P<sub>i</sub>: \_\_\_\_\_Temp Pump  
Bath : \_\_\_\_\_x<sub>i</sub>: \_\_\_\_\_Temp  
Room : \_\_\_\_\_x<sub>f</sub>: \_\_\_\_\_Time<sub>f</sub>: \_\_\_\_\_P<sub>f</sub>: \_\_\_\_\_ $\Delta V$ : \_\_\_\_\_Solute  $\rho = \text{_____}$  M. Wt. = \_\_\_\_\_  
( ) $\Delta n$  solute = \_\_\_\_\_ n total: \_\_\_\_\_

n solute = \_\_\_\_\_ x solute: \_\_\_\_\_

OBSERVATIONS: \_\_\_\_\_

Figure 8. Injection Sheet

3. By subtracting the initial volume reading from the final volume reading of the injection pump, the volume of mercury injected is calculated. This value must be adjusted slightly to determine the amount of solvent injected to the equilibrium cell since the mercury density changes as it moves from one air bath temperature to the other. The adjustment factor is calculated by dividing the density of mercury at the temperature of the cell bath (ECAB) into the density of mercury at the temperature of the pump bath (IPB). The moles of solvent injected are then calculated from the following equation:

$$n_{\text{HC}} = \left[ \rho_{\text{HC}} (V_2 - V_1) \frac{\rho_{\text{Hg}} (T_{\text{pb}})}{\rho_{\text{Hg}} (T_{\text{cb}})} \right] / \text{MW}_{\text{HC}} \quad (5.1)$$

4. After calculating the moles of solvent injected, close V6, open V10, and return the injection pump to the original volume read before the injection. As the injection pump is drawn back, fill the void left in the injection pump with mercury from the cleaning pump. When the injection pump has been returned to its original position, open V5 to monitor the pressure in the equilibrium cell. The pressure in the equilibrium cell should be equal to the vapor pressure of the injected solvent. If the vapor pressure of the injected solvent is less than atmospheric pressure, more mercury should be injected into the equilibrium cell until the pressure in the cell is above atmospheric pressure so that no air can enter the equilibrium cell from a possible leak under vacuum.

### Injecting the Solute Gas

1. Once the amount of solvent injected into the equilibrium cell has been calculated, a desired mole fraction of solute is chosen at which to measure the first mixture bubble-point pressure. The mole fraction chosen depends on the nature of the solvent and the desired range of solubilities to be measured. Using the chosen mole fraction and the moles of solvent injected, an estimate of the moles of solute gas to be injected is calculated from the following equation:

$$n_{SG} = \frac{n_{HC} x_{SGi}}{(1 - x_{SGi})}. \quad (5.2)$$

2. Set the solute gas injection pump (GIP) initial reading to zero and allow the pressure in the injection pump to stabilize at some pressure between 600 and 900 psia. This pressure range is chosen because the solute gas densities used in this work are relatively insensitive to T, P variations within this range as shown in Figure 9. Appendix A explains how Figure 9 was developed. Record this pressure on the injection sheet. At the recorded pressure and temperature of the pump bath, calculate the solute gas density. A program was developed for calculating density of carbon dioxide as a function of temperature and pressure (Appendix B) using equations published by IUPAC (26). This program provides an accurate and efficient means of calculating CO<sub>2</sub> gas phase densities.

3. Record the solute gas density on the injection sheet and use the following equation to calculate an estimate of the volume of solute gas to be injected.

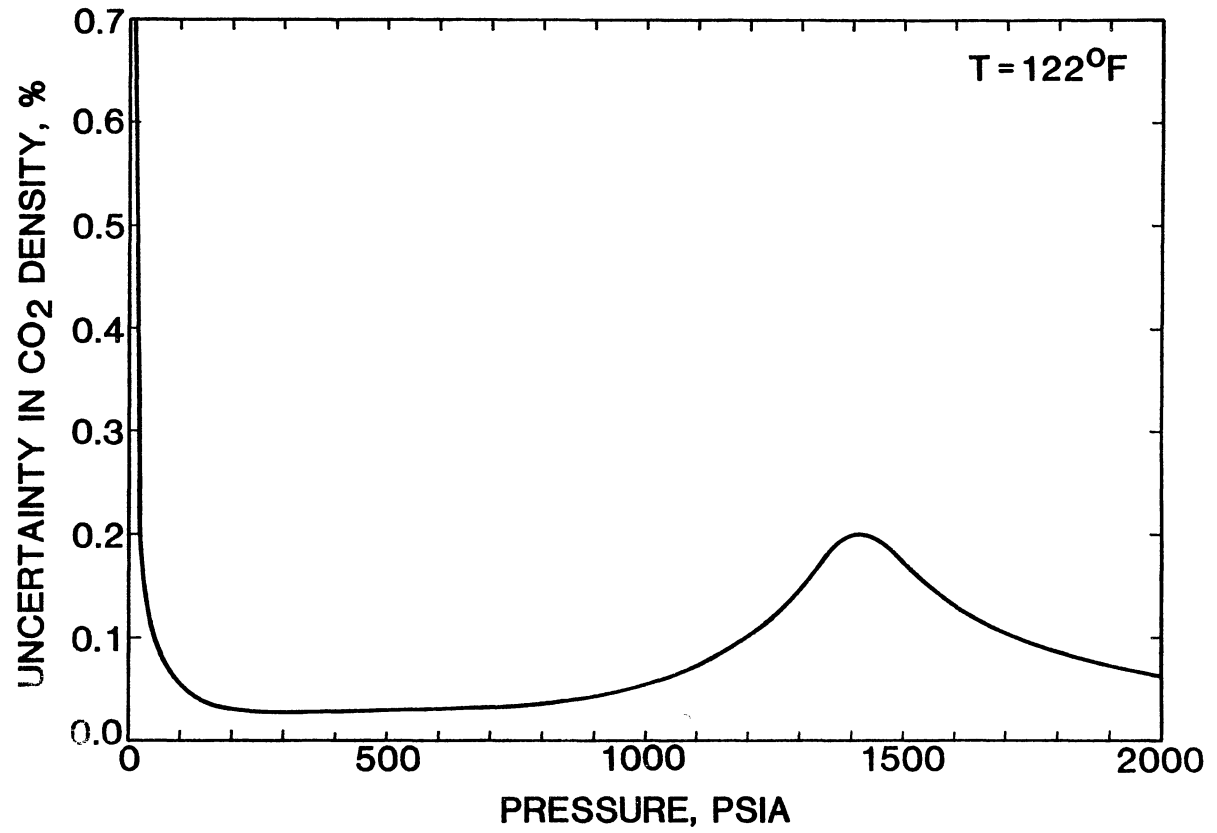


Figure 9. Percentage Uncertainty in CO<sub>2</sub> Density Versus Pressure

$$V_{SG} = n_{SG} MW_{SG} / \rho_{SG} (T_{GIP}, P_{GIP}). \quad (5.3)$$

Advance the piston in the solute injection pump by the amount calculated in Equation (5.3). Carefully and slowly open OV3 and allow the pressure in the solute injection pump to return to approximately the original pressure reading recorded on the injection sheet. Quickly close OV3, then adjust the solute injection pump until the exact original pressure reading is reestablished in the pump. After allowing sufficient time for the pressure in the solute injection pump to reach the original value (normally requires 2 to 3 minutes to stabilize at recorded pressure), note the volume reading on the pump and record this value on the injection sheet. Calculate the actual moles of solute gas injected from the tabulated density, the solute molecular weight, and the final volume read from the injection pump. When the actual moles of solute injected are known, the actual mole fraction of solute can be calculated by the following relation and the injection is complete.

$$x_{SG} = \frac{n_{SG}}{n_{SG} + n_{HC}} \quad (5.4)$$

#### Measuring the Bubble Point

1. Usually after injection of the solvent and solute, the vapor-liquid interface is about 10 cc below the top of the equilibrium cell. The gas phase must be totally collapsed for the bubble-point pressure to be determined. To accomplish this, open V10 and V5, and turn on the stirrer. Use the cleaning pump to introduce mercury into the

equilibrium cell until the gas phase is forced into solution, being careful not to exceed the 2,000 psia limit on the pressure transducer.

2. Allow the pressure to stabilize at a level approximately 200 psi above the expected bubble-point pressure of the mixture. This will assure the solute is completely dissolved in the solvent and a single-phase fluid exists in the equilibrium cell. Isolate the cleaning pump from the apparatus by closing V10.

3. When the pressure stabilizes, note the volume reading on the solvent injection pump. A P-V data sheet (Figure 10) is used to record all data points taken during the bubble point measuring procedure. Record on this sheet the volume from the pump, the temperature of both air baths, and the corresponding stabilized pressure read from the hydrocarbon transducer.

4. Rotate the solvent pump handle counter-clockwise 0.01 cc removing that volume of mercury from the equilibrium cell. Record the new volume reading from the pump on the P-V data sheet. Allow the pressure to stabilize, exercising patience to assure the proper (stabilized) pressure is tabulated. Record the pressure on the data sheet.

5. Repeat step four three times. Plot the data recorded on the P-V data sheet as  $P_i$  vs  $(V_i - V_0)$ , where  $P_i$  and  $V_i$  represent the system pressure and volume of point  $i$ , respectively, and  $V_0$  represents the original volume reading on the P-V data sheet. Figure 11 shows results for a typical P-V traverse. The steep slope of the single phase line indicates an all-liquid composition in the equilibrium cell because liquids are relatively incompressible and the pressures are greatly effected by small changes in volume. Fit the best line possible through

PVT DATA

System: \_\_\_\_\_ No. \_\_\_\_\_

Temp: \_\_\_\_\_

x( ): \_\_\_\_\_

| DATE | TIME | ROOM TEMP. | $V_I$ |  |  | $\Delta V,$<br>cc | P<br>( ) | Pump Bath Temp. | Cell Bath Temp. |
|------|------|------------|-------|--|--|-------------------|----------|-----------------|-----------------|
|      |      |            |       |  |  |                   |          |                 |                 |
|      |      |            |       |  |  |                   |          |                 |                 |
|      |      |            |       |  |  |                   |          |                 |                 |
|      |      |            |       |  |  |                   |          |                 |                 |
|      |      |            |       |  |  |                   |          |                 |                 |
|      |      |            |       |  |  |                   |          |                 |                 |
|      |      |            |       |  |  |                   |          |                 |                 |
|      |      |            |       |  |  |                   |          |                 |                 |
|      |      |            |       |  |  |                   |          |                 |                 |
|      |      |            |       |  |  |                   |          |                 |                 |
|      |      |            |       |  |  |                   |          |                 |                 |
|      |      |            |       |  |  |                   |          |                 |                 |
|      |      |            |       |  |  |                   |          |                 |                 |
|      |      |            |       |  |  |                   |          |                 |                 |
|      |      |            |       |  |  |                   |          |                 |                 |

Chart No.: \_\_\_\_\_

$P_B$ : \_\_\_\_\_

Initials: \_\_\_\_\_

Figure 10. P-V Data Sheet

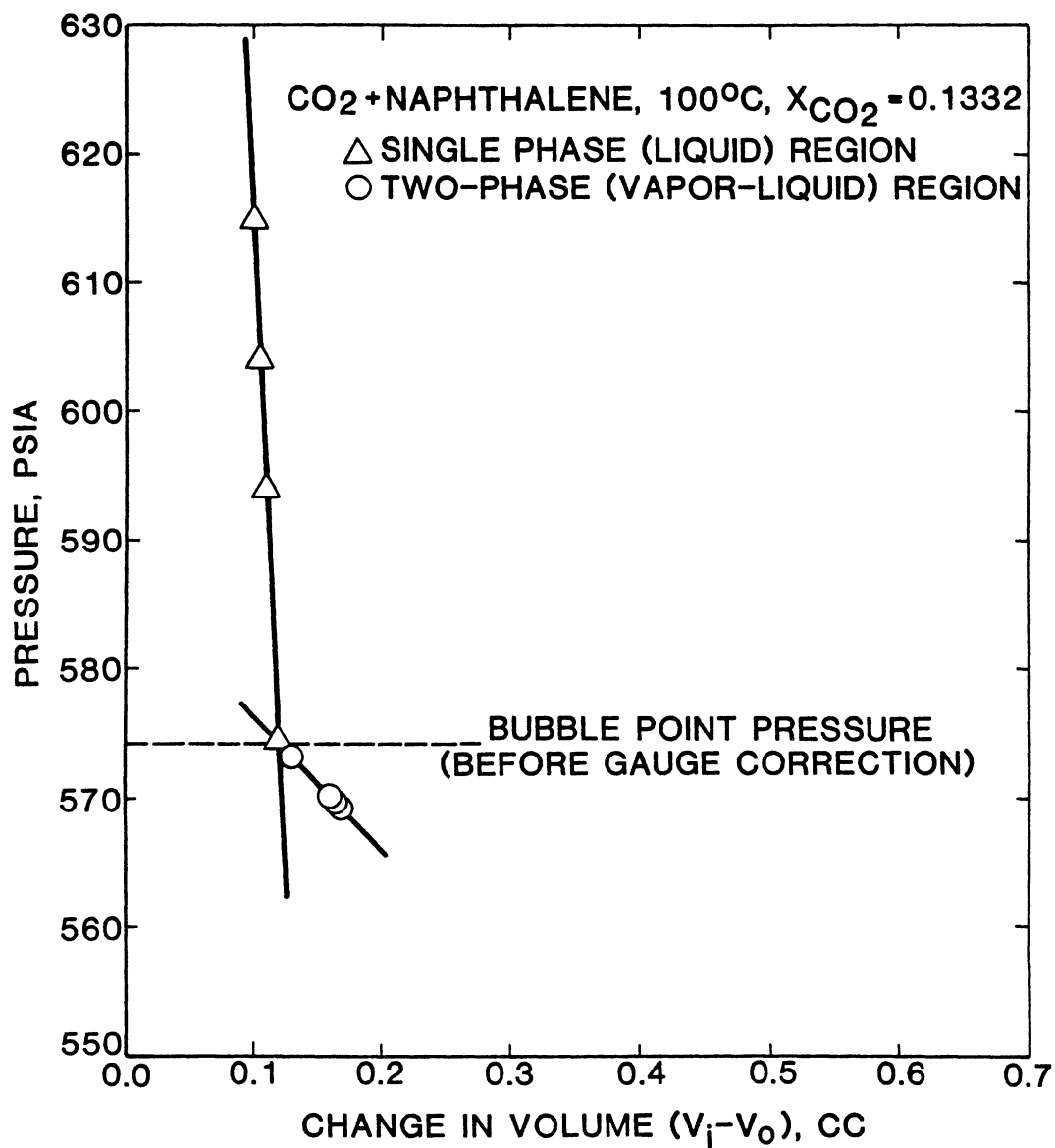


Figure 11. Graphical Bubble-Point Determination



the four data points and extrapolate the line down to a pressure level below the expected bubble-point pressure.

6. Rotate the pump handle counter-clockwise again, but only remove 0.005 cc of mercury from the equilibrium cell (smaller increments in volume are used nearer the bubble-point pressure to more accurately determine the correct pressure). After the pressure stabilizes, record it and the volume reading from the solvent injection pump on the P-V data sheet. Plot this point as before and check to see if it lies on the extrapolated single phase line. If the point is on the line, the fluid in the equilibrium cell is still single-phase liquid.

7. Repeat step six until the measured pressure deviates from the extrapolated single-phase line when it is plotted on the  $P_i$  vs  $(V_i - V_0)$  graph (this P will lie above the line). Such a behavior indicates that the fluid in the equilibrium cell has separated into vapor and liquid phases.

8. Withdraw 0.005 cc from the equilibrium cell, again recording the volume reading from the solvent pump and the corresponding pressure after it has stabilized.

9. Plot the resulting data point and repeat step eight until enough points have been plotted (as described in step five) to establish a two-phase line (three or four points are usually sufficient).

10. Extrapolate the two-phase line to intersect the single-phase line. As indicated in Figure 11, the intersection of the two lines determines the bubble-point pressure of the composition under study.

11. From the transducer calibration record find two transducer pressure readings which bound the experimentally measured bubble point. A typical transducer calibration record is shown in Appendix C

(see HYDROCARBON TRANSDUCER CORRECTIONS, Appendix C computer output). Linearly interpolate between the two boundary values to find the transducer gauge correction which corresponds to the measured bubble point. Adjust the measured bubble point by the corresponding gauge correction and the measurement is complete.

#### Proper Determination of the Isothermal Solubility Curves

Because no visible observation of the cell contents is possible to check the exact amount of material charged to the cell, other methods must be used to determine experimentally whether the solubilities measured are acceptable. A useful method is described below.

To properly establish an experimental pressure-composition isotherm, a system combining the bubble-point pressure measurements from two separate hydrocarbon solvent injections is used. First solvent is injected following the proper procedure. Solute gas is then injected and bubble-point pressures measured at three or four mole fractions of solute gas. After the final pressure has been measured, the equilibrium cell is cleaned and a second solvent injection is made at the same temperature. Additional solute injections are made with the second solvent injection and their respective pressures are measured.

The relation between the mole fraction of solute,  $x$ , and the bubble-point pressure,  $P_b$  can be conveniently observed by plotting the experimental values as  $P_b/x$  vs  $x$ . The points should lie on a smooth curve as demonstrated in Figure 12. If the points from the separate solvent injections do not lie on single smooth curve, then at least one of the two runs is in error, and another solvent injection must be made to determine which of the injections is incorrect.

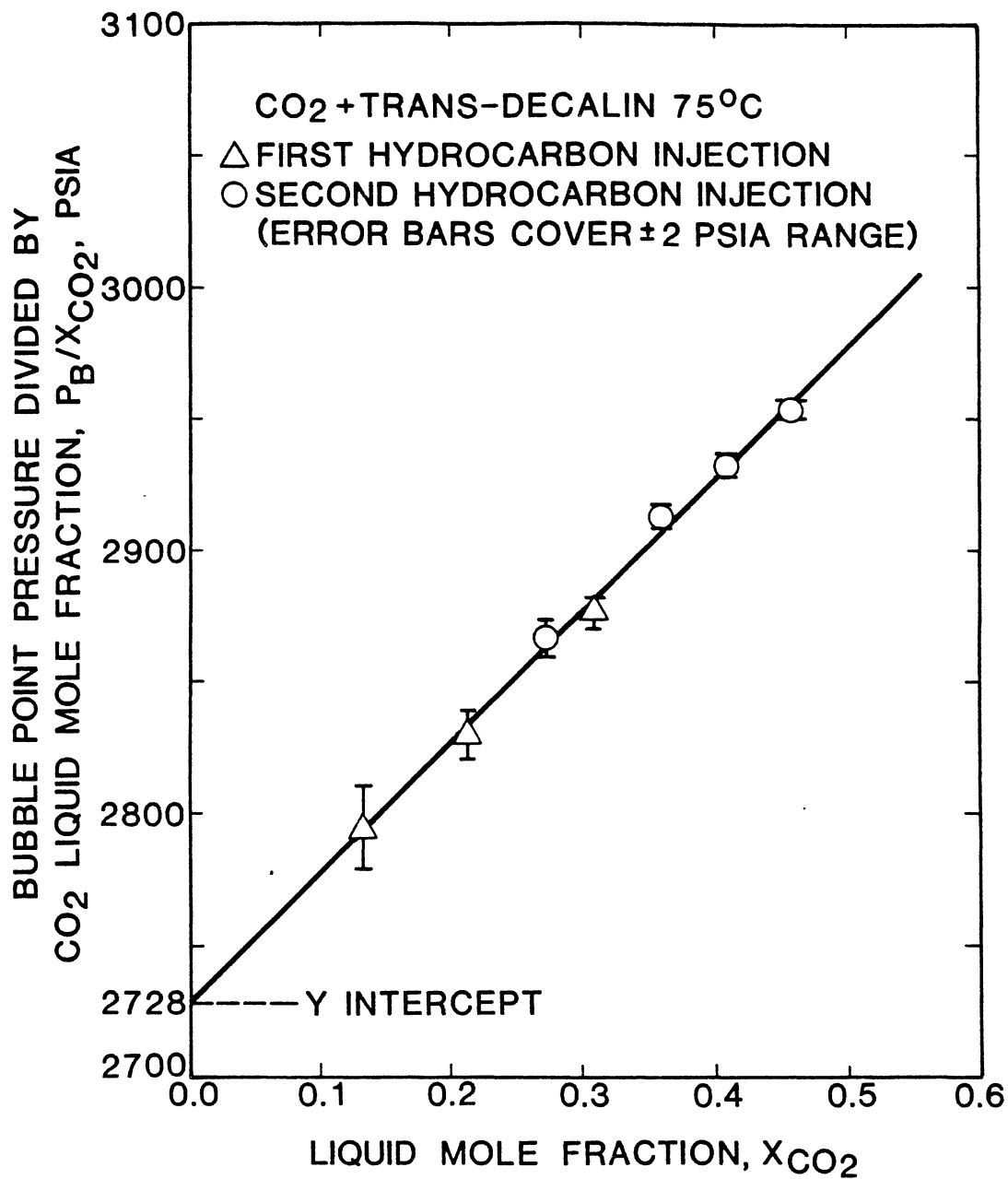


Figure 12. Typical Bubble-Point Data for CO<sub>2</sub> + Solvent

The above mentioned method is a convenient means of determining erroneous solubilities because the  $P/x$  values magnify any inherent pressure errors by the reciprocal of the mole fraction. The magnified error is easily identified on the graph as a point which does not lie on the smooth curve created by the correct measurements. Also, by matching two separate solvent injections, a check is made on the measurements of the actual amounts of materials injected (both solvent and solute). If an error is made in either injection, the bubble-point pressures will not form a smooth curve when plotted as described above. Another reason the method works so well is that the  $P/x$  values cover a range less than  $P$  and, in fact, would be constant if Henry's Law was obeyed at all compositions studied.

The above method is a necessary test to be performed on each isotherm. The method, of course, does not guarantee that the data are correct. There is a possibility that the solvent is not properly degassed prior to injection. If this is the case, both solvent injections might match as described above, but the resulting isotherm would still be in error. To check for this occurrence, the solvent should be degassed a second time and then checked using the method as described earlier.

#### Calibration of Pressure Transducers

The hydrocarbon pressure transducer was calibrated on a regular basis (after each system studied) to assure proper pressure readings during operation. The previously discussed apparatus was designed for easy access to the dead weight gauge, so calibration of the pressure transducers is simple and requires little time. Because the equations

used to evaluate the transducer gauge corrections involved numerous repetitive calculations, a computer program was developed (Appendix C) to quickly perform the calculations and determine the transducer corrections. The proper procedure for calibration of the pressure transducers is listed as follows.

1. Using an accurate cathetometer, measure the heights of the transducers (in the injection pump bath), mercury-oil interface, and dead weight gauge reference point. Calculate the head correction from these measured heights to account for the difference in fluid levels between the reference line on the dead weight gauge and the pressure transducers (see Appendix C).

2. Open V10, IV, DW1, DW2, and DW3. Check the mercury level in the Jergusen gauge to make sure it is level with the black reference line marked on the outside cover of the gauge. This black line is the height of the the mercury-oil interface used to calculate the head correction so it is important that the mercury-oil interface is always set at this height. If the mercury level is not even with the black reference mark, open PV1 and adjust the cleaning pump to return the mercury level in the Jergusen gauge to the proper mark. Isolate the cleaning pump by closing PV1 once the mercury-oil interface has been returned to the correct height.

3. Now the dead weight gauge is linked directly to the pressure transducer, and the calibration is begun by placing the appropriate disk weights on the floating piston of the dead weight gauge. The choice of weights depends on the particular pressure range over which the apparatus will be operated. Appendix C shows a useful combination of disk weights and the resulting pressures the various combinations of

weights produce. Once the weights have been placed on the gauge, adjust the pump handle on the dead weight gauge so that the reference mark on the floating piston aligns with the reference mark on the piston housing. While keeping the two reference marks aligned, monitor the pressure reading on the pressure transducer readout and record the pressure when it stabilizes. Change the weight(s), and align the reference marks after each change, then record the corresponding pressure readings.

4. After the desired range of pressures has been covered, return the weights to their respective places in the storage box. Return the floating piston to its original position by reversing the pump of the dead weight gauge until the floating piston rests on the piston housing. Isolate the dead weight gauge from the apparatus by closing valves DW1, DW2, DW3, and IV1. Calculate the transducer gauge corrections using the program mentioned earlier and print out the transducer calibration record. This calibration record is used to correct bubble-point pressures measured with the apparatus. Further information concerning the dead weight gauge operation and maintenance is found in the manual which accompanies the gauge (27).

## CHAPTER VI

### ERROR ANALYSIS AND DATA REDUCTION

Experimental data must be obtained with precision and accuracy if the analysis of such data is to yield useful results. The maximum expected experimental error in CO<sub>2</sub> solubilities and bubble-point pressures (presented later in this work) are calculated in this chapter to estimate the accuracy of the data presented. Following the error analysis is a description of the methods used to determine equation-of-state interaction parameters for the systems studied.

#### Error Analysis

In the measurement of experimental quantities, two types of errors are typically encountered. One is random error which results from non-recurring disturbances. The other is systematic error which is caused by improper measurement procedures. Random errors can be accounted for by the use of statistical methods, but systematic errors can only be eliminated by correcting improper measurement procedures (6).

To assure there were no systematic errors involved with data collection in this work, two checks were made on the apparatus and measurement procedure. First, the vapor pressures of several pure chemicals were measured and compared with literature values. Second, a binary mixture was studied and results compared with work performed by other experimenters. With no discrepancies seen between data collected

using the apparatus and other sources, systematic errors were assumed to have been eliminated.

Random error in calculated or dependent variables such as liquid mole fraction or pressure, respectively, can be determined by error propagation and considering prime errors.

Prime errors are due to imprecisions in temperature, volume, and pressure measurements. By repeated measurements and calibrations of the apparatus used in this study these errors are estimated to be

$$\epsilon_T = 0.05K \quad (6.1)$$

$$\epsilon_V = 0.0025\text{cc} \quad (6.2)$$

$$\epsilon_P = 0.05 \text{ psia} \quad (6.3)$$

The estimates for  $\epsilon_V$  and  $\epsilon_P$  are based on the ability to read the injection pumps and pressure transducer display, respectfully; while  $\epsilon_T$  is based on the ability of the temperature controller to hold a set point temperature.

Using Equation (J) of Appendix D, the estimated error in liquid mole fraction for this work can be calculated as follows

$$\begin{aligned} \epsilon_{x_1} = x_1 x_2 & \left[ (\epsilon_{\rho_1} / \rho_1)^2 + (\epsilon_{V_1} / \sum V_{i1})^2 \right. \\ & \left. + (\epsilon_{\rho_2} / \rho_2)^2 + (\epsilon_{V_2} / V_2)^2 \right]^{1/2} \end{aligned} \quad (6.4)$$

A typical data run consisted of three CO<sub>2</sub> injection of 3 cc each and one hydrocarbon injection of 7 cc. The uncertainty in CO<sub>2</sub> density was estimated to be 0.15% based on the variations of pressure and



temperature used in the CO<sub>2</sub> density program of Appendix B and the claimed uncertainty of the IUPAC (26) tables on which the program of Appendix B is based. The worst case error in hydrocarbon density was estimated to be 0.003 g/cc (based on the difference of two density measurements on pyrene). Substitution of these values in Equation (6.4) yields

$$\epsilon_{x_1} = 0.004 x_1 x_2. \quad (6.5)$$

Hence, the maximum error in liquid mole fraction, occurring at an equimolar mixture of CO<sub>2</sub> and solvent is 0.001.

Random error in bubble-point pressures due to prime and propagated errors can be estimated by use of Equation (K) of Appendix D,

$$\epsilon_p^2 = \epsilon_p^2 + (\partial P / \partial x_1)^2 \epsilon_{x_1}^2 + (\partial P / \partial T)^2 \epsilon_T^2. \quad (6.6)$$

Assuming the temperature term of Equation (6.7) is negligible and substituting the maximum error in liquid mole fraction calculated above Equation (K) becomes

$$\epsilon_p^2 = 0.05^2 + 0.001^2 (\partial P / \partial x_1)^2. \quad (6.7)$$

Using the maximum value of  $\partial P / \partial x_1$  for each system studied in this work the maximum error in bubble-point pressure was calculated to be that shown in Table III.

TABLE III  
 MAXIMUM ERROR IN BUBBLE  
 POINT PRESSURE

| Solvent      | Maximum Error<br>(psi) |
|--------------|------------------------|
| Benzene      | 1.2                    |
| Naphthalene  | 5.8                    |
| Phenanthrene | 7.9                    |
| Pyrene       | 10.3                   |

#### Data Reduction

The primary goal of this study was to obtain the solubility of CO<sub>2</sub> in a series of aromatic solvents. These solubilities were then used to estimate optimum values of binary interaction parameters for each binary system to be used in the SRK and P-R equations of state.

Optimum values of interaction parameters were estimated from the solubility data obtained in this work using a non-linear regression package modified and explained in detail by Gasem (6). The optimality criterion used by this package involves minimizing the weighted error in bubble-point pressures:

$$Q = \sum_{i=1}^N \frac{(p_i^{\text{Exp}} - p_i^{\text{Calc}})^2}{\epsilon_p^2} \quad (6.8)$$

The solubility data of this work was also used to estimate Henry's constants and partial molar volumes of CO<sub>2</sub> in the systems studied. These estimates were made by use of an equation proposed by Krichevsky and Kasarnovsky (20). A regression program written by Gasem (6) using the Krichevsky-Kasarnovsky equation calculated Henry's constants and CO<sub>2</sub> partial molar volumes by minimizing the sum of the squares of the error in the logarithm of the CO<sub>2</sub>-fugacity-to-mole-fraction ratio.

$$Q = \sum_{i=1}^N \{ [\ln (f^0_{\text{CO}_2, \text{P}}/x_{\text{CO}_2})]^{\text{Exp}} - [\ln (f^0_{\text{CO}_2, \text{P}}/x_{\text{CO}_2})]^{\text{Calc}} \}^2 \quad (6.9)$$

## CHAPTER VII

### EXPERIMENTAL RESULTS AND DISCUSSION

This study began with the design and construction of the bubble-point apparatus. Upon completion of the apparatus, the measurement equipment was calibrated and the expected experimental error in bubble-point pressures using the apparatus was estimated. Error propagation calculations, discussed in Chapter VI, resulted in an expected error of  $\pm 1.2$  to  $\pm 10.3$  psia in bubble-point pressure, depending on the system (see Table III), and of  $\pm 0.001$  in  $\text{CO}_2$  mole fractions.

Vapor pressure measurements were made on some pure chemicals to see if the apparatus could reproduce known vapor pressure data. Pentane and benzene vapor pressures were measured with a maximum error of 0.5 psia as shown in Table IV.

TABLE IV  
VAPOR PRESSURE TEST RESULTS

| Temperature<br>(°C) | Experimental Vapor<br>Pressure (psia) |         | Literature Vapor<br>Pressure (psia)* |         |
|---------------------|---------------------------------------|---------|--------------------------------------|---------|
|                     | Pentane                               | Benzene | Pentane                              | Benzene |
| 40                  | 17.8                                  | 3.9     | 17.3                                 | 3.5     |
| 50                  | 24.1                                  | 5.4     | 23.8                                 | 5.2     |

\*Vapor Pressure Reference (28)

Next, a test binary system was selected to demonstrate the reliability of data produced by the apparatus. Benzene was used as the test solvent because of the large amount of data available on the binary  $\text{CO}_2$  + benzene. Five investigators (2-6) have studied the phase behavior of  $\text{CO}_2$  + benzene at  $40^\circ\text{C}$ .

The data obtained in this study for  $\text{CO}_2$  + benzene at  $40^\circ\text{C}$  is listed in Table V. Figure 13 compares the data of Table V with the data obtained by the other investigators for  $\text{CO}_2$  + benzene at  $40^\circ\text{C}$ . In this figure, the ordinate is the difference between bubble-point pressure of the mixture and the vapor pressure of benzene at  $40^\circ\text{C}$ , divided by the corresponding  $\text{CO}_2$  liquid mole fraction. The abscissa is the  $\text{CO}_2$  liquid mole fraction. Plotting bubble-point data in this manner shows how the system deviates from Henry's Law and magnifies any error in uniformity of the data by the reciprocal of the  $\text{CO}_2$  liquid mole fraction.

Examination of Figure 13 shows the  $\text{CO}_2$  + benzene data generated in this work to be very consistent with the majority of the other experimenters cited, particularly at  $\text{CO}_2$  liquid mole fractions greater than 0.3. The data in Table IV is in best agreement with the bubble-point data of Gupta et al. At  $\text{CO}_2$  liquid mole fractions less than 0.3, the data begin to scatter. Inspection of Figure 13 shows the data of this work appears to be in best agreement with the bubble-point work of Gupta. The worst agreement with Ohgaki, whose data is lower than the other experimenters at  $\text{CO}_2$  liquid mole fraction less than 0.4 but moves towards the data of others as mole fraction increases.

Binary interaction parameters,  $k_{ij}$  and  $l_{ij}$ , for the system  $\text{CO}_2$  + benzene were regressed from the data of Table IV for both the SRK and P-R equation of state (refer to Table VI). The case of using a single

TABLE V  
SOLUBILITY OF CO<sub>2</sub> IN BENZENE

| Mole Fraction<br>CO <sub>2</sub> | Pressure<br>MPa (psia) |
|----------------------------------|------------------------|
| -----313.2K (40°C, 104°F)-----   |                        |
| 0.139                            | 1.644 (238.4)          |
| 0.181                            | 2.106 (305.5)          |
| 0.325                            | 3.544 (514.0)          |
| 0.401                            | 4.186 (607.1)          |
| 0.500                            | 4.925 (714.3)          |
| 0.602                            | 5.572 (808.1)          |

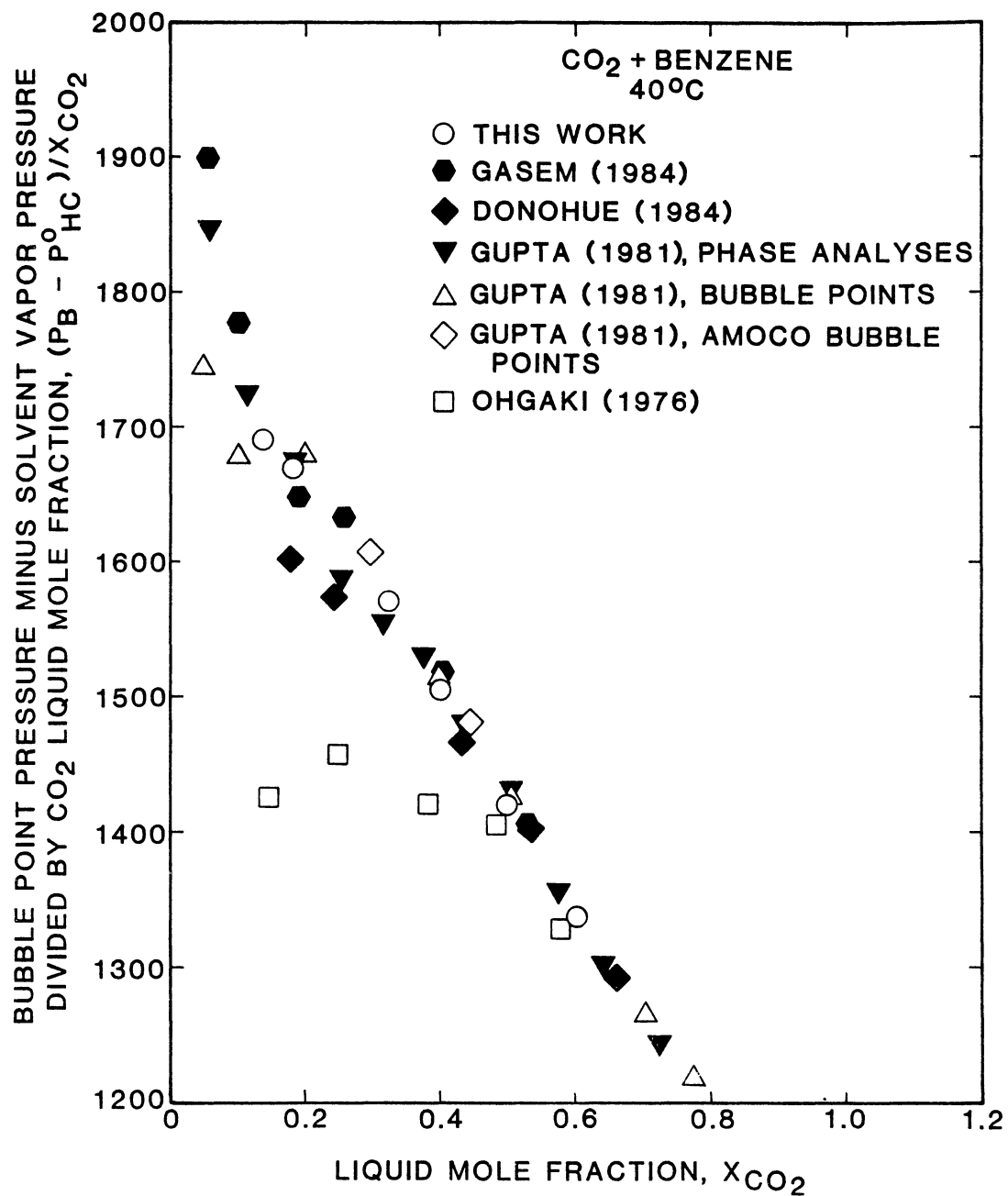


Figure 13. Comparison of Bubble-Point Data for CO<sub>2</sub> + Benzene at 40°C

TABLE VI

SOAVE AND PENG-ROBINSON EQUATION OF STATE  
REPRESENTATIONS OF CO<sub>2</sub> SOLUBILITY DATA

| Temperature<br>K (°F)                    | Soave Parameters (P-R) |                 | Error in CO <sub>2</sub><br>Mole Fraction |        |
|--|------------------------|-----------------|---|--------|
|  | k <sub>12</sub>        | l <sub>12</sub> | RMS                                       | Max.   |
| -----CO <sub>2</sub> + Benzene-----      |                        |                 |   |        |
| 313.2 (104)                              | 0.068 (0.066)          | 0.035 (0.037)   | 0.003                                     | 0.005  |
|  | 0.090 (0.089)          | -- --           | 0.018                                     | 0.031  |
| -----CO <sub>2</sub> + Naphthalene-----  |                        |                 |   |        |
| 373.2 (212)                              | 0.079 (0.075)          | 0.027 (0.030)   | <0.001                                    | <0.001 |
|  | 0.118 (0.116)          | -- --           | 0.007                                     | <0.009 |
| 423.2 (302)                              | 0.068 (0.064)          | 0.031 (0.032)   | <0.001                                    | <0.001 |
|  | 0.119 (0.115)          | -- --           | 0.004                                     | 0.005  |
| 373.2 and<br>423.2                       | 0.082 (0.079)          | 0.024 (0.025)   | 0.002                                     | 0.004  |
|  | 0.119 (0.116)          | -- --           | 0.006                                     | 0.010  |
| -----CO <sub>2</sub> + Phenanthrene----- |                        |                 |   |        |
| 383.2 (230)                              | 0.100 (0.096)          | 0.021 (0.023)   | <0.001                                    | <0.001 |
|  | 0.153 (0.152)          | -- --           | 0.004                                     | 0.005  |
| 423.2 (302)                              | 0.103 (0.096)          | 0.016 (0.019)   | <0.001                                    | <0.001 |
|  | 0.147 (0.145)          | -- --           | 0.002                                     | 0.003  |
| 383.2 and<br>423.2                       | 0.113 (0.145)          | 0.014 --        | 0.003                                     | 0.005  |
|  | 0.150 (0.149)          | -- --           | 0.004                                     | 0.006  |



TABLE VI (Continued)

| Temperature<br>K(°F)               | Soave Parameters (P-R) |                 | Error in CO <sub>2</sub><br>Mole Fraction |        |
|------------------------------------|------------------------|-----------------|---|--------|
|                                    | k <sub>12</sub>        | l <sub>12</sub> | RMS                                       | Max.   |
| -----CO <sub>2</sub> + Pyrene----- |                        |                 |   |        |
| 433.2 (320)                        | 0.256 (0.234)          | 0.017 (0.018)   | <0.001                                    | <0.001 |
|                                    | 0.310 (0.289)          | -- --           | 0.001                                     | 0.002  |

interaction parameter,  $k_{ij}$ , to model the data of Table V is also presented. In both cases, using both interaction parameters,  $k_{ij}$  and  $l_{ij}$ , or  $k_{ij}$  alone, the values of interaction parameters for use with the SRK equation were very similar to those for the P-R equation. Table VI also shows the errors in predicted  $\text{CO}_2$  mole fractions using these interaction parameters. Both equations yield similar errors in predicted  $\text{CO}_2$  mole fractions. Figure 14 shows the abilities of the SRK equation, using two interaction parameters,  $k_{ij}$  and  $l_{ij}$ , (fitted to the data of this work) to predict the data of Table V and the other investigators cited. Here the solubility deviations for the bubble point work of Gupta most closely follow this work (as should be expected from Figure 14).

Figures 13 and 14 show the data obtained in this work using the bubble-point apparatus to be consistent with the results of most of the other investigators for this system. With these results and considering the accuracy of the vapor pressure data reproduced, the apparatus was deemed operational.

The system  $\text{CO}_2$  + naphthalene was studied at 100 and 150°C. Isotherm temperatures were selected to be slightly over the melting point of the solvent and arbitrarily to 150°C for the second isotherm of  $\text{CO}_2$  + naphthalene and  $\text{CO}_2$  + phenanthrene. The  $\text{CO}_2$  liquid mole fractions studied with corresponding bubble-point pressures for these isotherms are listed in Table VII. Figures 15 and 16 show the bubble-point pressure divided by the  $\text{CO}_2$  liquid mole fraction versus the  $\text{CO}_2$  liquid mole fraction for the data at 100 and 150°C, respectively. The error bars of Figures 15 and 16 (as well as the other figures of this chapter displaying bubble-point pressure divided by  $\text{CO}_2$  liquid mole fraction as

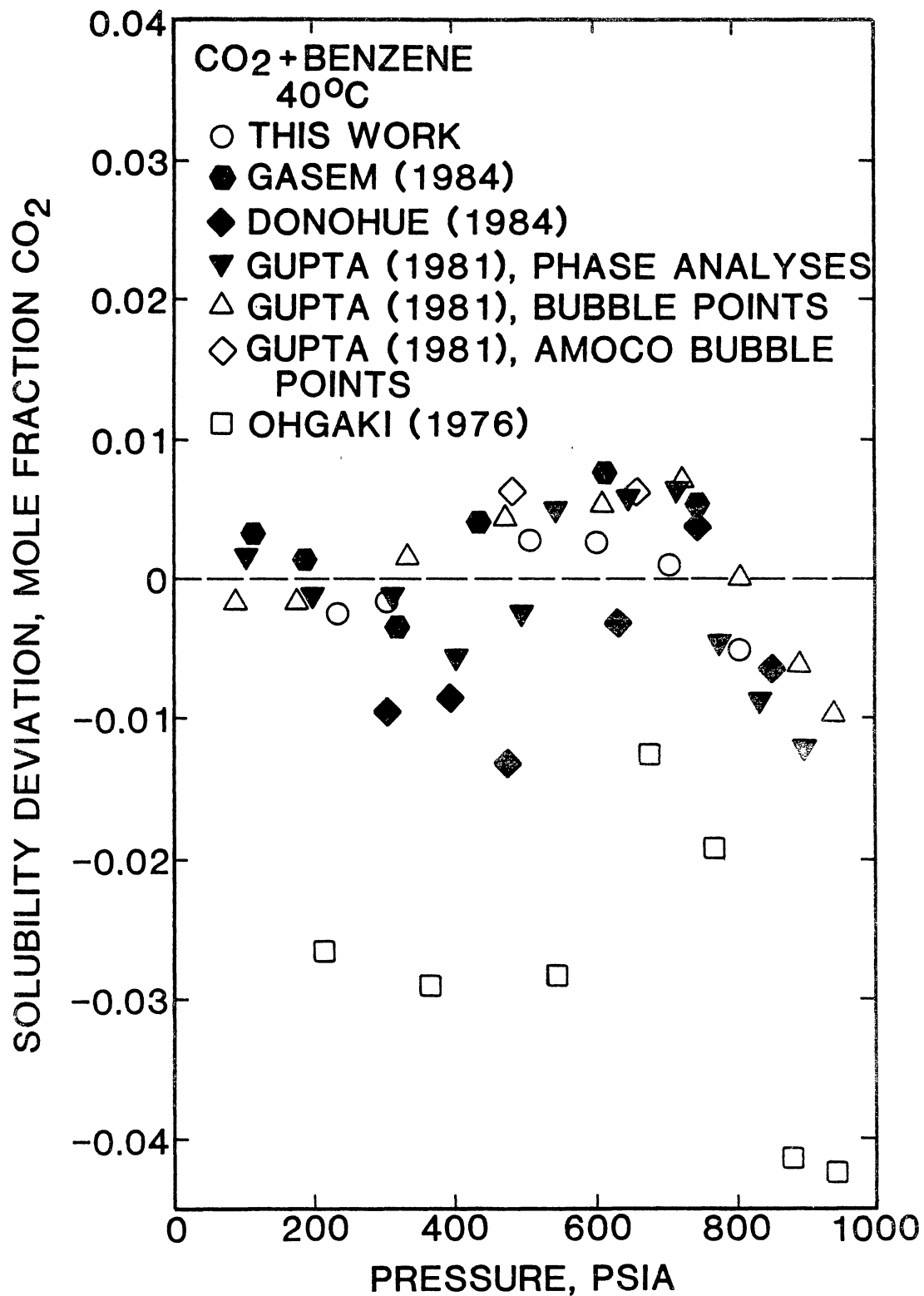


Figure 14. Comparison of Solubility Data for CO<sub>2</sub> in Benzene at 40°C

TABLE VII  
SOLUBILITY OF CO<sub>2</sub> IN NAPHTHALENE

| Mole Fraction<br>CO <sub>2</sub> | Pressure |          |
|----------------------------------|----------|----------|
|                                  | MPa      | (psia)   |
| -----373.2K (100°C, 212°F)-----  |          |          |
| 0.047                            | 1.385    | (200.9)  |
| 0.107                            | 3.196    | (463.5)  |
| 0.133                            | 3.978    | (577.0)  |
| 0.162                            | 4.852    | (703.7)  |
| 0.202                            | 6.091    | (883.4)  |
| 0.248                            | 7.586    | (1100.2) |
| 0.336                            | 10.451   | (1515.8) |
| -----423.2K (150°C, 302°F)-----  |          |          |
| 0.051                            | 1.925    | (279.2)  |
| 0.107                            | 4.129    | (598.9)  |
| 0.110                            | 4.229    | (613.4)  |
| 0.151                            | 5.873    | (851.8)  |
| 0.201                            | 7.879    | (1142.8) |
| 0.224                            | 8.845    | (1282.9) |
| 0.252                            | 9.965    | (1445.2) |

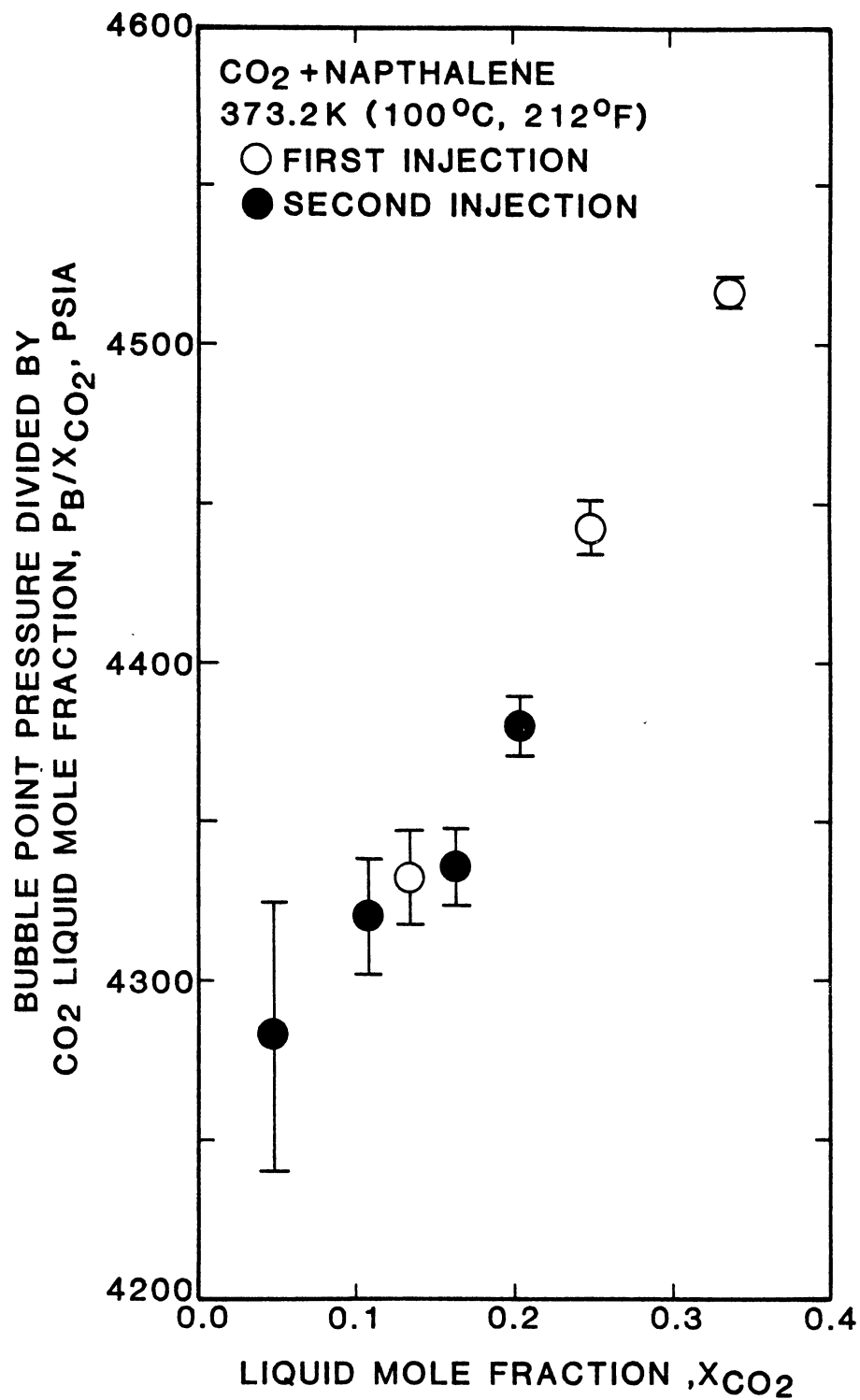


Figure 15. Bubble-Point Data for CO<sub>2</sub> + Naphthalene at 100°C

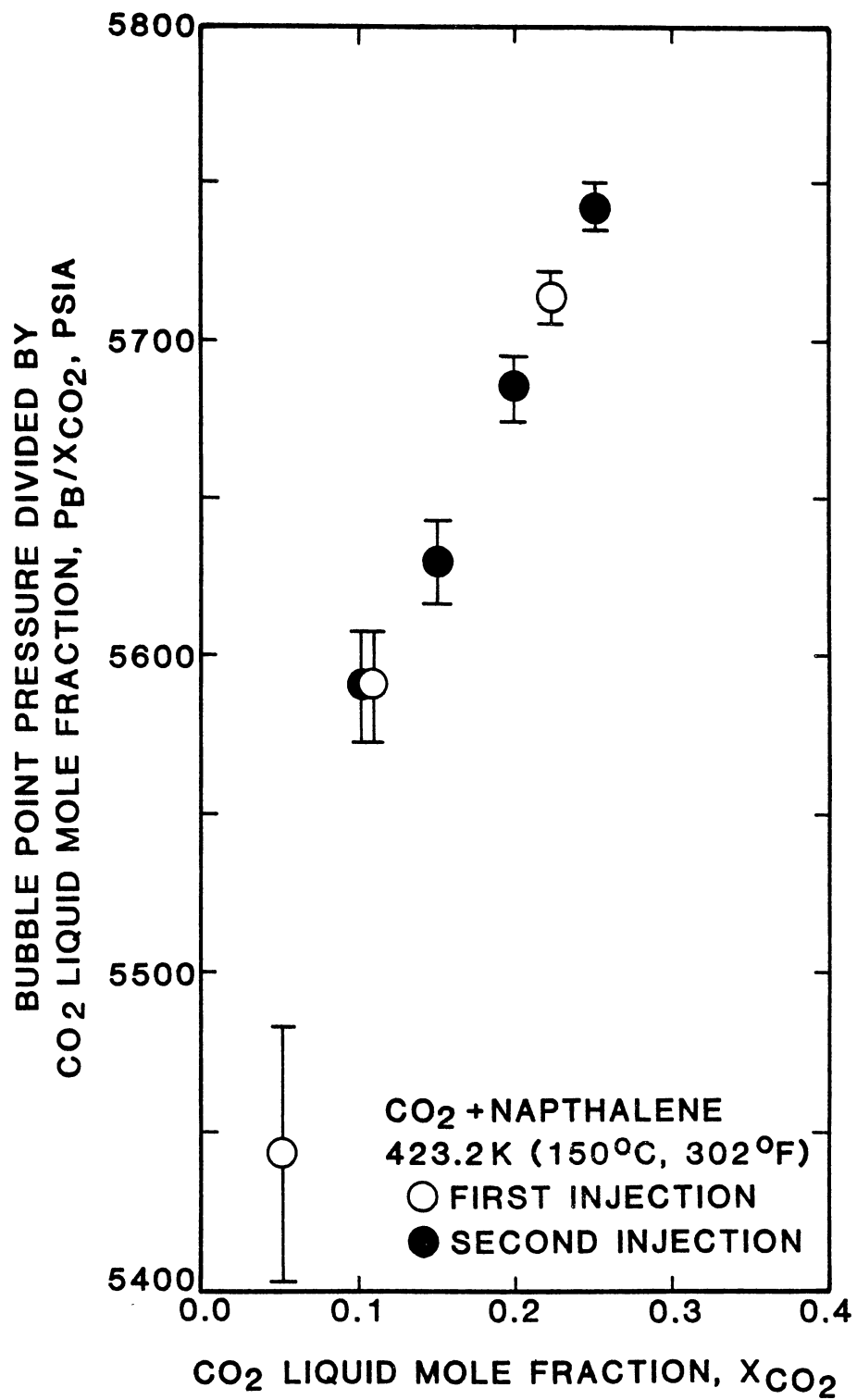


Figure 16. Bubble-Point Data for CO<sub>2</sub> + Naphthalene at 150°C

a function of CO<sub>2</sub> liquid mole fraction) correspond to  $\pm 2$  psi in bubble-point pressure for representation purposes. The vapor pressure of the solvent (naphthalene) is negligible at these temperatures and therefore not subtracted from the bubble-point pressures as was done in Figure 13.

Table VI presents the binary interaction parameters,  $k_{ij}$  and  $l_{ij}$  for both the SRK and P-R equations at each temperature studied. Here again, the case of using one interaction parameter,  $k_{ij}$ , to model the data for this system is also presented. The data for all isotherms were then lumped and regressed together to obtain interaction parameters based on a wider range of conditions. Interaction parameters for this lumped case showed no dramatic differences from parameters obtained using the individual isotherms (see Table VI).

The interaction parameters for the SRK and P-R equations are very similar and again had the same error in predicted CO<sub>2</sub> mole fraction. Figure 17 shows the SRK and P-R prediction error of the data on CO<sub>2</sub> + naphthalene, using both  $k_{ij}$  and  $l_{ij}$ . In general, Figure 17 shows the SRK and P-R equations predicting solubilities well within the claimed uncertainties in CO<sub>2</sub> mole fraction, 0.001, with one point of each isotherm outside this uncertainty. These points were omitted during data regression.

Orlov and Cherkasova (9) studied the system CO<sub>2</sub> + naphthalene but a translation of their work could not be obtained to compare with the data of this work.

The next system studied was the binary CO<sub>2</sub> + phenanthrene. The CO<sub>2</sub> liquid mole fractions studied with corresponding bubble-point pressures for isotherms at 110 and 150°C are given in Table VIII. Figures 18 and 19 show the data of Table VIII for the isotherms at 110 and 150°C, respectively, in the same format as was used with CO<sub>2</sub> + naphthalene.

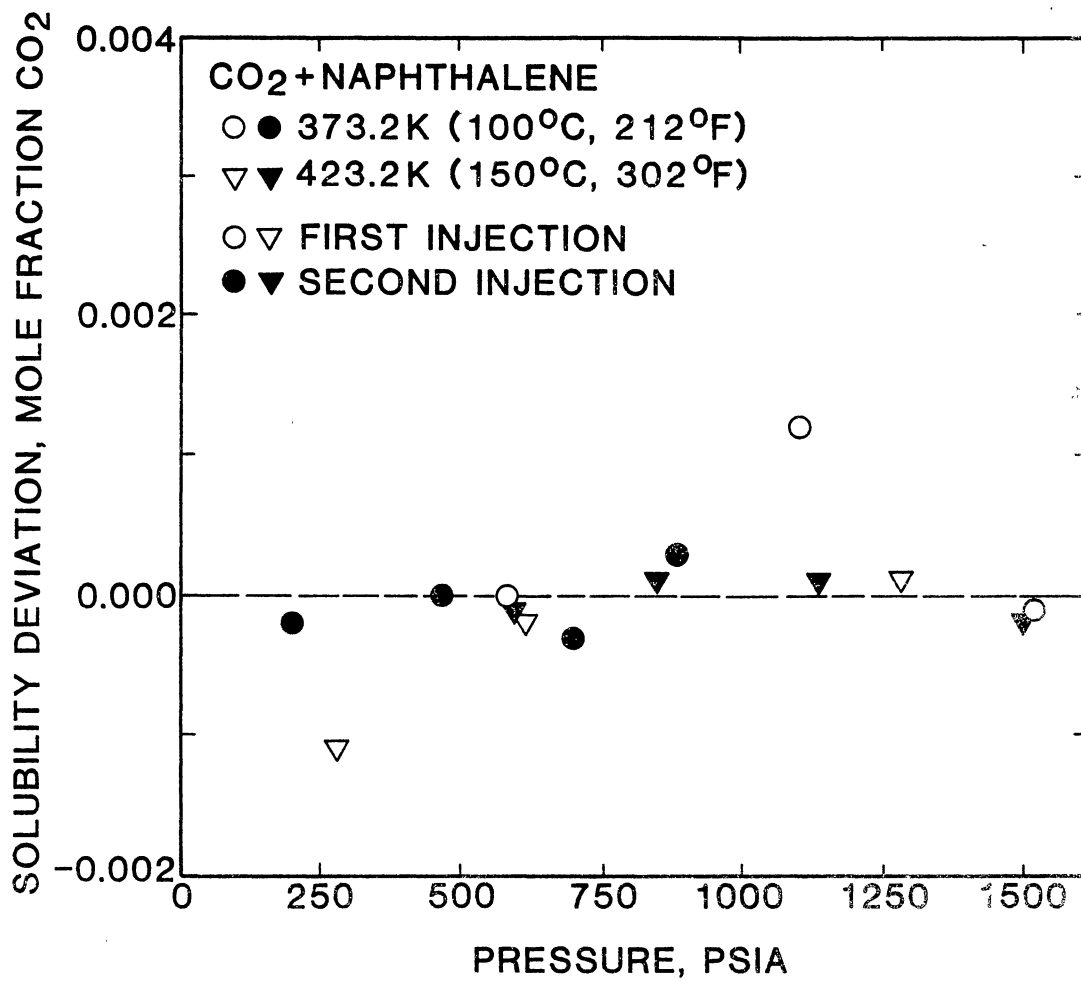


Figure 17. Soave and Peng-Robinson Representations of CO<sub>2</sub> Solubility in Naphthalene



TABLE VIII  
SOLUBILITY OF CO<sub>2</sub> IN PHENANTHRENE

| Mole Fraction<br>CO <sub>2</sub> | Pressure |          |
|----------------------------------|----------|----------|
|                                  | MPa      | (psia)   |
| -----383.2K (110°C, 230°F)-----  |          |          |
| 0.047                            | 1.877    | (272.3)  |
| 0.069                            | 2.810    | (407.5)  |
| 0.086                            | 3.606    | (523.0)  |
| 0.108                            | 4.575    | (663.5)  |
| 0.127                            | 5.414    | (785.3)  |
| 0.164                            | 7.197    | (1043.8) |
| 0.229                            | 10.615   | (1539.6) |
| -----423.2K (150°C, 302°F)-----  |          |          |
| 0.058                            | 2.761    | (400.5)  |
| 0.087                            | 4.182    | (606.6)  |
| 0.102                            | 4.957    | (719.0)  |
| 0.140                            | 6.991    | (1014.0) |
| 0.149                            | 7.526    | (1091.5) |
| 0.178                            | 9.151    | (1327.3) |
| 0.195                            | 10.208   | (1480.5) |

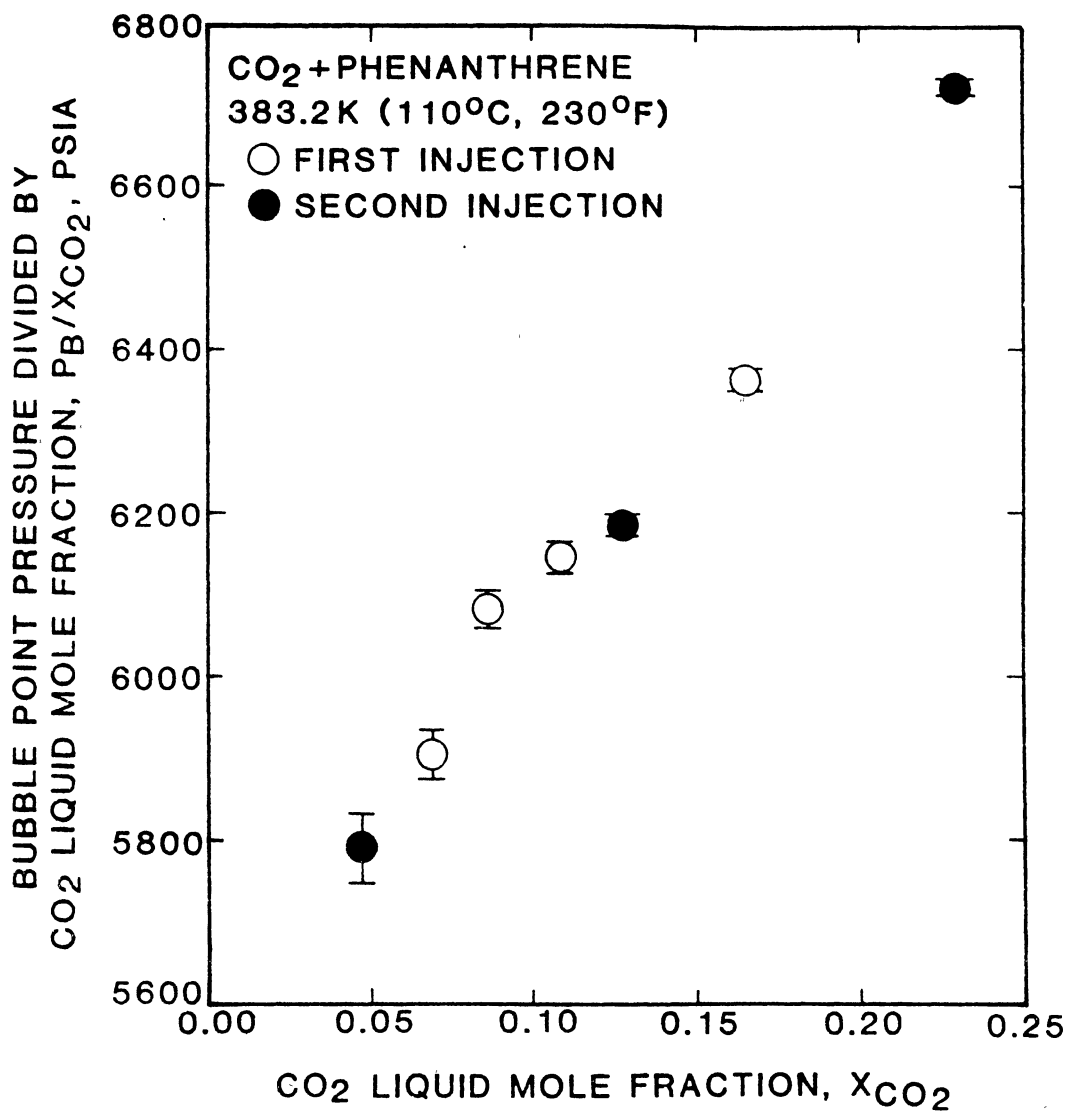


Figure 18. Bubble-Point Data for CO<sub>2</sub> + Phenanthrene at 110°C

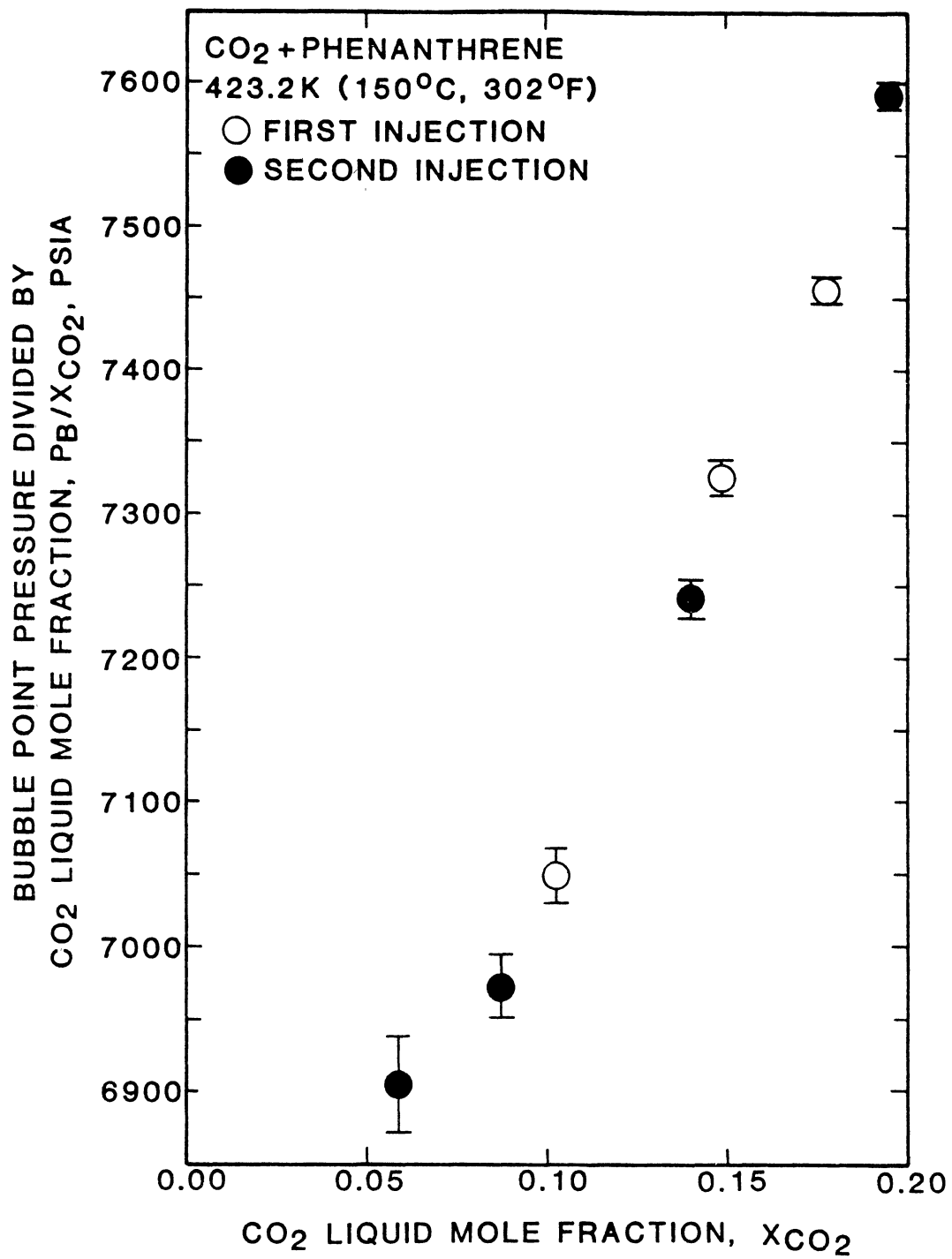


Figure 19. Bubble-Point Data for CO<sub>2</sub> + Phenanthrene at 150°C

Table VI presents the binary interaction parameters regressed from the data of Table VIII (for both  $k_{ij}$  and  $l_{ij}$  and for  $k_{ij}$  regressed alone) for the SRK and P-R equations. In addition to the parameters determined for each isotherm, lumped-isotherm interaction parameters are also given. Again, interaction parameters for the lumped case were not significantly different from parameters for the individual isotherms.

As was the case for  $\text{CO}_2$  + benzene and  $\text{CO}_2$  + naphthalene, the parameters for the SRK and P-R equations are similar and resulted in the same error in predicted  $\text{CO}_2$  mole fraction. Figure 20 shows the error of the SRK and P-R equations in predicting the data of Table VIII on  $\text{CO}_2$  + phenanthrene using both  $k_{ij}$  and  $l_{ij}$ . The Soave and Peng-Robinson equations have predicted the solubility data of Table VII within the expected uncertainty of 0.001 in  $\text{CO}_2$  liquid mole fraction with the exception of one point of the 150°C isotherm. This point was omitted during data regression.

Two other investigators have studied the binary  $\text{CO}_2$  + phenanthrene. Y.-K. Chen et al. (7) studied the solubility of  $\text{CO}_2$  in phenanthrene at one atmosphere and temperatures ranging from 105 to 145°C. DeVaney et al. (8) measured vapor-liquid equilibria for  $\text{CO}_2$  + phenanthrene at temperatures from 104.4 to 426.7°C and pressures from 200 to 1600 psia.

Values for  $k_{ij}$  were regressed from the data of these authors and plotted against temperature for comparison with the optimum values of  $k_{ij}$  from this work (Figure 21). This comparison was made using the single interaction parameter,  $k_{ij}$ , because values for both  $k_{ij}$  and  $l_{ij}$  could not be regressed from Chen's solubility data (single datum point at each temperature). At low temperature, Figure 21 shows that binary

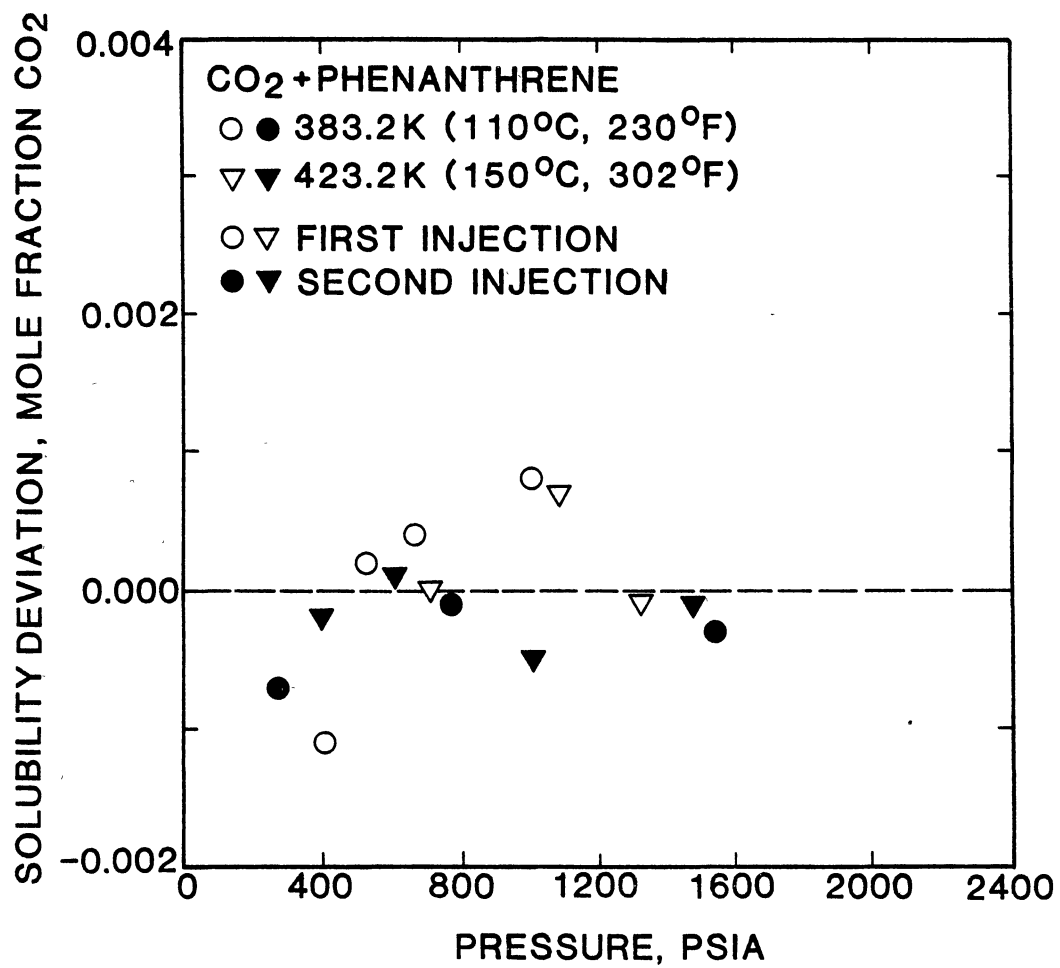


Figure 20. Soave and Peng-Robinson Representations of CO<sub>2</sub> Solubility in Phenanthrene

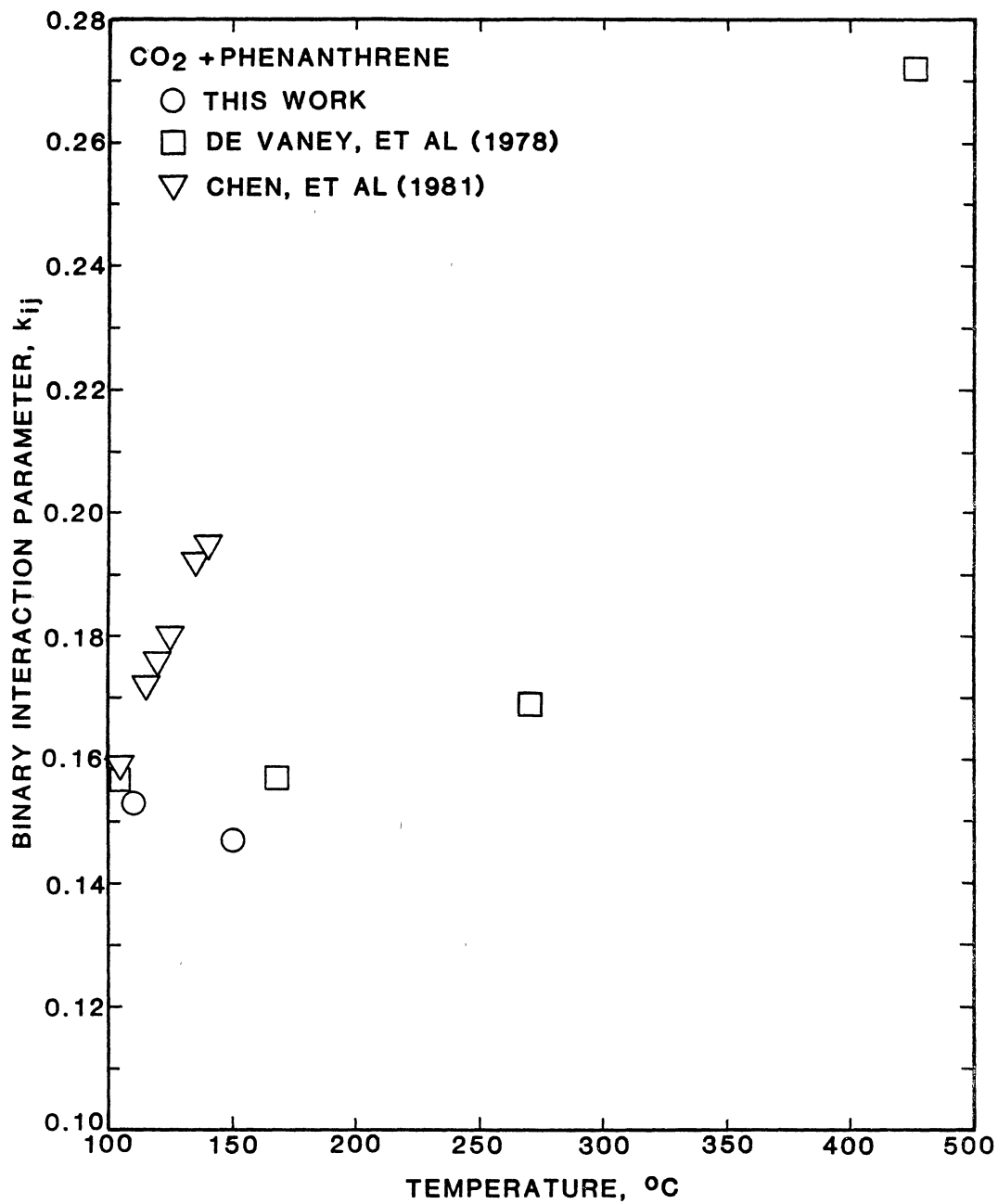


Figure 21. Comparison of Binary Interaction Parameters for CO<sub>2</sub> + Phenanthrene

interaction parameters regressed from the work of Chen and DeVaney at 105 and 104.4°C, respectively, agree well with the interaction parameter regressed at 110°C from this work. However, as temperature increases the interaction parameters of each author show different trends. Interaction parameters regressed from Chen increase with temperature in a linear fashion while those of DeVaney increase exponentially with temperature. The interaction parameters regressed from this work decrease with temperature.

The solubility of CO<sub>2</sub> in phenanthrene at one atmosphere pressure was estimated from the data of this work and of DeVaney at the temperatures studied by extrapolating  $P_b/x_{CO_2}$  versus  $x_{CO_2}$  plots to a pressure of one atmosphere. Figure 22 compares the work of Y. K. Chen with these estimates. The atmospheric solubilities of CO<sub>2</sub> in phenanthrene from extrapolating the data of this work show reasonable agreement with Chen. Extrapolating the work of DeVaney produces a trend of consistently lower values of atmospheric solubilities.

The last system investigated study was CO<sub>2</sub> + pyrene at 160°C. Table IX presents the CO<sub>2</sub> liquid mole fraction studied and corresponding bubble-point pressure for this system. Figure 23 shows the data of Table IX in the same format used for the data for CO<sub>2</sub> + naphthalene and CO<sub>2</sub> + phenanthrene.

The values of interaction parameters (using both  $k_{ij}$ ,  $l_{ij}$  and  $k_{ij}$  regressed alone) for this system are given in Table VI. As with the other systems examined in this work, the interaction parameters for the SRK and P-R equations are very similar and yield the same error in predicted CO<sub>2</sub> mole fraction. Figure 24 shows the precision of the SRK and P-R equations in their ability to model the data of Table VIII for

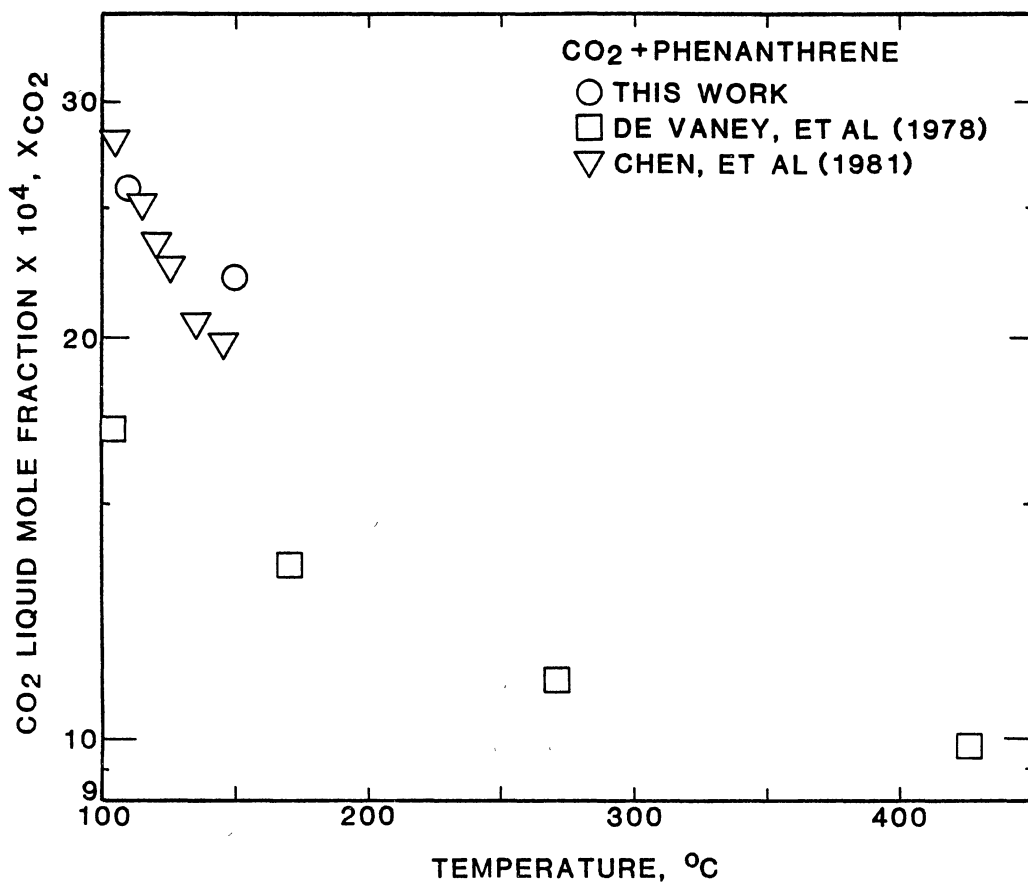


Figure 22. Solubility of CO<sub>2</sub> in Phenanthrene at One Atmosphere



TABLE IX  
SOLUBILITY OF CO<sub>2</sub> IN PYRENE

| Mole Fraction<br>CO <sub>2</sub> | Pressure<br>MPa | (psia)   |
|----------------------------------|-----------------|----------|
| -----433.2K (160°C, 320°F)-----  |                 |          |
| 0.040                            | 0.734           | (106.4)  |
| 0.057                            | 3.135           | (454.7)  |
| 0.069                            | 3.898           | (565.4)  |
| 0.100                            | 5.817           | (843.7)  |
| 0.156                            | 9.662           | (1401.4) |
| 0.159                            | 9.843           | (1427.6) |
| 0.168                            | 10.572          | (1533.4) |

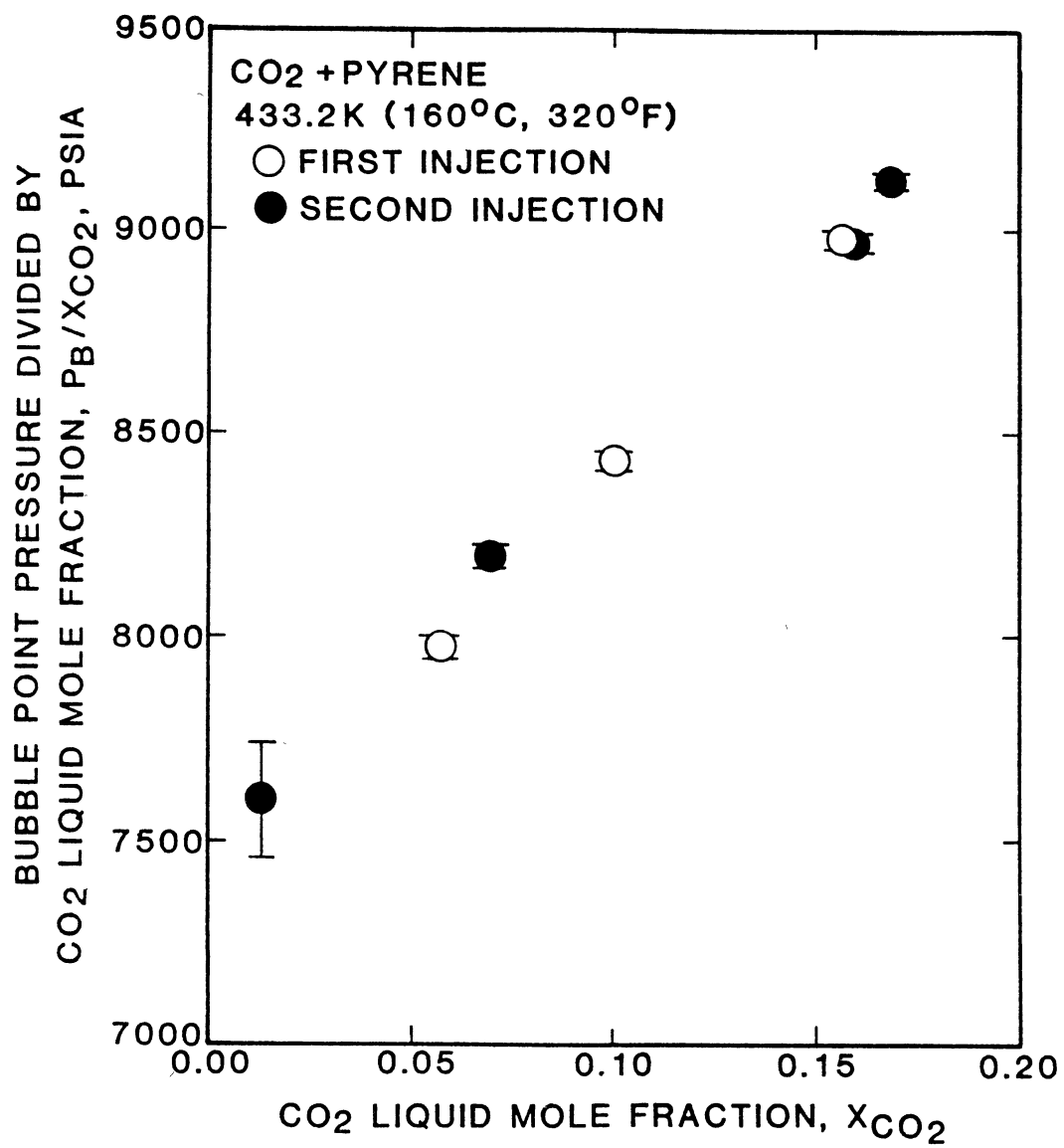


Figure 23. Bubble-Point Data for CO<sub>2</sub> + Pyrene at 160°C

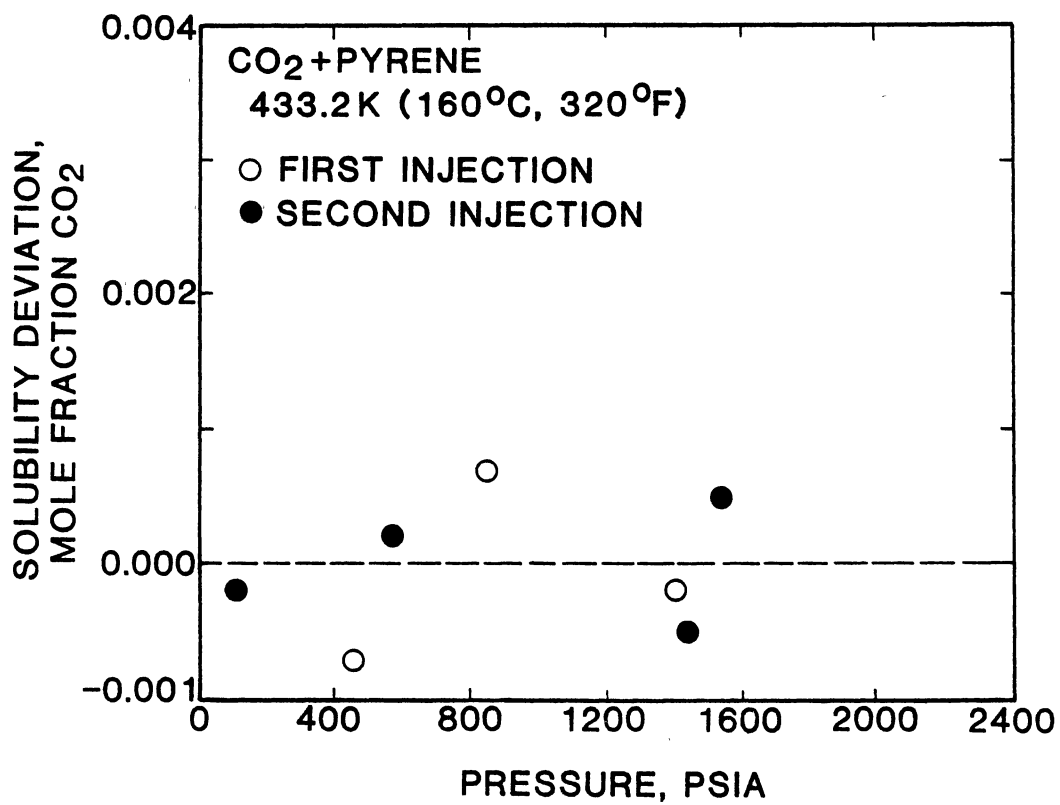


Figure 24. Soave and Peng-Robinson Representations of CO<sub>2</sub> Solubility in Pyrene

CO<sub>2</sub> + pyrene using two interaction parameters,  $k_{ij}$  and  $l_{ij}$ . Here the deviations between the experimental and predicted solubilities all lie within the claimed uncertainty of 0.001 in CO<sub>2</sub> liquid mole fraction.

Comparing the values of  $k_{ij}$  and  $l_{ij}$  for CO<sub>2</sub> + pyrene to values estimated for the other systems studied in this work reveals a large increase in the value of  $k_{ij}$  and a larger than expected value of  $l_{ij}$ . These larger than expected values for  $k_{ij}$  and  $l_{ij}$  may be due to the estimated values of critical properties used for pyrene in data regression (pyrene begins to thermally decompose before critical conditions can be reached for measurement; hence critical properties can only be estimated). The equations of state used in this study require the critical properties of the components of a system they are to model. Discrepancies in the estimated critical properties used and the (unknown) real critical properties would cause error in the resulting values of  $k_{ij}$  and  $l_{ij}$  regressed from experimental data. Table X lists the critical properties for the solvents studied in this work.

TABLE X  
CRITICAL PROPERTIES USED IN EQUATIONS OF STATE

| Solvent      | Pressure<br>(MPa) | Temperature<br>(K) | Acentric<br>Factor | Reference |
|--------------|-------------------|--------------------|--------------------|-----------|
| Benzene      | 4.898             | 561.7              | 0.225              | (29)      |
| Naphthalene  | 4.114             | 748.4              | 0.315              | (30)      |
| Phenanthrene | 3.30              | 873.2              | 0.540              | (31)      |
| Pyrene       | 2.60              | 938.2              | 0.344              | (32)      |

Figures 25 and 26 show the change in the lumped parameter values of  $k_{ij}$  and  $l_{ij}$  (using the SRK equation for representation purposes) with the number of benzene rings in the solvent molecule and with solvent molecular weight, respectively. Figure 27 shows the change in the values of  $k_{ij}$  and  $l_{ij}$  for each isotherm as a function of the solvent density. These figures show that the value of  $k_{ij}$  has a tendency to increase exponentially with solvent complexity and density. The value of  $l_{ij}$  has a tendency to decrease linearly with solvent complexity and density.

All the interaction parameters of Table VI show the same trend when comparing values of  $k_{ij}$  when regressed with  $l_{ij}$  and when regressed alone. The value of  $k_{ij}$  increases with temperature and is larger when regressed alone than when regressed with  $l_{ij}$ . The values for  $l_{ij}$  all decrease with temperature as well as with the complexity of the solvent.

The error in predicted  $\text{CO}_2$  mole fractions presented in Table VI (when using either the Soave or P-R equation) show the greater ability of equations of state to model the data of this work when using both parameters,  $k_{ij}$  and  $l_{ij}$ , than with  $k_{ij}$  alone.

Henry's constants and partial molar volumes for  $\text{CO}_2$  were estimated for the systems examined in this work. Values for these parameters obtained using the Krichevsky-Kasarnovsky (K-K) equation (presented in detail in Chapter III) are listed in Table XI. The use of the K-K equation to estimate the Henry's constant and partial molar volume of  $\text{CO}_2$  for the system  $\text{CO}_2 + \text{benzene}$  is questionable due to the high volatility of benzene at  $40^\circ\text{C}$  (see assumptions constraining the use of the K-K equation in Chapter III).

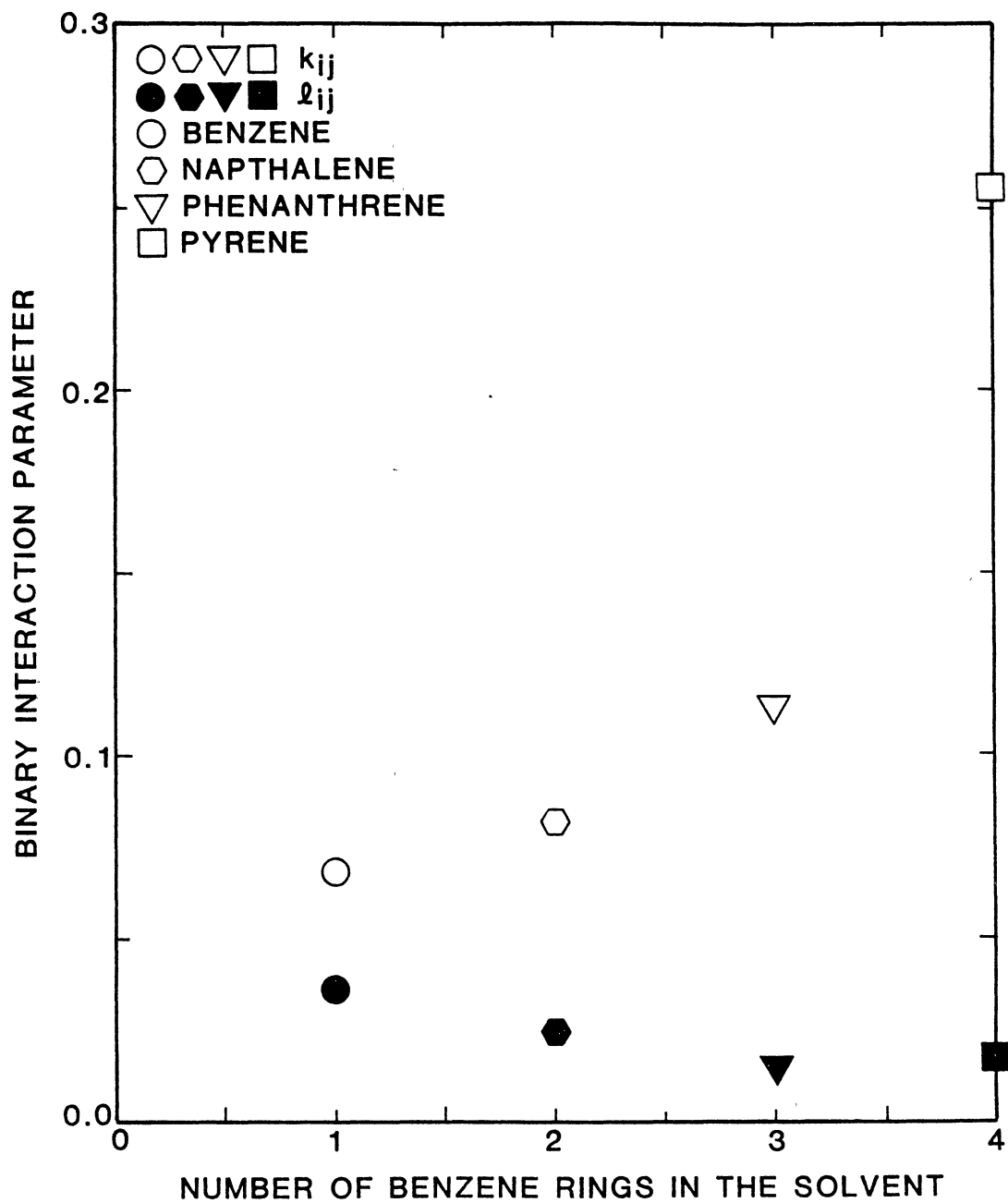


Figure 25. Binary Interaction Parameters Versus the Number of Benzene Rings in the Solvent

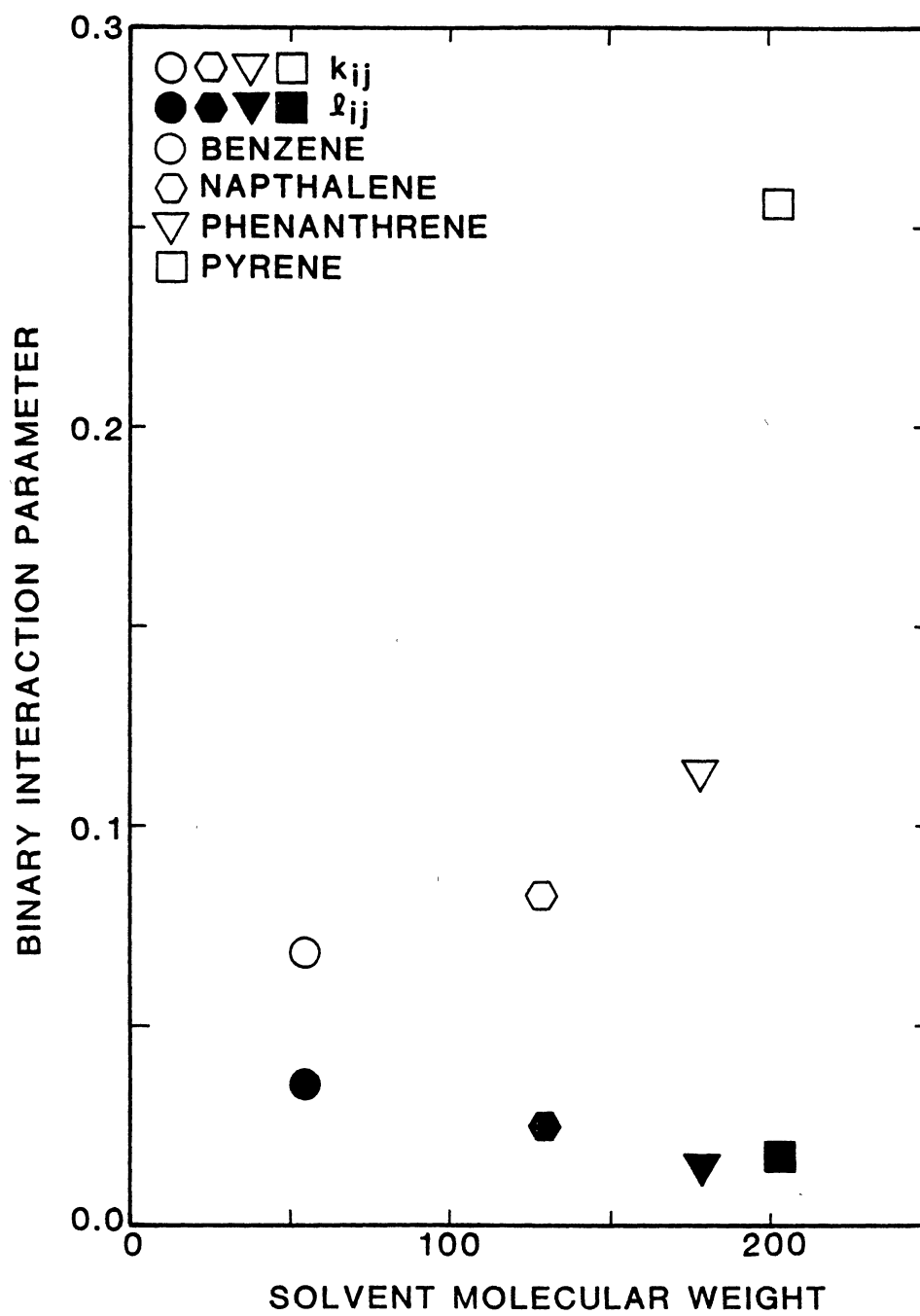


Figure 26. Binary Interaction Parameters Versus Solvent Molecular Weight

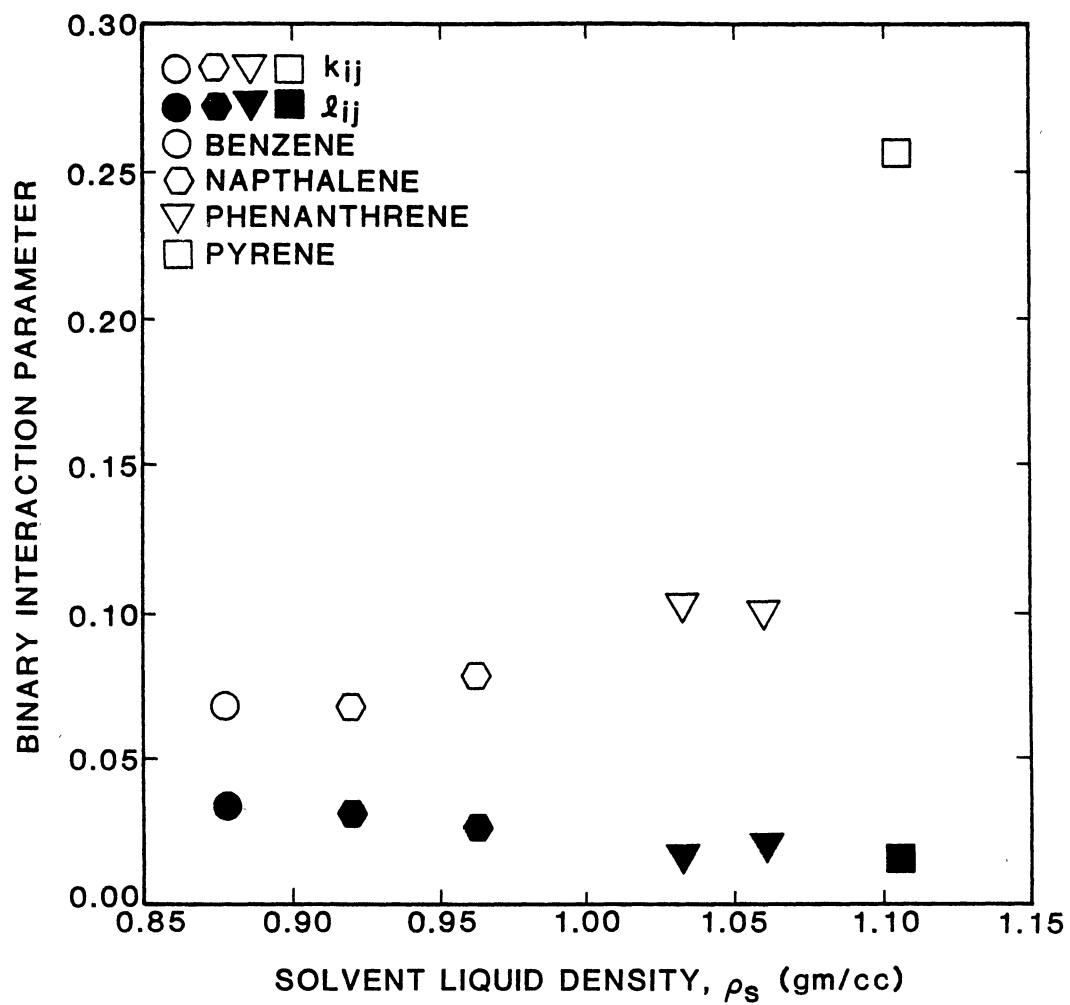


Figure 27. Binary Interaction Parameters Versus the Solvent Liquid Density



Examination of Table XI shows the Henry's constant increasing with complexity of the solvent as well as temperature. The Henry's constants of Table XI in the column labeled estimated were obtained by linear regression of the data shown in Figures 13, 15, 16, 18, 19 and 23 and determining the y-intercept (or Henry's constant) of these figures. The resulting estimated Henry's constants are within 5% of the results of the K-K analysis.

The partial molar volumes of  $\text{CO}_2$  listed in Table XI begin at largely negative values and become more positive with solvent complexity and temperature. The negative partial molar volumes suggesting the solvent volume shrinks upon mixture of  $\text{CO}_2$  with the solvent. The partial molar volumes obtained from K-K analysis are subject to larger uncertainties than Henry's constants and care should be observed in attributing physical significance to these values.

Henry's constant and partial molar volume data for these systems could not be found in the literature for comparison purposes.

A summary of the densities of  $\text{CO}_2$  and solvents and the volumes of each injected during collection of experimental data is given in Table XII. The references from which the solvent densities were obtained are also listed in Table XII with the exception of pyrene.

No density data could be found on pyrene, so its density was measured. This was done by removing the equilibrium cell from the apparatus and mounting a pre-weighed bottle in its place. The hydrocarbon injection pump was then used to inject a known volume of pyrene into the bottle at conditions similar to the experimental temperature and pressure at which pyrene was studied. The bottle was then removed from the apparatus, allowed to cool to room temperature,

TABLE XI  
HENRY'S CONSTANTS AND PARTIAL  
MOLAR VOLUMES FOR CO<sub>2</sub>

| Solvent      | Temperature<br>(°C) | Henry's<br>Constant,<br>K-K<br>(psia) | Henry's<br>Constant,<br>estimated<br>(psia) | Partial Molar<br>Volume CO <sub>2</sub><br>(g/cc) |
|--------------|---------------------|---------------------------------------|---|---|
| Benzene      | 40                  | 1935                                  | 1835  | -283.1  |
| Naphthalene  | 100                 | 4240                                  | 4210  | -56.9   |
|              | 150                 | 5436                                  | 5570  | -30.9   |
| Phenanthrene | 110                 | 5672                                  | 5610  | -17.6   |
|              | 150                 | 6619                                  | 6600  | -4.2  |
| Pyrene       | 160                 | 7522                                  | 7425  | 18.9  |

TABLE XII  
 DENSITIES AND VOLUMES USED  
 TO CALCULATE SOLUBILITIES

| Solvent*<br>Density<br>(g/cc)<br>$\rho_{HC}$ | Volume<br>of Solvent<br>Injected<br>(cc)<br>$V_{HC}$ | Injection<br>Pressure for<br>CO <sub>2</sub> at 50°C<br>(psia) | Calculated<br>CO <sub>2</sub> density<br>(g/cc)<br>$\rho_{CO_2}$ | Volume<br>of CO <sub>2</sub><br>Injected<br>(cc)<br>$V_{iCO_2}$ | Solvent<br>Injection |
|--|--|--|--|---|----------------------|
| -----Benzene 40°C-----                       |  |  |  |   |                      |
| 0.8577                                       | 6.80   | 589.3  | 0.0830   | 6.39  | 1                    |
|  |  | 589.3  | 0.0830   | 12.72   | 1                    |
|  |  | 595.6  | 0.0839   | 7.63  | 1                    |
|  | 4.14   | 576.7  | 0.0808   | 5.48  | 2                    |
|  | 7.06   | 748.2  | 0.1108   | 30.76   | 3                    |
|  | -----Naphthalene 100°C-----                          |  |  |   |                      |
| 0.9628                                       | 6.74   | 693.4  | 0.0989   | 3.46  | 1                    |
|  |  | 693.4  | 0.0989   | 3.96  | 1                    |
|  |  | 693.4  | 0.0989   | 4.01  | 1                    |
|  | 7.30   | 756.9  | 0.1112   | 1.07  | 2                    |
|  |  | 756.9  | 0.1112   | 1.54  | 2                    |
|  |  | 756.9  | 0.1112   | 1.61  | 2                    |
|  |  | 756.9  | 0.1112   | 1.27  | 2                    |
|  |  | 756.9  | 0.1112   | 1.27  | 2                    |

TABLE XII (Continued)

| Solvent*<br>Density<br>(g/cc)<br>PHC | Volume<br>of Solvent<br>Injected<br>(cc)<br>$V_{HC}$ | Injection<br>Pressure for<br>$CO_2$ at 50°C<br>(psia) | Calculated<br>$CO_2$ density<br>(g/cc)<br>$\rho_{CO_2}$ | Volume<br>of $CO_2$<br>Injected<br>(cc)<br>$V_{iCO_2}$ | Solvent<br>Injection |
|--------------------------------------|--|---|---|--|----------------------|
| -----Naphthalene 150°C-----          |  |   |   |  |                      |
| 0.9219                               | 7.55   | 670.9   | 0.0948  | 1.36   | 1                    |
|                                      |  | 670.9   | 0.0948  | 1.74   | 1                    |
|                                      |  | 670.9   | 0.0948  | 1.74   | 1                    |
|                                      | 5.72   | 742.3   | 0.1083  | 2.00   | 2                    |
|                                      |  | 742.3   | 0.1083  | 0.97   | 2                    |
|                                      |  | 742.3   | 0.0183  | 1.86   | 2                    |
|                                      |  | 742.3   | 0.0183  | 0.77   | 2                    |
| -----Phenanthrene 110°C-----         |  |   |   |  |                      |
| 1.0613                               | 7.24   | 833.1   | 0.1270  | 1.11   | 1                    |
|                                      | 7.78   | 815.3   | 0.1232  | 0.81   | 2                    |
|                                      |  | 815.3   | 0.1232  | 1.60   | 2                    |
|                                      | 7.49   | 786.8   | 0.1132  | 5.01   | 3                    |
|                                      | 7.55   | 786.8   | 0.1172  | 2.05   | 4                    |
|                                      |  | 786.8   | 0.1172  | 1.25   | 4                    |
|                                      | 7.86   | 775.5   | 0.1149  | 1.70   | 5                    |

TABLE XII (Continued)

| Solvent*<br>Density<br>(g/cc)<br>$\rho_{HC}$ | Volume<br>of Solvent<br>Injected<br>(cc)<br>$V_{HC}$ | Injection<br>Pressure for<br>$CO_2$ at 50°C<br>(psia) | Calculated<br>$CO_2$ density<br>(g/cc)<br>$\rho_{CO_2}$ | Volume<br>of $CO_2$<br>Injected<br>(cc)<br>$V_{iCO_2}$ | Solvent<br>Injection |
|--|--|---|---|--|----------------------|
| -----Phenathrene 150°C-----                  |  |   |   |  |                      |
| 1.0613†                                      | 7.86   | 775.5   | 0.1149  | 2.06   | 1                    |
|  |  | 775.5   | 0.1149  | 1.08   | 1                    |
|  |  | 775.5   | 0.1149  | 0.74   | 1                    |
| 1.0326                                       | 8.42   | 768.5   | 0.1135  | 1.17   | 2                    |
|  |  | 768.5   | 0.1135  | 0.62   | 2                    |
|  |  | 768.5   | 0.1135  | 1.29   | 2                    |
|  |  | 768.5   | 0.1135  | 1.50   | 2                    |
| -----Pyrene 160°C-----                       |  |   |   |  |                      |
| 1.107  | 6.57   | 743.6   | 0.1085  | 0.87   | 1                    |
|  |  | 743.6   | 1.1085  | 0.73   | 1                    |
|  |  | 743.6   | 0.1085  | 1.08   | 1                    |
|  | 7.34   | 723.6   | 0.1046  | 0.24   | 2                    |
|  |  | 723.6   | 0.1046  | 1.02   | 2                    |
|  |  | 723.6   | 0.1046  | 1.94   | 2                    |
|  |  | 723.6   | 0.1046  | 0.21   | 2                    |

†Solvent injection made at 110°C.

\*Density references: Benzene (33), Napthalene (34), Phenanthrene (34)

and vented to allow equalization of air pressure inside the bottle to the atmosphere. A mettler balance (Mettler Instrument Corporation, type B6, number 63592) was used to measure the weight of the bottle and pyrene, from which the weight of the bottle was subtracted. Two density measurements were made, the first yielding 1.10830 g/cc and the second 1.1053 g/cc, with an average density of 1.10682 g/cc which was rounded 1.107 g/cc for calculations.

The solubilities of CO<sub>2</sub> for all bubble points presented in this work can be recalculated in the event that discrepancies are found between CO<sub>2</sub> or solvent densities used in this work and those of some other source (by use of Table XII). Using the preferred CO<sub>2</sub> or solvent density, in conjunction with the volume data of Table XII, corrected CO<sub>2</sub> solubilities can be obtained from the following equation:

$$x_{CO_2} = \frac{\rho_{CO_2} \sum_{i=1}^N V_{iCO_2} / MW_{CO_2}}{\rho_{CO_2} \sum_{i=1}^N V_{iCO_2} / MW_{CO_2} + \rho_{HC} V_{HC} / MW_{HC}} \quad (7.1)$$

Overall, the bubble-point apparatus operated very well over the course of data collection with a few inconveniences. Occasionally the higher melting point solvents solidified in exposed portions of heated tubing during clean up. This problem was overcome by applying direct heat to the tubing using a heat gun. The 1/16" tubing used for pressure measuring lines restricted the mercury flow through these lines, increasing the time required to clean the apparatus. And last, the temperature controller of the injection pump air bath was more powerful

than the needs of this air bath. This required fine tune temperature adjustments to occasionally be made to this controller.

## CHAPTER VIII

### CONCLUSIONS AND RECOMMENDATIONS

This work involved the measurement of high pressure solubilities of  $\text{CO}_2$  in the aromatic solvents benzene, naphthalene, phenanthrene, and pyrene. Based on this work, the following conclusions and recommendations are made.

#### Conclusions

1. A magnetically stirred bubble-point apparatus has successfully been constructed and tested.
2. Measurement of vapor pressures of pure pentane and benzene have been made and agree within 0.5 psi with literature data.
3. The solubility of  $\text{CO}_2$  in benzene at  $40^\circ\text{C}$  has been measured at several  $\text{CO}_2$  mole fractions using the apparatus. This solubility data is consistent with the work of several other experimenters who studied this system.
4. The solubility of  $\text{CO}_2$  in the aromatic solvents naphthalene, phenanthrene, and pyrene have been measured at temperature of 100 to  $160^\circ\text{C}$  and pressures from 200 to 1550 psia.
5. Binary interaction parameters for these systems have been regressed from resulting experimental data for the SRK and P-R equations of state.



6. Solubilities of  $\text{CO}_2$  predicted by the SRK and P-R equations, using the binary interaction parameters  $k_{ij}$  and  $l_{ij}$ , are generally within the expected experimental error of 0.001 in  $\text{CO}_2$  mole fraction. Exceptions are three data points (two for the system  $\text{CO}_2$  + naphthalene and one for the system  $\text{CO}_2$  + phenanthrene) which were omitted during data regression. Errors in predicted  $\text{CO}_2$  solubilities were as large as 0.01 when a single interaction parameter  $k_{ij}$  was used for predictions.
7. Henry's constants and partial molar volumes of  $\text{CO}_2$  for the systems studied in this work have been regressed from experimental data using the K-K equation. Henry's constants obtained using the K-K equation were within 5% of Henry's constants estimated from the y-intercept of plots of bubble-point pressure divided by  $\text{CO}_2$  liquid mole fraction as a function of  $\text{CO}_2$  liquid mole fraction. Partial molar volumes resulting from K-K analysis yielded some negative values.

#### Recommendations

1. Further studies are recommended on  $\text{CO}_2$  + cyclic hydrocarbons (naphthenic and aromatic) that are constituents found in coal to better define the behavior of these systems. Not only would these data benefit the design and operation of coal conversion processes, but they would aid in the search of generalized interaction parameter correlations for these systems.
2. The 1/16" tubing used for pressure measuring lines hindered the cleaning the apparatus. Mercury flow was restricted in these small

lines, increasing the time required to clean the apparatus. These lines should be replaced by 1/8" tubing to correct this problem.

3. A variable-resistance resistor should be placed in series with the injection pump air bath heater coil to reduce the amount of power supplied to the heater coil by the temperature controller. This resistance should then be adjusted to optimize the temperature control in the injection pump air bath.

## A SELECTED BIBLIOGRAPHY

- (1) Robinson, R. L. Phase Behavior of Coal Fluids: Data for Correlation Development. Oklahoma State University. Proposal No. EN 83-R-102, to U.S. Department of Energy Pittsburgh Energy Technology Center, 1983.
- (2) Donohue, Marc D. Personal Communication. Johns Hopkins University, Baltimore, Maryland, July 10, 1984.
- (3) Gupta, Mukesh K., Ying-Hsiao Li, Barry L. Hulsey, and Robert L. Robinson, Jr. "Phase Equilibrium for Carbon Dioxide-Benzene at 313.2, 353.2, and 593.2K." Journal of Chem. and Engr. Data, 27 (1982), 55-57.
- (4) Nagarajan, N., Y.-K. Chen, and Robert L. Robinson, Jr. Interfacial Tensions in Carbon Dioxide - Hydrocarbon Systems: Development of Experimental Facilities and Acquisition of Experimental Data. Experimental Data for CO<sub>2</sub> + Benzene. Progress Report to Amoco Production Co., Stillwater, Oklahoma, June 15, 1984.
- (5) Ohgaki, K. and T. Katayama. "Isothermal Vapor-Liquid Equilibrium Data for Binary Systems Containing Carbon Dioxide at High Pressures: Methanol - Carbon Dioxide, n-Hexane - Carbon Dioxide Systems." Journal of Chem. and Engr. Data, 21 (1976), 53-55.
- (6) Gasem, K. A., Ph.D. Dissertation, Oklahoma State University, Stillwater, Oklahoma (in preparation), 1985.
- (7) Chen, Y.-K., John J. Heidman, Phillip J. Carlberg, and Robert L. Robinson, Jr. The Equilibrium Phase Behavior of Several Solute Gases in the Solvent Phenanthrene. Research Report RR-54, Gas Processors Association, Tulsa, Oklahoma, 1981.
- (8) DeVaney, Will, James M. Berryman, Pen-Li Kao, and Bert Eakin. High Temperature V-L-E Measurements for Substitute Gas Components. Research Report RR-30, 1978, Gas Processors Association, Tulsa, Oklahoma.
- (9) Orlov, M. L., A. M. Cherkasova, M. I. Tyaptina, and V. P. Mashkina, Vopr. Tekhnol. Ulavliraniya I. Pererab Produktor Koksovaniya, 6, 46 (1977); Ca 89, 113674 (1978).

- (10) Huron, Marie-Jose, Gery-Noel Dufarn, and Jean Vidal. "Vapour-Liquid Equilibrium and Critical Locus Curve Calculations With the Soave Equation for Hydrocarbon Systems with Carbon Dioxide and Hydrogen Sulphide." Fluid Phase Equilibria, 1 (1977), 247-265.
- (11) Graboski, Michael S. and Thomas E. Daubert. "A Modified Soave Equation of State for Phase Equilibrium Calculations. 2. Systems Containing CO<sub>2</sub>, H<sub>2</sub>S, N<sub>2</sub> and CO." Ind. Eng. Chem. Process Des. Dev., 17, 4 (1978), 448-454.
- (12) Mundis, C. J., L. Yarborough, and R. L. Robinson, Jr., "Vaporization Equilibrium Ratios for CO<sub>2</sub> and H<sub>2</sub>S in Paraffinic, Naphthenic, and Aromatic Solvents." Ind. Eng. Chem., Process Des. Dev., 16, 2 (1977) 254-259.
- (13) Lin, H.-M. "Peng-Robinson Equation of State for Vapor-Liquid Equilibrium Calculations for Carbon Dioxide + Hydrocarbon Mixtures." Fluid Phase Equilibria, 16 (1984), 151-169.
- (14) Turek, Edward A., R. S. Metcalfe, L. Yarborough, and R. L. Robinson, Jr., "Phase Equilibria in CO<sub>2</sub>-Multicomponent Hydrocarbon Systems: Experimental Data and an Improved Prediction Technique." Society of Petroleum Engineers Journal, June, 1984, pp. 308-324.
- (15) Yarborough, L. "Application of a Generalized Equation of State to Petroleum Reservoir Fluid" in Equations of State in Engineering and Research, Advances in Chemistry Series, 182, K. C. Chao and R. L. Robinson, Jr., (Editors), American Chemical Society, Washington, D.C. (1979).
- (16) Robinson, R. L., Jr., "Review of Phase Equilibrium Thermodynamics", Class Notes, Cheng 5843, Oklahoma State University, Spring 1984.
- (17) Robinson, R. L., Jr., "Fugacity", Class Notes, Cheng 5843, Oklahoma State University, Spring 1984.
- (18) Soave, G. "Equilibrium Constants from a Modified Redlich-Kwong Equation of State", Chem. Eng. Sci., 27 (1972) 1197-1203.
- (19) Robinson, Donald B. and Ding-Yu Peng, "A New Two-Constant Equation of State". Ind. Eng. Chem., Fundam., 15 (1976) 59-64.
- (20) Krichevsky, I. R. and J. S. Kasarnovsky, "Thermodynamical Calculations of Solubilities of Nitrogen and Hydrogen in Water at High Pressures". J. Chem. Soc., 57 (1935) 2168-2171.

- (21) Eubank, P. T., K. R. Hall, and J. C. Holste. "A Review of Experimental Techniques for Vapor-Liquid Equilibria", in 2nd International Conference on Phase Equilibria and Fluid Properties in the Chemical Industry, H. Knapp and S. I. Sandler (Editors), DECHEMA, Frankfurt, Part II, 675-687 (1980).
- (22) Malanowski, S. "Experimental Methods for Vapor-Liquid Equilibria. Dew- and Bubble-Point Method". Fluid Phase Equilibria, 9 (1982) 311-317.
- (23) Sage, B. H., J. H. Schasfsma, and W. N. Lacey. "Phase Equilibria in Hydrocarbon Systems." Ind. Eng. Chem., 26 (1934), 1218-1224.
- (24) Tiffin, D. L., A. DeVera, K. D. Luks, and J. P. Kohn. "Phase Equilibria Behavior of the Systems Carbon Dioxide + n-Dotriacontane and Carbon Dioxide + n-Docosane." J. Chem. Engr. Data, 23 (1978) 45-47.
- (25) Anderson, J. M., M.S. Thesis, Oklahoma State University, Stillwater, Oklahoma (in preparation), 1985.
- (26) Angus, S., B. Armstrong, and K. M. deRueck. International Thermodynamic Tables of the Fluid State - 3. Carbon Dioxide, Pergamon Press, Oxford, 1973.
- (27) Miks, C. E., "Test Report, Ruska Dead Weight Gauge", (Cat. No. 2400.1, Serial No. 10381) Ruska Instrument Company, Houston, Texas, 1963.
- (28) "Lange's Handbook of Chemistry", 12th Edition, John A. Dean (Editor), McGraw-Hill Book Co., New York, 1979.
- (29) "Engineering Data Book", 9th Edition, Gas Processors Suppliers Associations, Tulsa, 1972.
- (30) Reid, Robert C., John M. Prausnitz, and Thomas K. Sherwood. The Properties of Gases and Liquids. 2nd Edition, New York: McGraw-Hill Book Co., 1977.
- (31) API Monograph Series. Anthracene and Phenanthrene. Washington, D.C.: American Petroleum Institute. Monograph No. 708, January 1979.
- (32) API Monograph Series. Four-Ring Condensed Aromatic Compounds. Washington D.C.: American Petroleum Institute. Monograph No. 709, March 1979.
- (33) API Research Project 44, Selected Values of Properties of Hydrocarbons and Related Compounds. Thermodynamics Research Center, Texas A&M College, College Station, Texas, Oct. 1972.

- (34) Gurevich, B. S. and V. M. Bednov. "Temperature Variation of the Density and Viscosities of Aromatic Substances." Russian Journal of Physical Chemistry, 46 (1972), 1532.

## APPENDIXES

## APPENDIX A

### EXPLANATION OF THE PROGRAM USED TO CALCULATE PERCENTAGE UNCERTAINTY IN CO<sub>2</sub> DENSITY

This program calculates the percentage uncertainty in CO<sub>2</sub> density as a function of pressure at a constant temperature using the Soave-Redlich-Kwong equation of state discussed in Chapter III and the following equation developed by error propagation of the CO<sub>2</sub> density (which is a function of both temperature and pressure):

$$\epsilon_{\rho_{\text{CO}_2}} = \left[ \left( \frac{\partial \rho_{\text{CO}_2}}{\partial P} \epsilon_P \right)^2 + \left( \frac{\partial \rho_{\text{CO}_2}}{\partial T} \epsilon_T \right)^2 \right]^{0.5}$$

The partial derivatives are calculated from the SRK equation of state, while the values for  $\epsilon_T$  and  $\epsilon_P$ , 0.1 K and 0.05 psi, respectively, are unique to the apparatus used in this study. Using these values, the program generates a table showing the percent uncertainty in CO<sub>2</sub> density as a function of pressure.



APPENDIX B  
COMPUTER PROGRAM USED TO CALCULATE  
CO<sub>2</sub> DENSITY AS A FUNCTION  
OF TEMPERATURE AND PRESSURE

This program calculates the density of carbon dioxide at a given temperature and pressure using an analytical equation of state developed by IUPAC (26). The program was set up interactively so that a density value could be calculated conveniently at the temperature and pressure conditions of a CO<sub>2</sub> injection. The program can handle a variety of units on the input variables which makes it very user friendly.

```

$JOB
C2345678901234567890
C
C
C      CALCULATE PRESSURE USING ANALYTICAL EQUATION OF STATE
C
C
1  IMPLICIT REAL *8 (A-G,O-Z)
2  DIMENSION BIJ(10,7),A(4),C(2),D(2)
3  DATA BIJ/-7.25854437D-01,4.47869183D-01,-1.72011999D-01,
C4.46304911D-03,2.55491571D-01,5.94667298D-02,
C-1.47960010D-01,1.36710441D-02,3.92284575D-02,
C-1.19872097D-02,-1.68332974D00,1.26050691D00,
C-1.83458178D00,-1.76300541D00,2.37414246D00,
C1.16974683D00,-1.69233071D00,-1.00492330D-01,
C4.41503812D-01,-8.46051949D-02,2.59587221D-01,
C5.96957049D00,-4.61487677D00,-1.11436705D01,
C7.50925141D00,7.43706410D00,-4.68219937D00,
C-1.63653806D00,8.86741970D-01,4.64564370D-02,
C3.76945574D-01,1.54645885D01,-3.82121926D00,
C-2.78215446D01,6.61133318D00,1.50646731D01,
C-3.13517448D00,-1.87082988D00,0.0D00,0.0D00,
C-6.70755370D-01,1.94449475D01,3.60171349D00,
C-2.71685720D01,-2.42663210D00,9.57496845D00,
C0.0D00,0.0D00,0.0D00,0.0D00,-8.71456126D-01,
C8.64880497D00,4.92265552D00,-6.42177872D00,
C-2.57944032D00,0.0D00,0.0D00,0.0D00,0.0D00,0.0D00,
C-1.49156928D-01,0.0D00,0.0D00,0.0D00,0.0D00,0.0D00,
C0.0D00,0.0D00,0.0D00,0.0D00/
4  DATA A/-6.8849249D00,-9.5924263D00,1.3679755D01,
C-8.6056439D00/
5  DATA C/3.822502D-01,4.2897885D-01/
6  WRITE(6,73)
7  73  FORMAT(/15X,'***** DETERMINATION OF CARBON DIOXIDE DENSITY *****
C*')
8  WRITE(6,74)
9  74  FORMAT(/20X,'ENTER TEMPERATURE UNITS')
10 WRITE(6,175)
11 175  FORMAT(20X,'1-FARENHEIT, 2-RANKINE, 3-KELVIN, 4-CELSIUS?')
12 READ(5,176) L1
13 176  FORMAT(I1)
14 WRITE(6,500) L1
15 500  FORMAT(20X,I1)
16 WRITE(6,177)
17 177  FORMAT(/20X,'ENTER PRESSURE UNITS')
18 WRITE(6,178)
19 178  FORMAT(20X,'1-PSIA, 2-ATM, 3-BAR ?')
20 READ(5,79) L2
21 79  FORMAT(I1)
22 WRITE(6,502) L2
23 502  FORMAT(20X,I1)
24 WRITE(6,81)
25 81  FORMAT(/20X,'ENTER DESIRED DENSITY UNITS')
26 WRITE(6,82)
27 82  FORMAT(20X,'1-G/CM3, 2-LB/FT3 ?')
28 READ(5,83) L3
29 83  FORMAT(I1)
30 WRITE(6,503) L3
31 503  FORMAT(20X,I1)

```

```

00000080
00000090
00000100
00000110
00000120
00000130
00000140
00000150
00000160
00000170
00000180
00000190
00000200
00000210
00000220
00000230
00000240
00000250
00000260
00000270
00000280
00000290
00000300
00000310
00000320
00000330
00000340
00000350
00000360
00000370
00000380
00000390
00000400
00000410
00000420
00000430
00000440
00000450
00000460
00000470
00000480
00000490
00000500
00000510
00000520
00000530
00000540
00000550
00000560
00000570
00000580
00000590
00000600
00000610
00000620
00000630
00000640
00000650
00000651
00000652

```

```

32      WRITE(6,199)
33 199  FORMAT(/5X,'FIX DECIMAL POINT WHEN ENTERING ALL REQUESTED DATA
      C'//)
34      WRITE(6,84)
35 84   FORMAT(/5X,'ENTER INITIAL TEMPERATURE')
36      READ(5,86) T
37 86   FORMAT(D10.4)
38      WRITE (6,504) T
39 504  FORMAT (5X,F7.2)
40      WRITE(6,87)
41 87   FORMAT(/5X,'ENTER FINAL TEMPERATURE')
42      READ(5,88) TFIN
43 88   FORMAT(D10.4)
44      WRITE (6,505) TFIN
45 505  FORMAT (5X,F7.2)
46      WRITE(6,89)
47 89   FORMAT(/5X,'ENTER TEMPERATURE INCREMENT')
48      READ(5,91)TINC
49 91   FORMAT(D10.4)
50      WRITE (6,506) TINC
51 506  FORMAT (5X,F7.2)
52      WRITE(6,92)
53 92   FORMAT(/5X,'ENTER INITIAL PRESSURE')
54      READ(5,93)P
55 93   FORMAT(D10.4)
56      WRITE (6,507) P
57 507  FORMAT (5X,F7.2)
58      WRITE(6,94)
59 94   FORMAT(/5X,'ENTER FINAL PRESSURE')
60      READ(5,95) PFIN
61      WRITE (6,508) PFIN
62 508  FORMAT (5X,F7.2)
63 95   FORMAT(D10.4)
64      WRITE(6,96)
65 96   FORMAT(/5X,'ENTER PRESSURE INCREMENT')
66      READ(5,97)PINC
67 97   FORMAT(D10.4)
68      WRITE (6,509) PINC
69 509  FORMAT (5X,F7.2)
70      WRITE(6,135)
71 135  FORMAT(/5X,'OUTPUT UNITS ARE ')
72      IF(L1.EQ.1)GO TO 251
73      IF(L1.EQ.2)GO TO 252
74      IF(L1.EQ.4)GO TO 253
75      IF(L1.EQ.3)GO TO 302
76 251  T=(T+460)/1.8
77      TFIN=(TFIN+460.0)/1.8
78      TINC=TINC/1.8
79      WRITE(6,136)
80 136  FORMAT(5X,'TEMPERATURE - DEGREES FARENHEIT')
81      GO TO 254
82 252  T=T/1.8
83      TFIN=TFIN/1.8
84      TINC=TINC/1.8
85      WRITE(6,137)
86 137  FORMAT(5X,'TEMPERATURE - DEGREES RANKINE')
87      GO TO 254
88 253  T=T+273.15
89      TFIN=TFIN+273.15
90      WRITE(6,138)

```

```

00000660
00000670
00000680
00000690
00000700
00000710
00000720
00000721
00000722
00000730
00000740
00000750
00000760
00000761
00000762
00000770
00000780
00000790
00000800
00000801
00000802
00000810
00000820
00000830
00000840
00000841
00000842
00000850
00000860
00000870
00000871
00000872
00000880
00000890
00000900
00000910
00000920
00000921
00000922
00000930
00000940
00000950
00000960
00000970
00000980
00000990
00001000
00001010
00001020
00001030
00001040
00001050
00001060
00001070
00001080
00001090
00001100
00001110
00001120
00001130

```

```

91 138 FORMAT(5X,'TEMPERATURE - DEGREES CELSIUS') 00001140
92 GO TO 254 00001150
93 302 WRITE(6,303) 00001160
94 303 FORMAT(5X,'TEMPERATURE - DEGREES KELVIN') 00001170
95 254 IF(L2 EQ 1)GO TO 155 00001180
96 IF(L2 EQ 2)GO TO 156 00001190
97 IF(L2 EQ 3)GO TO 305 00001200
98 155 P=0 068947*P 00001210
99 PINC=0 068947*PINC 00001220
100 PFIN=0 068947*PFIN 00001230
101 WRITE(6,141) 00001240
102 141 FORMAT(5X,'PRESSURE - PSIA') 00001250
103 GO TO 257 00001260
104 156 P=1 01325*P 00001270
105 PINC=1 01325*PINC 00001280
106 PFIN=1 01325*PFIN 00001290
107 WRITE(6,142) 00001300
108 142 FORMAT(5X,'PRESSURE - ATMOSPHERES') 00001310
109 GO TO 257 00001320
110 305 WRITE(6,306) 00001330
111 306 FORMAT(5X,'PRESSURE - BAR') 00001340
112 257 IF (L3 EQ 1)GO TO 310 00001350
113 WRITE(6,311) 00001360
114 311 FORMAT(5X,'DENSITY - POUNDS PER CUBIC FT') 00001370
115 GO TO 340 00001380
116 310 WRITE(6,312) 00001390
117 312 FORMAT(5X,'DENSITY - GRAMS PER CM3') 00001400
118 340 WRITE(6,98) 00001410
119 98 FORMAT(//10X,'PRESSURE',8X,'TEMPERATURE',8X,'CO2 DENSITY',13X,'Z') 00001420
120 WRITE(6,99) 00001430
121 99 FORMAT(9X,'-----',6X,'-----',6X, 00001440
C'-----',7X,'-----'/) 00001450
122 401 PIN=P 00001460
123 402 P=PIN 00001470
124 78 TC=304.21 00001480
125 PC=73.825 00001490
126 RHOC=0.010589 00001500
127 R=83 143 00001510
128 IF(T.GT TC)GO TO 22 00001520
129 PSUM=0 0 00001530
130 DO 23 I=1,4 00001540
131 PCONST=A(I)*(TC/T-1)**I 00001550
132 PSUM=PSUM+PCONST 00001560
133 23 CONTINUE 00001570
134 PSAT=PC*DEXP(11.3774*(1-T/TC)**1 935+PSUM) 00001580
135 IF(P.LT PSAT)GO TO 22 00001590
136 SUM=0 0 00001600
137 DO 26 I=1,2 00001610
138 CON=C(I)*((1-T/TC)**((I+1 0)/3 0)) 00001620
139 SUM=SUM+CON 00001630
140 26 CONTINUE 00001640
141 RHO=RHOC*(1+1 9073793*(1-T/TC)**0 347+SUM) 00001650
142 GO TO 41 00001660
143 22 RHO=P/(R*T) 00001670
144 41 M=0 00001680
145 31 SUM=0 0 00001690
146 TAU=304 2/I 00001700
147 OMEGA=RHO/O 01063 00001710
148 DO 100 J=1,7 00001720
149 DO 90 I=1,10 00001730

```

```

150          CONST=BIJ(I,J)*(1AU-1)**(J-1)*(OMEGA 1)**(I-1)          00001740
151          SUM=SUM+CONST          00001750
152      90      CONTINUE          00001760
153      100     CONTINUE          00001770
154          Z=1 O+OMEGA*SUM          00001780
155          R=83 143          00001790
156          PA=RHO*Z*R*T          00001800
C          00001810
C          00001820
C          00001830
C          00001840
C          CALCULATE CRITICAL EQUATION PARAMETERS          00001850
C          00001860
C          00001870
157          DELT=DABS((T-TC)/TC)          00001880
158          DELRHO=DABS((RHO-RHOC)/RHOC)          00001890
159          R=DELT +(O 6471102*DELRHO**2)**1 4409          00001900
160      25      X=R-O 6471102*R**O 306*DELRHO**2-DELT          00001910
161          ABSX=DABS(X)          00001920
162          IF (ABSX LT 1E-5)GO TO 20          00001930
163          DX=1-O 198016*DELRHO**2/R**O 694          00001940
164          R=R-X/DX          00001950
165          GO TO 25          00001960
166      20      THETA=O 670302*DELRHO/R**O 347          00001970
167          QT1=37 26895-82 70074*THETA**2+57 08947*THETA**4 O          00001980
168          IF (T GE TC)GO TO 30          00001990
169          CCAL=-53.81157          00002000
170          GO TO 40          00002010
171      30      CCAL=-34 92493          00002020
172      40      QT2=CCAL*DABS(1 O-1 440248*THETA**2.O)**1 934872          00002030
173          QTHETA=QT1+QT2          00002040
174          DELP=R**1 9348*QTHETA+6 98*DELT+28.362          00002050
C          *R**1 5879*THETA*(1-THETA**2)          00002060
175          PS=PC*(1+DELP)          00002070
C          00002080
C          THE FINAL EQUATION          00002090
C          00002100
176          EXP1=1-DEXP(-(O O1/R)**1 5)          00002110
177          EXP2=1-DEXP(-(O O5/R)**3 O)          00002120
178          FR=1-EXP1*EXP2          00002130
179          PCALC=FR*PA+(1-FR)*PS          00002140
180          ERR=DABS(P-PCALC)/P          00002150
181          IF (ERR.LT 1E-4)GO TO 160          00002160
182          IF (M EQ O)GO TO 131          00002170
183          DRHODP=(RHODEL-RHOOLD)/(PCALC-POLD)          00002180
184          RHO=RHOOLD+DRHODP*(P-POLD)          00002190
185          GO TO 41          00002200
186      131     M=1          00002210
187          POLD=PCALC          00002220
188          RHOOLD=RHO          00002230
189          DEL=O OOO1          00002240
190          RHODEL=RHO+DEL          00002250
191          RHO=RHODEL          00002260
192          GO TO 31          00002270
193      160     RHO=RHO*44 O09          00002280
194          IF (L1 EQ 1)GO TO 350          00002290
195          IF (L1 EQ 2)GO TO 351          00002300
196          IF (L1 EQ 4)GO TO 352          00002310
197          GO TO 353          00002320
198      350     HT4=1 8*T-460          00002330

```

```

199      GO TO 453                                00002340
200  351 HT4=1 8*T                                00002350
201      GO TO 453                                00002360
202  352 HT4=T-273 15                             00002370
203      GO TO 453                                00002380
204  353 HT4=T                                      00002390
205  453 IF(L2 EQ 1)GO TO 354                     00002400
206      IF(L2 EQ 2)GO TO 255                     00002410
207      GO TO 356                                 00002420
208  354 HP4=14 504*P                              00002430
209      GO TO 256                                 00002440
210  255 HP4=P/1 01325                             00002450
211      GO TO 256                                 00002460
212  356 HP4=P                                      00002470
213  256 IF(L3 EQ 1)GO TO 378                     00002480
214      HRHO4=RHO*62 371                         00002490
215      GO TO 379                                 00002500
216  378 HRHO4=RHO                                 00002510
217  379 R=83 143                                  00002520
218      Z=(PCALC*44 009)/(RHO*R*T)              00002530
219      HZ=Z                                       00002540
220      WRITE(6,170)HP4,HT4,HRHO4,HZ            00002550
221  170 FORMAT(7X,F10 2.8X,F10 2.10X,F10 6.8X,F10 5/) 00002560
222      P=P*PINC                                  00002570
223      IF(PINC EQ 0 0)GO TO 75                   00002580
224      IF (P GT PFIN)GO TO 75                   00002590
225      GO TO 78                                    00002600
226  75 T=T + TINC                                  00002610
227      IF(TINC EQ 0 0)GO TO 77                  00002620
228      IF (T GT TFIN)GO TO 77                   00002630
229      GO TO 402                                  00002640
230  77 STOP                                        00002650
231      END                                        00002660

$ENTRY                                           00002670

```

\*\*\*\*\* DETERMINATION OF CARBON DIOXIDE DENSITY \*\*\*\*\*

ENTER TEMPERATURE UNITS  
1-FARENHEIT, 2 RANKINE, 3 KELVIN, 4-CELSIUS?  
1

ENTER PRESSURE UNITS  
1-PSIA, 2-AIM, 3-BAR ?  
1

ENTER DESIRED DENSITY UNITS  
1-G/CM3, 2 LB/FT3 ?  
1

FIX DECIMAL POINT WHEN ENTERING ALL REQUESTED DATA

ENTER INITIAL TEMPERATURE  
212 00

ENTER FINAL TEMPERATURE  
212.00

ENTER TEMPERATURE INCREMENT  
0.00

ENTER INITIAL PRESSURE  
700.00

ENTER FINAL PRESSURE  
730.00

ENTER PRESSURE INCREMENT  
10.00

OUTPUT UNITS ARE:  
TEMPERATURE - DEGREES FARENHEIT  
PRESSURE - PSIA  
DENSITY - GRAMS PER CM3

| <u>PRESSURE</u> | <u>TEMPERATURE</u> | <u>CO2 DENSITY</u> | <u>Z</u> |
|-----------------|--------------------|--------------------|----------|
| 700.01          | 212.00             | 0.077497           | 0.88298  |
| 710.01          | 212.00             | 0.078758           | 0.88125  |
| 720.01          | 212.00             | 0.080024           | 0.87953  |
| 730.01          | 212.00             | 0.081295           | 0.87780  |

STATEMENTS EXECUTED= 5512

CORE USAGE OBJECT CODE= 9936 BYTES, ARRAY AREA= 624 BYTES, TOTAL AREA AVAILABLE= 129024 BYTES

DIAGNOSTICS NUMBER OF ERRORS= 0, NUMBER OF WARNINGS= 0, NUMBER OF EXTENSIONS= 0

COMPILE TIME= 0 09 SEC, EXECUTION TIME= 0.07 SEC, 11.02 39 THURSDAY 4 OCT 84 WATFIV - MAR 1980 V2LO

C\$STOP

## APPENDIX C

### COMPUTER PROGRAM USED IN CALIBRATION OF PRESSURE TRANSDUCERS

This is an iterative program which calculates the hydrocarbon transducer correction used to adjust experimental pressure measurements taken with the bubble point apparatus. The gauge correction is calculated as the difference between the transducer pressure readout and the Ruska dead weight gauge reference pressure. The Ruska pressure is calculated from an equation supplied in the manual which accompanied the dead weight gauge tester (27). The equation (shown in lines 24-28 of the program) is a function of several variables; the sum of the masses placed on the floating piston (SUMMAS (M)), the tare mass of the floating piston (TARMAS), acceleration due to gravity (C1), the temperature of the floating piston hydraulic oil (TEMP), the transducer pressure reading (GAUGE (N,M)), and five constants (C2-C6) which are supplied by the manual. After the reference pressure is calculated, the head correction is subtracted from it to account for the difference in fluid levels between the mercury in the equilibrium cell and the dead weight gauge tester reference line. The head correction is calculated as follows:

$$HC = g[\rho_{Hg}(h_{Hgcell} - h_{if}) - \rho_{oil}(h_{ref} - h_{if})] \quad (A)$$



After substituting the values of the various heights measured with the cathetometer,  $h_{\text{Hgcell}} = 577.5\text{mm}$ ,  $h_{if} = 116.95\text{mm}$ , and  $h_{\text{ref}} = 223.3\text{mm}$ , as well as an appropriate value for the acceleration due to gravity, a value for HC is calculated from the equation to be 8.7 psi. Once the values for the head correction and the various transducer gauge pressure readings have been read into the program, a table is printed out which can be used to determine the gauge correction required at any pressure within the set range of calibration. A useful list of weight combinations (Table A) is included to show the combinations of weights used and the corresponding dead weight reference pressures calculated using those combinations.

TABLE A

| Weight Combination | Resulting Reference Pressure, psig |
|--------------------|------------------------------------|
| Q                  | 49.94                              |
| P                  | 79.90                              |
| O                  | 129.84                             |
| O, P               | 179.77                             |
| M                  | 229.71                             |
| M, Q               | 249.68                             |
| M, P               | 279.65                             |
| N, O, P            | 379.52                             |
| M, N               | 429.08                             |
| M, N, O            | 529.33                             |
| L, O               | 629.21                             |
| L, M               | 729.08                             |
| L, M, O            | 829.03                             |
| L, M, N            | 928.83                             |
| L, M, N, O         | 1028.70                            |
| A, O               | 1128.58                            |
| A, N               | 1228.42                            |
| A, M, O            | 1328.30                            |
| A, M, N            | 1428.17                            |
| A, M, N, O         | 1528.05                            |
| A, L, O            | 1627.93                            |

```

$JOB
C
C
C      THIS PROGRAM CALCULATES TRANSDUCER CORRECTIONS FOR THE PRESSURE
C      HYDROCARBON TRANSDUCER LOCATED IN EN412 FROM DEAD WEIGHT
C      TEST DATA
C
C      USER I D U14702F
C      PROGRAM NAME TCRSS CNTL
C
C
1      DIMENSION SUMMAS(21),GAUGE(2,21),DWP(2,21),GC(2,21),
2      TRANSP(2,21),HEAD(2),GAUGE(2)
3      DOUBLE PRECISION C1,C2
4      DATA C1,C2,C3,C4/O 998951759.0,0260416.1 0,0 000017/
5      DATA C5,C6/25 0,0 2356E-08/
6      DATA TEMP/24 4/
7      DATA HEAD/8 7,0 0/
8      DATA NUMP,TARMAS/21,0 78107/
9      DATA MONTH,NDATE,NYEAR/8,28,84/
10     DO 20 N=1,2
11     DO 10 M=1,NUMP
12     READ (5,5) TRANSP(N,M)
13     5    FORMAT (F9 3)
14     10   CONTINUE
15     20   CONTINUE
16     DO 40 N=1,2
17     DO 30 M=1,NUMP
18     GAUGE(N,M) = TRANSP(N,M) - 14 696
19     30   CONTINUE
20     40   CONTINUE
21     READ (5,50) (SUMMAS(I),I=1,NUMP)
22     50   FORMAT (F10 6)
23     DO 70 N=1,2
24     DO 60 M=1,NUMP
25     DWP(N,M) = (SUMMAS(M) + TARMAS)*C1
26     DWP(N,M) = DWP(N,M) + C2*(C3 + C4*(TEMP - C5))*(C3 - C6*GAUGE(N,M))
27     DWP(N,M) = DWP(N,M) / DWP(N,M)
28     TRUEP(N,M) = DWP(N,M) - HEAD(N)
29     GC(N,M) = TRUEP(N,M) - GAUGE(N,M)
30     60   CONTINUE
31     70   CONTINUE
32     WRITE (6,120) MONTH,NDATE,NYEAR
33     120  FORMAT (///40X,'DATE ',1X,I2,'/',1X,I2,'/',1X,I2,'/',12//)
34     WRITE (6,130)
35     130  FORMAT (10X,'INPUT UNITS ARE DEG C AND PSIA'////)
36     WRITE (6,80)
37     80   FORMAT (///20X,'HYDROCARBON TRANSDUCER CORRECTIONS'///)
38     WRITE (6,90)
39     90   FORMAT (15X,'TRANS PRESS',5X,D W PRESS',5X,'TRANSD CORR'///)
40     WRITE (6,100) (TRANSP(1,M),DWP(1,M),GC(1,M),M=1,NUMP)
41     100  FORMAT (18X,F7 2.8X,F7 2.9X,F5 2)
42     WRITE (6,110)
43     110  FORMAT (/1X,'-----'
44     '-----',//)
45     110  FORMAT (///25X,'GAS TRANSDUCER CORRECTIONS'///)
46     WRITE (6,90)
47     WRITE (6,100) (TRANSP(2,M),DWP(2,M),GC(2,M),M=1,NUMP)

```

43        STOP  
44        END  
  
\$ENTRY

00000640  
00000650  
00000660

DATE: 8/28/84

INPUT UNITS ARE DEG C AND PSIA

HYDROCARBON TRANSDUCER CORRECTIONS

| TRANS PRESS | D.W PRESS | TRANSD CORR |
|-------------|-----------|-------------|
| 57.90       | 49.94     | -1.97       |
| 87.60       | 79.90     | -1.70       |
| 137.30      | 129.84    | -1.47       |
| 186.90      | 179.77    | -1.13       |
| 236.50      | 229.71    | -0.79       |
| 256.30      | 249.68    | -0.62       |
| 286.10      | 279.65    | -0.46       |
| 385.30      | 379.52    | 0.22        |
| 435.00      | 429.46    | 0.45        |
| 534.10      | 529.33    | 1.23        |
| 633.40      | 629.21    | 1.80        |
| 732.50      | 729.08    | 2.58        |
| 831.70      | 829.03    | 3.33        |
| 930.90      | 928.83    | 3.93        |
| 1030.00     | 1028.70   | 4.70        |
| 1129.20     | 1128.58   | 5.38        |
| 1228.30     | 1228.42   | 6.12        |
| 1327.40     | 1328.30   | 6.90        |
| 1426.50     | 1428.17   | 7.67        |
| 1525.60     | 1528.05   | 8.44        |
| 1624.60     | 1627.93   | 9.32        |

-----

STATEMENTS EXECUTED= 442

CORE USAGE        OBJECT CODE=        2672 BYTES,ARRAY AREA=        772 BYTES,TOTAL AREA AVAILABLE= 129024 BYTES

## APPENDIX D

### ERROR PROPAGATION IN MOLE FRACTION AND BUBBLE POINT PRESSURE

The mole fraction of component 1,  $x_1$ , in a binary mixture is expressed as

$$x_1 = \frac{n_1}{n_1 + n_2} \cdot \quad (A)$$

We define the total moles injected for component 1,  $n_1$ , as

$$n_1 = \sum_i \rho_{i1} V_i \quad (B)$$

The total moles of component 2 injected is similarly defined as

$$n_2 = \rho_2 V_2 \quad (C)$$

Assuming all of the component 1 injections are made at the same temperature and pressure, substitution of Equation (B) and (C) into Equation (A) yields

$$x_i = \frac{\rho_1 \sum V_{i1}}{\rho_1 \sum V_{i1} + \rho_2 V_2} \quad (D)$$

The uncertainty in the mole fraction of component 1,  $\epsilon_{x_1}$ , can be defined by error propagation as

$$\begin{aligned} \epsilon_{x_1} = & \left(\frac{\partial x_1}{\partial \rho_1}\right)^2 \epsilon_{\rho_1}^2 + \sum \left(\frac{\partial x_1}{\partial V_{i1}}\right)^2 \epsilon_{V_{i1}}^2 \\ & + \left(\frac{\partial x_1}{\partial \rho_2}\right)^2 \epsilon_{\rho_2}^2 + \left(\frac{\partial x_1}{\partial V_2}\right)^2 \epsilon_{V_2}^2 \end{aligned} \quad (E)$$

Expressions for the partial derivatives in Equation (E) can be derived by differentiation of Equation (D) with respect to  $\rho_1$ ,  $V_{i1}$ ,  $\rho_2$ , and  $V_2$  which yields

$$\frac{\partial x_1}{\partial \rho_1} = \frac{\rho_2 V_2 \sum V_{i1}}{(\rho_1 \sum V_{i1} + \rho_2 V_2)^2} \quad (F)$$

$$\frac{\partial x_1}{\partial V_{i1}} = \frac{\rho_1 \rho_2 V_2}{(\rho_1 \sum V_{i1} + \rho_2 V_2)^2} \quad (G)$$

$$\frac{\partial x_1}{\partial \rho_2} = \frac{-\rho_1 V_2 \sum V_{i1}}{(\rho_1 \sum V_{i1} + \rho_2 V_2)^2} \quad (H)$$

$$\frac{\partial x_1}{\partial V_2} = \frac{-\rho_1 \rho_2 \sum V_{i1}}{(\rho_1 \sum V_{i1} + \rho_2 V_2)^2} \quad (I)$$

respectively.

Substituting Equations (F) through (I) into Equation (E) and with some algebraic manipulation, Equation (E) becomes

$$\begin{aligned} \epsilon_{x_1} = & x_1 x_2 \left[ \left( \frac{\epsilon_{\rho_1}}{\rho_1} \right)^2 + \left( \frac{\epsilon_{V_1}}{\sum V_{i1}} \right)^2 + \left( \frac{\epsilon_{\rho_2}}{\rho_2} \right)^2 \right. \\ & \left. + \left( \frac{\epsilon_{V_2}}{V_2} \right)^2 \right]^{1/2} \end{aligned} \quad (J)$$

The uncertainty in bubble-point pressure can also be estimated through error propagation. This uncertainty (by analogy to Equation (E)) can be expressed as

$$\epsilon_{P_b}^2 = \epsilon_P^2 + \left( \frac{\partial P}{\partial x_1} \right)^2 \epsilon_{x_1}^2 + \left( \frac{\partial P}{\partial T} \right)^2 \epsilon_T^2. \quad (K)$$

VITA 2

MARK WILLIAM BARRICK

Candidate for the Degree of

Master of Science

Thesis: HIGH PRESSURE SOLUBILITIES OF CARBON DIOXIDE IN THE AROMATIC SOLVENTS BENZENE, NAPHTHALENE, PHENANTHRENE, AND PYRENE

Major Field: Chemical Engineering

Biographical:

Personal Data: Born in El Dorado, Kansas, July 12, 1960. The son of W. Ray and Mary Barrick.

Education: Graduated from Tulsa Memorial High School, Tulsa, Oklahoma in May 1978; received Bachelor of Science degree in Chemical Engineering from Oklahoma State University in July, 1983; completed requirements for Master of Science degree from Oklahoma State University in January, 1985.

Professional Experience: Employed by Getty Refining and Marketing, Process Engineering Division; as an engineer intern, Summer, 1982; Research Assistant, Department of Chemical Engineering, Oklahoma State University, September, 1983 to September, 1984; Member of American Institute of Chemical Engineers, Tau Beta Pi, and Omega Chi Epsilon.